

V347M
NO. 5-77-10
col. 3



MISCELLANEOUS PAPER S-77-10

A PROBABILISTIC ANALYSIS OF EMBANKMENT STABILITY PROBLEMS

by

Lawrence W. Gilbert

Soils and Pavements Laboratory
U. S. Army Engineer Waterways Experiment Station
P. O. Box 631, Vicksburg, Miss. 39180

July 1977

Final Report

Approved For Public Release; Distribution Unlimited



Prepared for **Office, Chief of Engineers, U. S. Army**
Washington, D. C. 20314

Under **CWIS 31173, Task 21**

LIBRARY BRANCH
TECHNICAL INFORMATION CENTER
US ARMY ENGINEER WATERWAYS EXPERIMENT STATION
VICKSBURG, MISSISSIPPI

REPORT DOCUMENTATION PAGE		READ INSTRUCTIONS BEFORE COMPLETING FORM
1. REPORT NUMBER Miscellaneous Paper S-77-10	2. GOVT ACCESSION NO.	3. RECIPIENT'S CATALOG NUMBER
4. TITLE (and Subtitle) A PROBABILISTIC ANALYSIS OF EMBANKMENT STABILITY PROBLEMS	5. TYPE OF REPORT & PERIOD COVERED Final report	
	6. PERFORMING ORG. REPORT NUMBER	
7. AUTHOR(s) Lawrence W. Gilbert	8. CONTRACT OR GRANT NUMBER(s)	
9. PERFORMING ORGANIZATION NAME AND ADDRESS U. S. Army Engineer Waterways Experiment Station Soils and Pavements Laboratory P. O. Box 631, Vicksburg, Miss. 39180	10. PROGRAM ELEMENT, PROJECT, TASK AREA & WORK UNIT NUMBERS CWIS 31173, Task 21	
11. CONTROLLING OFFICE NAME AND ADDRESS Office, Chief of Engineers, U. S. Army Washington, D. C. 20314	12. REPORT DATE July 1977	
	13. NUMBER OF PAGES 150	
14. MONITORING AGENCY NAME & ADDRESS (if different from Controlling Office)	15. SECURITY CLASS. (of this report) Unclassified	
	15a. DECLASSIFICATION/DOWNGRADING SCHEDULE	
16. DISTRIBUTION STATEMENT (of this Report) Approved for public release; distribution unlimited.		
17. DISTRIBUTION STATEMENT (of the abstract entered in Block 20, if different from Report)		
18. SUPPLEMENTARY NOTES This report was submitted as a thesis in partial fulfillment of the requirement of the degree of Master of Science in Civil Engineering at the Massachusetts Institute of Technology, August 1974.		
19. KEY WORDS (Continue on reverse side if necessary and identify by block number) Embankment stability Embankments Models Probability theory		
20. ABSTRACT (Continue on reverse side if necessary and identify by block number) In this thesis, a probabilistic model is developed to predict the reliability of an embankment constructed on soft saturated clay. The model is based on a circular arc method of analysis, supplemented with a measure of the uncertainty in the resisting and overturning moments. The uncertainty in the overturning moment was considered negligible in this thesis. The uncertainty in the resisting moment was considered due to the uncertainties of bias, random testing error, and inherent soil variability. (Continued)		

20. ABSTRACT (Continued)

Two case studies were analyzed in this thesis by both the conventional method of analysis and the probability model. The results indicate that the uncertainties in bias correction factors are the dominant sources for both field vane testing and unconfined compression testing.

The basic probability model is then extended to include the effect of embankment length on the computed failure probability. Two approaches are taken. The first is a direct extension of the basic model, considering the actual embankment length as a multiple of the minimum embankment length required to satisfy the assumption of "plane strain." The second approach is a three dimensional probability model developed from a first passage failure criterion.

PREFACE

The thesis study reported herein was conducted at Massachusetts Institute of Technology (MIT) by Mr. Lawrence William Gilbert while on a graduate study leave sponsored by the U. S. Army Engineer District, New Orleans.

Permission to publish this thesis was granted by MIT. The thesis was published by the U. S. Army Engineer Waterways Experiment Station (WES) under the Civil Works Research and Development Program of the Office, Chief of Engineers (OCE) under CWIS 31173, "Special Studies for Civil Works Soils Problems," in partial fulfillment of Task 21, "Application of Probabilistic Methods to Soil Mechanics," Special studies were under the direction of Mr. C. L. McAnear, Chief, Soil Mechanics Division, under the general supervision of Mr. J. P. Sale, Chief, Soils and Pavements Laboratory, WES. Mr. R. R. W. Beene was OCE technical monitor.

COL John L. Cannon, CE, was Commander and Director of WES and Mr. F. R. Brown was Technical Director at the time of publication.

CONVERSION FACTORS, U. S. CUSTOMARY TO METRIC (SI)
UNITS OF MEASUREMENT

U. S. customary units of measurement used in this report can be converted to metric (SI) units as follows:

<u>Multiply</u>	<u>By</u>	<u>To Obtain</u>
inches	25.4	millimetres
feet	0.3048	metres
pounds (force) per square foot	47.88026	pascals

A PROBABILISTIC ANALYSIS
OF
EMBANKMENT STABILITY PROBLEMS

by

LAWRENCE WILLIAM GILBERT

BS, Tulane University

(1969)

Submitted in partial fulfillment
of the requirements of the degree of
Master of Science in Civil Engineering

at the

Massachusetts Institute of Technology

August, 1974

Signature of Author . . . *Lawrence William Gilbert* . . .
Department of Civil Engineering, August 25, 1974

Certified by *Charles C. Ladd*
Thesis Supervisor

and *Erik H. Vanmarcke*
Thesis Supervisor

Accepted by
Chairman, Departmental Committee on Graduate
Students of the Department of Civil Engineering

ABSTRACT

A PROBABILISTIC ANALYSIS OF EMBANKMENT STABILITY PROBLEMS

by

LAWRENCE WILLIAM GILBERT

Submitted to the Department of Civil Engineering on (August, 1974) in partial fulfillment of the requirements for the degree of Master of Science in Civil Engineering.

In this thesis, a probabilistic model is developed to predict the reliability of an embankment constructed on soft saturated clay. The model is based on a circular arc method of analysis, supplemented with a measure of the uncertainty in the resisting and in the overturning moments. The uncertainty in the overturning moment was considered negligible in this thesis. The uncertainty in the resisting moment was considered due to the uncertainties of bias, random testing error, and inherent soil variability.

Two case studies were analyzed in this thesis by both the conventional method of analysis and the probability model. The results indicate that the uncertainties in bias correction factors are the dominant sources for both field vane testing and unconfined compression testing.

The basic probability model is then extended to include the effect of embankment length on the computed failure probability. Two approaches are taken. The first is a direct extension of the basic model, considering the actual embankment length as a multiple of the minimum embankment length required to satisfy the assumption of "plane strain." The second approach is a three dimensional probability model developed from a first passage failure criterion.

Thesis Supervisors:

Charles Cushing Ladd
Professor of Civil Engineering

Erik H. Vanmarcke
Associate Professor of Civil Engineering

ACKNOWLEDGEMENTS

I wish to express my gratitude to Professor Charles C. Ladd and Professor Erik H. Vanmarcke, my thesis supervisors, for the friendship, encouragement, and assistance which they have so willingly given to me during the past year and especially during the writing of this thesis.

I would also like to thank the U.S. Army Corps of Engineers, New Orleans District, for being so interested in furthering the education of its employees as to sponsor my year of study at M.I.T.

Finally, I am grateful to my wife, Donna, and my daughter, Erin, for their love and understanding, and for helping me keep this year in its proper perspective.

TABLE OF CONTENTS

	<u>Page</u>
TITLE PAGE	1
ABSTRACT	2
ACKNOWLEDGEMENTS	3
TABLE OF CONTENTS	4
LIST OF FIGURES	7
LIST OF TABLES	10
INTRODUCTION	11
CHAPTER 1: SAFETY FACTORS AND FAILURE PROBABILITIES	14
1.1 General	14
1.2 Limitations of Current Design Approach	16
1.3 Uncertainty in the Method of Analysis	19
1.3.1 Safety Factor Definition	19
1.3.2 Simplifying Model Assumptions	21
1.4 Uncertainty in the Resistance	22
1.4.1 Measurement of In situ Strength	22
1.4.2 Input Value of Strength	27
1.5 Uncertainty in the Load	28
1.5.1 Density and Configuration Measurements	28

	<u>Page</u>
1.5.2 External Loads	29
1.6 Influence of Embankment Length	29
1.7 Advantages of a Probability Model	30
 CHAPTER 2: THE PROBABILITY MODEL	 38
2.1 General	38
2.2 Statistical Tools	38
2.3 Basic Probability Model	41
2.4 Load and Resistance Uncertainty	46
2.5 Model Uncertainty	50
2.6 Measurement of Resistance Uncertainty	51
2.6.1 Uncertainty Due to Bias	52
2.6.2 Uncertainty Due to Random Testing Error	54
2.6.3 Uncertainty Due to Inherent Soil Variability	56
2.6.4 Combined Uncertainty	60
2.7 Probability Model for Layered Foundations	61
 CHAPTER 3: CASE STUDIES	 76
3.1 General	76
3.2 Fore River Test Section	76
3.2.1 Conventional Analysis	76
3.2.2 Probabilistic Analysis	82

	<u>Page</u>
3.3 Atchafalaya Basin Test Section	88
3.3.1 Conventional Analysis	88
3.3.2 Probabilistic Analysis	93
CHAPTER 4: THE INFLUENCE OF EMBANKMENT LENGTH ON FAILURE PROBABILITY	120
4.1 General	120
4.2 Series System Failure Criterion	121
4.3 "First Passage" Failure Criterion	123
CHAPTER 5: CONCLUSIONS AND RECOMMENDATIONS	132
5.1 General	132
5.2 Conclusions	132
5.2.1 Need to Recognize Uncertainty	132
5.2.2 Safety Factors as a Measure of Reliability	134
5.2.3 The Uncertainty of Bias	137
5.3 Recommendations	140
5.3.1 Other Failure Modes	140
5.3.2 Spatial Variability	141
5.3.3 Other Measures of Strength	142
APPENDIX A	143
NOTATION	144
REFERENCES	146

LIST OF FIGURES

<u>Figure No.</u>	<u>Title</u>	<u>Page No.</u>
1-1	Safety Factor Definitions	34
1-2	Uncertainty Due to Random Testing Error and Soil Variability	35
1-3	Uncertainty in Bias Correc- tion Factor	36
1-4	Design Optimization	37
2-1	Basic Statistical Terms	66
2-2	Covariance, Correlation Coefficient and Correla- tion Distance	67
2-3	Definition of Safety Factor, Circular Arc Analysis	68
2-4	Standardized Normal Distri- bution and β versus pf	69
2-5	Reliability Index versus Safety Factor	70
2-6	Variance Function versus h/δ_s	71
2-7	One and Two-Dimensional Variability	72
2-8	Modelled Failure Plane	73
2-9	Spatial Variability of Layer Thickness	74

<u>Figure No.</u>	<u>Title</u>	<u>Page No.</u>
2-10	Safety Factor for Layered Foundation	75
3-1	Fore River Test Section, Plan	100
3-2	FRT Test Section, UC Test Data	101
3-3	FRT Test Section, FV Test Data	102
3-4	FRT Test Section, Critical Arc	103
3-5	Revised Bjerrum Correction	104
3-6	W_u Correction	105
3-7	FRT Simplified Failure Surface	106
3-8	FRT Failure Probabilities versus Safety Factors	107
3-9	Atchafalaya Basin Test Section III, Plan for Raising Levee Grade	108
3-10	Plan of Test Section III	109
3-11	Centerline FV Strength (TS III)	110
3-12	105 feet Floodwayside FV Strength (TS III)	111
3-13	180 feet Floodwayside FV Strength (TS III)	112
3-14	Centerline UC Strength (TS III)	113
3-15	105 feet Floodwayside UC Strength (TS III)	114
3-16	180 feet Floodwayside UC Strength (TS III)	115

<u>Figure No.</u>	<u>Title</u>	<u>Page No.</u>
3-17	Circular Arc Analyses (TS III), Field Vane Strengths	116
3-18	Circular Arc Analysis (TS III), Unconfined Compression Strengths	117
3-19	TS III Simplified Failure Surface	118
3-20	Calculated pf at Test Section III and pf versus FS	119
4-1	Standardized Safety Margin versus Position Along Embankment Length	130
4-2	P_f versus Actual Embankment Length	131

TABLES

<u>Table No.</u>	<u>Title</u>	<u>Page No.</u>
1-1	Design Safety Factors and Approximate Failure Rates	16
3-1	Stability of FRT Test Embank- ment	80
3-2	Fore River Test Section Data	98
3-3	Stability of TS III Main (Floodwayside) Embankment	92
3-4	Atchafalaya Basin Test Section III Data	99
4-1	Failure Probabilities Including Length Effect	123

Introduction

Probabilistic methods only recently have been introduced into the field of geotechnical engineering. There has been some skepticism as to the worth of probability models in the field. The two main reasons for the skepticism are:

1. Measurements of soil properties such as undrained shear strength (S_u) can be biased. The magnitude of bias has to be evaluated if the results from probability models are to have meaning.
2. The scatter of soil property measurement is not purely random. The geologic history of a soil deposit can result in zones of soil having a strength difference from the average for the layer. The problem of test bias for the most common strength tests (e.g. the field vane and the unconfined compression) and the inherent variability of soil properties are treated in a rational manner.

Models developed from probability theory are subject to limitations, as are all engineering models. Probability models do not replace "engineering judgement". Rather, they provide frameworks that allow the engineer to exercise this judgement in a systematic manner. Probabilistic models can assist one to evaluate both the

limitations and consequences of design.

This thesis presents a probability model for analyzing the undrained stability of earth embankments constructed on soft, saturated clay. It consists of five chapters.

Chapter One presents the reasons why the conventional safety factor does not indicate the true reliability of an embankment. It also presents in general terms the advantage of expressing the safety of an embankment by its probability of failure rather than its conventional safety factor.

Chapter Two introduces the basic concepts and tools that will be applied throughout this report. Then, a two-dimensional probability model is developed for an embankment on a homogeneous foundation. This is the case of an embankment having an assumed failure plane within a single layer of uniform strength, of constant inherent variability, and uniformly tested. Next, the model is extended to include layered soils. The chapter also includes a presentation of the methodology for determining the input for the model.

Chapter Three analyzes case studies with the probability model. It is the intent of this chapter to clarify the

model by applying it to real problems on which typical soil data are available. Differences between the conventional safety factor and the probability of failure also are illustrated in this chapter.

Chapter Four contains an extension of the general two-dimensional model. In this chapter the influence of embankment length on the probability of failure of an embankment are evaluated. The examples in chapter three are used to illustrate this extension.

Chapter Five presents the conclusions from the study and makes recommendations for future research.

Chapter 1 Safety Factors and Failure Probabilities

1.1 General Faced with the responsibility of designing an earth embankment against a shear failure, an engineer practicing the current design approach begins by selecting the appropriate method of stability analysis. Since the probability model developed in this thesis is for embankments on soft saturated clays, stability during and immediately after construction is most critical. As an embankment is constructed, positive pore pressures are induced in the soft foundation clays. As the excess pore pressure dissipates, the strength of the foundation increases. This means that the safety of the embankment improves with time.

The appropriate method of stability analysis for the above case is the total stress analysis (TSA). The strength parameter required for a total stress analysis is the undrained shear strength, S_u .

Once the method of analysis is ascertained, the engineer seeks information on the soil types and layering geometry under the proposed embankment. This is accomplished with sub surface exploration (and soil classification of recovered samples) at the site of the proposed embankment. Hopefully, the site exploration is aided by a knowledge of the geology of the area.

Next, the engineer tries to measure the undrained

strength with depth and embankment length along the proposed embankment. The undrained strength can be measured with either field tests or laboratory tests on "undisturbed" samples. Current engineering practice usually uses either field vane tests or unconfined compression (or triaxial unconsolidated-undrained) tests on representative "undisturbed" samples.

With the proposed embankment geometry, a series of total stress stability analyses are performed to locate the most critical failure plane. The most critical failure plane is that which produces the minimum safety factor. (*) The design engineer would compare this minimum safety factor to a specified "design" safety factor and adjust the configurations of the section, if necessary, until the safety factor of the section is equal to or slightly greater than the "design" safety factor.

Historically, ranges of design safety factors have been used to account for unknowns associated with different types of foundation designs (Meyerhof, 1970). These design safety factors reflect values that have led

(*) The assumption of a circular failure mechanism is made in this thesis. Based on this assumption the safety factor is generally defined as equal to the resisting moment divided by the overturning moment, i.e.

$$FS = \frac{M_R}{M_O}$$

to satisfactory performance based on both stability and deformation. The magnitude of the safety factor in some way reflects uncertainties due to simplified soil and embankment configurations, simplified stability analyses and loads and resistances generated by a given structure.

A set of design safety factors was proposed by Terzaghi and Peck (1967) and is given in Table 1-1. The lower and upper limits reflect those that should be used for maximum and average design loads, respectively. Also shown in Table 1-1 are the failure rates of the three classes of structures as estimated by Meyerhof (1970).

Class	(T&P, 1967) Safety Factor	(Meyerhof, 1970) Approximate Failure Rates (per 1000)
Earthworks	1.3 to 1.5	5
Earth Retaining Structures	1.5 to 2.0	1
Foundations	2.0 to 3.0	0.5

Design Safety Factors and Approximate Failure Rates

TABLE 1-1

1.2 Limitations of Current Design Approach

The current design approach for analyzing the stability of earth embankments on soft saturated clays involves three basic steps. They are:

1. Select an appropriate method of total stress analysis, the selected method usually assumes

either a circular arc or a wedge type failure surface. These two types of failure mechanisms have different definitions of safety factor.

2. Estimate the input parameters for the selected method of analysis. The undrained shear strength is needed to calculate the resistance to failure. The total unit weight of the embankment and the foundation geometry are needed to calculate the overturning moment.
3. Subdivide the embankment length into sections of similar subsurface conditions. A separate design is made for each section.

There are four basic limitations to applying the current design approach. They are:

1. Uncertainty in the method of analysis. There is an uncertainty as to the true meaning of safety factors obtained from conventional methods of analysis. This uncertainty is due to inconsistencies in the definition of safety factor and to simplifying assumptions made in developing and applying conventional methods of analyses.
2. Uncertainty in the Resistance. This uncertainty is due to two sources. First, uncertainty is introduced in trying to measure the true in situ

strength of the foundation clays. Uncertainty due to bias error, random testing error, and inherent soil variability obscure the true or in situ undrained strength. The second source of uncertainty lies in what value of strength is input into the analysis. Some engineers use the mean value, while others use reduced means. There is also uncertainty as to whether the strength of fill and the fill crust strength should be considered.

3. Uncertainty in the Load. This uncertainty is due to uncertainties in measuring the total unit weight of the embankment material. Assuming that the embankment is constructed on level ground, the unit weight of the foundation clays does not contribute to the net load. Uncertainty in the load is also contributed by uncertainty in the embankment configuration and in externally applied loads.
4. Uncertainty due to embankment length. The safety factor of an embankment is generally independent of its length. If two embankments of different lengths are constructed to the same safety factor on the same foundation, the longer embank-

ment will have the higher failure probability.

These limitations will be explained in greater detail in the following section.

Determining the safety factor of an earth embankment requires selecting a method of analysis, estimating the loads and resistances, and subdividing the length of embankment into sections of similar subsurface conditions. Uncertainties are associated with each of these steps. It is a quantitative evaluation of these uncertainties, together with the embankment safety factor, that defines the probability of failure of an embankment. The uncertainties in these steps will be treated separately.

1.3 Uncertainty in the Method of Analysis.

1.3.1 Safety Factor Definition

Uncertainty as to the meaning of a safety factor is introduced with the definitions of safety factor. Consider first an example of an embankment investigated by the wedge method of analysis. Using the notation shown in Figure 1-1a, the safety factor against sliding is generally defined as:

$$FS = \frac{R_a + R_b + R_p}{D_a - D_p} \quad (1.3-1)$$

in which D = driving force; R = resisting force; a refers to the active wedge; b refers to the central block; P refers to the passive wedge.

The safety factor for the wedge method of analysis has been defined as:

$$FS = \frac{Ra + Rb + Rp + Dp}{Da} \quad (1.3-2)$$

Whether the term, Dp , is placed in the numerator or in the denominator of the equation of the safety factor will make a difference in the calculated safety factor of an embankment. The calculated safety factor for the two equations are the same only when the safety factor is equal to unity.

A similar inconsistency exists for the circular arc method of analysis. Considering the same embankment and the notation shown on Figure 1-lb, the safety factor is generally defined as:

$$FS = \frac{S\hat{L}r}{W_1 a_1 - W_2 a_2} \quad (1.3-3)$$

where S = shear strength; \hat{L} = failure arc length; r = radius of failure arc; a_1 and a_2 = moment arms; W_1 and W_2 = weights of masses 1 and 2. However, the safety factor for the circular arc method of analysis was initially defined by Terzaghi and Peck (1948) as:

$$FS = \frac{S\hat{L}r + W_2 a_2}{W_1 a_1} \quad (1.3-4)$$

Again, the location of the term, $W_2 a_2$, will result in different values of safety factor for safety factors greater than unity. Also, there is no reason why the

safety factors based on a circular arc analysis should be equal to the safety factors of a sliding wedge analysis (Wright and Duncan, 1972). Thus, an embankment can have at least four different safety factors depending on the selected method of analysis and on the definition of safety factor for that method of analysis.

This inconsistency in the definition of safety factor can be minimized in a probability model based on a circular arc method of analysis. The probability model begins with the definition of safety margin, M , or the net resisting moment.

$$M = \text{safety margin} = M_R - M_o \quad (1.3-5)$$

$$M = (SLr + W_2 a_2) - W_1 a_1 =$$

$$M = SLr - (W_2 a_2 - W_1 a_1) \quad (1.3-6)$$

Whether the term $W_2 a_2$ is considered as a negative overturning moment or a positive resisting moment does not change the safety margin.

1.3.2 Simplifying Model Assumptions

Simplifying assumptions made both in developing and in applying stability analyses result in methods of limited reliability. Some of these assumptions are:

1. Approximations of the embankment configuration, foundation layering, and failure surface shape are all sources of uncertainty.

2. The behavior of the embankment may not agree with the assumptions of the model (plastic deformations rather than rigid body motion, anisotropic versus isotropic strength, and strain softening material).
3. The conventional methods of analysis assume plane strain conditions. Many observed failures are bowl-shaped, far from plane strain.

1.4 Uncertainty in the Resistance

1.4.1 Measurement of In Situ Strength

Since this report is concerned with the undrained stability of an embankment constructed on soft saturated clays, the soil property needed for calculating resistance is the undrained shear strength. Selecting the in situ strength is usually a major source of uncertainty in stability analyses. The uncertainty in measuring strength will be illustrated with the field vane test as an example. The basic problems with other lab and field tests are similar to those of the field vane.

The first problem with the field vane test is bias. A test is biased when it consistently overpredicts or underpredicts the value of in situ strength, regardless of the number of tests performed. There are six disadvantages of the field vane test that lead to biased

measurement (Ladd, 1971). They are:

1. The stress system during shear is unlike any typical stress system applied to soils. Since the undrained strength of a soil is dependent upon the stress system at failure, the field vane can only be a semi-empirical measurement of strength.
2. Sample disturbance during testing leads to an underestimation of the in situ shear strength. For a series of tests on quick clay, field vanes left in the ground for one day after penetration gave substantially higher strengths than those sheared immediately after insertion. (Flaate, 1966). This is a measure of the disturbance due to the method of testing.
3. The presence of sand lenses, pieces of wood, or shells can increase the scatter of field vane tests and can increase the mean of the tests significantly. The field vane test is best suited for "homogeneous" soil deposits.
4. Since the test is performed in the field, close supervision by the engineer is essential. This will assure that the tests are performed in a standardized manner regardless of the drill crew.

5. The field vane test is not applicable to very stiff clays.
6. Partial drainage may occur in performing this field vane test thus altering the measured strength.

These sources of bias can be considered in part for by developing a correction factor. By correlating field vane measurements to "in situ" strengths back calculated from embankment failure, a correction factor can be obtained by relating the "in situ" to the measured field vane strength (Bjerrum, 1972). The product of the measured strength and the correction factor yields the best estimate of strength.

This allowance for test bias is essential to both the conventional method of analysis and the probability model. However, the conventional method does not explicitly allow for the uncertainty associated with the development of a correction factor. The reliability of such strength corrections can have a significant effect on the true probability of failure of an earth embankment.

The second problem with the field vane test is random testing error. Even if bias is completely eliminated the individual test results will be scattered about the mean strength due to testing errors. Increasing

scatter implies an increase in the probability of failure of an embankment. If a test had no bias and no random error it would be a perfect test, exactly measuring the in situ strength at a point. For this case there would be no uncertainty in measured strength. In general, the variability of test results from field vanes is high.

This uncertainty can have a significant effect on the probability of failure of an embankment, but can have no direct effect on safety factor determinations. However, some design engineers may use lower values of strength than normal to account for increased scatter.

The third problem is soil variability - how in situ strength varies with dimensions. This problem is due not to the type of test performed, but to the soil itself. If the field vane test were a perfect test, having no bias nor random error, the scatter of test results would reflect inherent soil variability. As inherent soil variability increases the probability of failure generally increases, but the conventional safety factor can be unaffected.

The three problems with field vane testing that introduce uncertainty into stability calculations are each illustrated on Figure 1-2 and 1-3.

Figure 1-2 demonstrates the qualitative importance

of random testing error and inherent soil variability. The first case presents the determination of strength for the same subsoil by two different unbiased testing methods. The same number of independent tests were performed with each method. The mean strength is the same for both type tests, but the scatter is larger for test B. The safety factors of an embankment constructed on this foundation are identical for both strength determinations based on the average S_u . However, the computed probability of failure for method A is lower due to the smaller scatter about the mean. This case illustrates the importance of random testing error.

The second case demonstrates the determination of strength for different subsoils using a "perfect" test for each. Again, the mean strength is the same for both subsoils but the scatter is different. The embankments on both subsoils will have the same safety factors, but different computed failure probabilities. This case presents the implications of inherent soil variability.

Figure 1-3 presents the importance of the scatter of correction factor correlations to compensate for bias. The sources of data for correction factor A were embankment failures on soft clays. These embankment failures were not restricted to a particular geologic deposit.

The sources of data for correction factor B were restricted to embankment failures on a particular geologic deposit (eg. Boston Blue Clay). The mean correction factors based on the same number of data are identical, but the scatter in developing correction factor A was larger than for B.

If an embankment were constructed on Boston Blue Clay, the safety factor would be identical regardless of which correction factor were applied to the measured strength. However, applying correction factor A would result in a higher computed probability of failure than correction factor B. The difference is due to the uncertainty in the bias correction.

1.4.2 Input Value of Strength. Once all available strength data are gathered, the engineer is faced with the decision of what value of strength to use in performing his stability analyses. Some engineers may select to use the true mean of the data, assuming that the safety factor will allow for the scatter of the data. Sowers (1970) recommends selecting a value of strength for which 25 percent of the data are lower and 75 percent higher. Other engineers may select the lowest observed strength for design.

Clearly, only by starting with the best estimate or mean strength (assuming no bias or after correcting it)

can one arrive at the mean safety factor. If lower strength values are assumed for design, the true mean safety factor of the embankment increases. For example, if one designs an embankment for a safety factor equalled to 1.5 and strengths selected were based on Sowers (1970) recommendation, the true mean safety factor could be closer to 2.

Because there is no universally accepted method of selecting the input strength, the mean safety factor of previously constructed embankments is uncertain. Also, a set of foundation strength data can have at least three different values of input strength - the mean value, Sowers value and the lowest value of strength. For a specified design safety factor and the three different values of input strength, three different embankment configurations can be designed. All three would have the same safety factor, but the calculated failure probabilities would be quite different.

1.5 Uncertainty in the Load

1.5.1 Density and Configuration Measurements. The soil property needed for load calculations is the total unit weight of the soil. This property is potentially subject to the same sources of uncertainty as is strength - namely bias, random testing error, and inherent soil

variability. However, unit weight determinations are considered to be unbiased tests.

Also required for calculating the load caused by the unbalanced mass of an earth embankment is the configuration of the embankment. For most man-made earth structures this configuration is well defined and variations in configurations are small.

1.5.2. External Loads. The uncertainty of external sources of loading also affects the failure probability. These external sources can be classified as dynamic and static. Dynamic loads include those due to earthquakes, explosives or impact. Both the magnitude and the uncertainty of these loads can be large. These type loads have uncertainty both in magnitude and in time of occurrence.

Although they may be of major consequence for certain slopes, the uncertainty of loading is usually much smaller than that of resistance. For the general case developed in this report, the uncertainty of the load is neglected in the probability model, i.e., the load is chosen to be deterministic.

1.6 Influence of Embankment Length. The current design approach does allow for length of the embankment in one respect. If noticeably different soil properties or

foundation geometry are uncovered along the length of a proposed embankment, the embankment is divided into sections having similar subsurface conditions. In fact, such subdivisions should also be made when applying a probability analysis to the embankment.

This subdivision of embankment length does not fully treat the uncertainty due to embankment length. Consider, for example, two embankments designed for a safety factor equalled to 1.50. One embankment is one mile long, the other is ten miles long. Assume that the subsurface conditions were similar for both embankments and that the embankment length was subdivided when necessary.

If both embankments were designed in a similar manner and all other uncertainties were equal, the longer embankment would have a higher probability of a failure occurring somewhere along the embankment length. This is true even though the safety factors are equal. The effects of embankment length will be developed in Chapter 4 of this thesis.

1.7 Advantages of a Probability Model. There are two main reasons why a probability model should supplement the current design approach. The first reason is to develop a methodology that can handle the limitations of the conventional safety factor method of analysis. The second

and most important is to have an expression for an earth embankment failure probability that can be combined with the costs associated with the structure to optimize design.

The previous section stated the main limitations of the current design approach. It is the ultimate goal of the probability model to give a meaning to all of the important factors that influence the probability of failure of a structure. The probability model will not minimize the role of "engineering judgement". Rather, it forces the engineer to further use "engineering judgement" in evaluating parameters such as soil variability, bias, and random error which are important for the ultimate safety of a structure.

Once the safety of a structure is expressed in terms of its probability of failure, a design optimization procedure can be developed. This procedure gives the engineer a method of determining what probability of failure to design for. In the past, design safety factors have been set based on intuitive judgement and past experience. In some cases the consequences of failure have been overlooked. By combining the consequences of failure with the probability of failure and the construction costs a logical decision can be made as to the required safety of a structure.

Consider the case of an earth dam analyzed for the end of construction stability. By evaluating the possibility of failures for different assumed geometries and by estimating the construction costs for each design, a plot of construction costs (cc) versus probability of failure (pf) can be made, see figure 4. The next step is to estimate the monetary consequence of a failure (CF). Then, plot the product of (CF) times (pf) versus (pf). The total expected costs (TEC) is equal to the sum of (cc) plus (CF) times (pf). The recommended design probability of failure is that which minimizes the total expected costs.

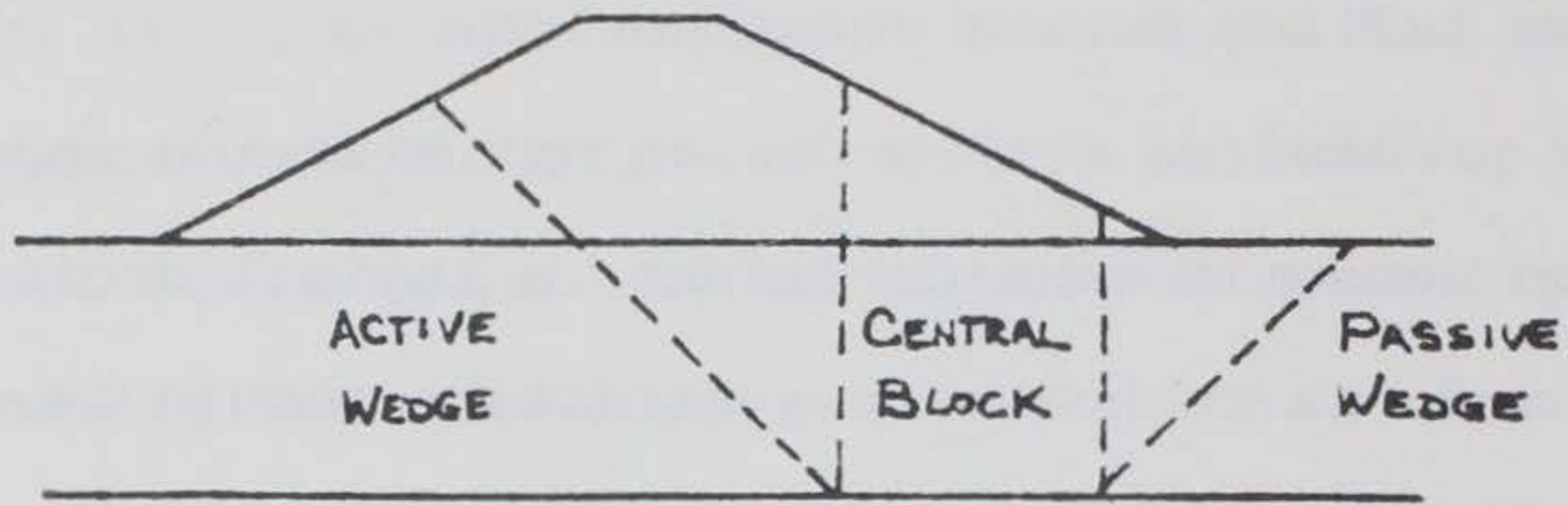
The above procedure assumes that the consequences of failure are only of an economic nature. This means that the risks of death or bodily injury and the major environmental consequences should also be assigned costs.

It can be seen how the current design method can overlook the process of optimization by considering an earth dam. An earth dam is usually designed for a safety factor of 1.50 for both the after construction case and the steady seepage case. Similar safety factors imply similar failure probabilities. However, the consequences of a dam failing during steady seepage with a reservoir full of water are orders of magnitude larger than those

of a dam failing during construction.

By proceeding with a design optimization approach based on economic considerations, a logical decision can be made as to how safe a structure should be. The probability model assumes that all earth embankments have a calculable probability of failure. By recognizing and evaluating this probability, the engineer is able to treat it in a logical manner.





D = DRIVING FORCE

R = RESISTING FORCE

A = REFERS TO ACTIVE WEDGE

B = REFERS TO CENTRAL BLOCK

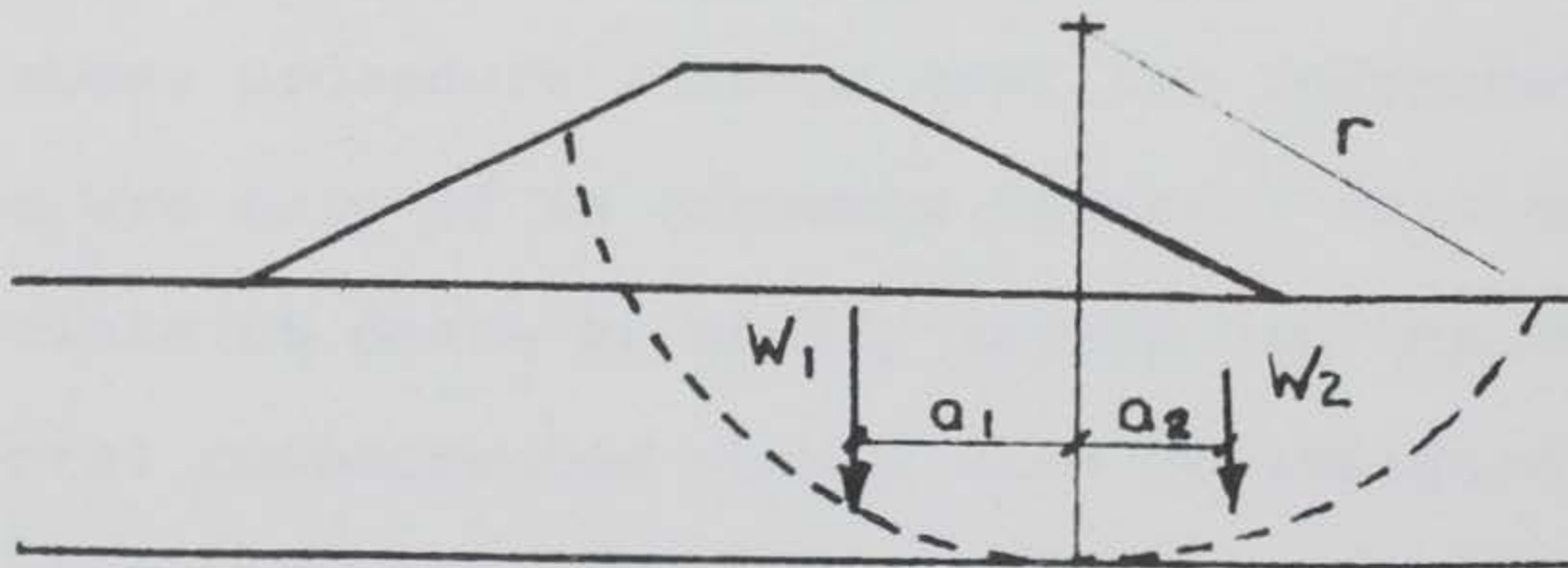
P = REFERS TO PASSIVE WEDGE

$$FS = \frac{R_A + R_B + R_P}{D_A - D_P}$$

OR

$$FS = \frac{R_A + R_B + R_P + D_P}{D_A}$$

WEDGE METHOD



S = SOIL STRENGTH

\hat{L} = FAILURE ARC LENGTH

r = RADIUS OF ARC

W = WEIGHT OF MATERIAL

a = MOMENT ARM

$$FS = \frac{S \hat{L} r}{W_1 a_1 - W_2 a_2}$$

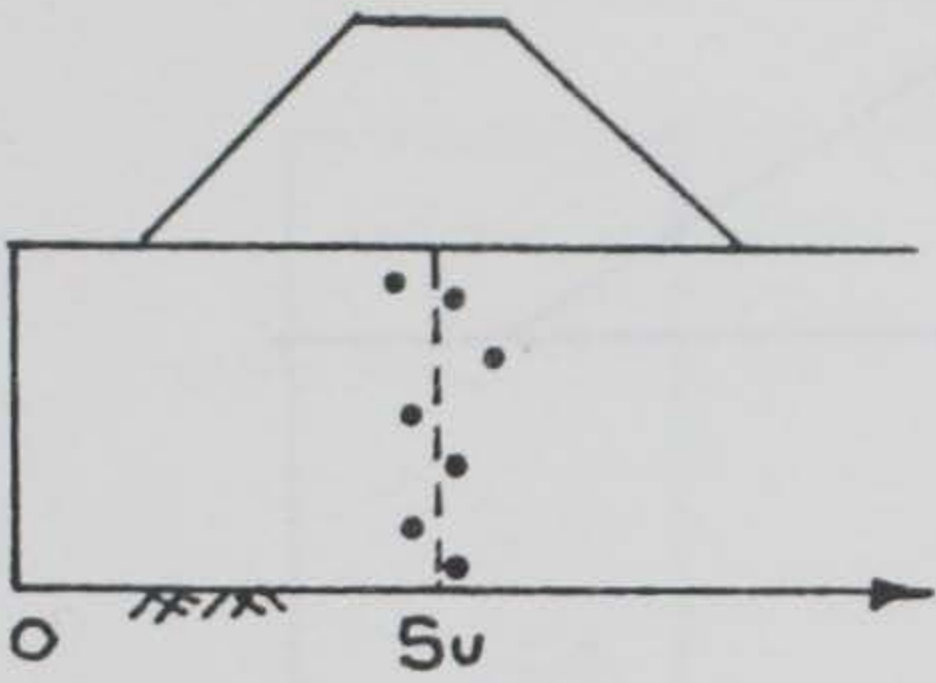
OR

$$FS = \frac{S \hat{L} r + W_2 a_2}{W_1 a_1}$$

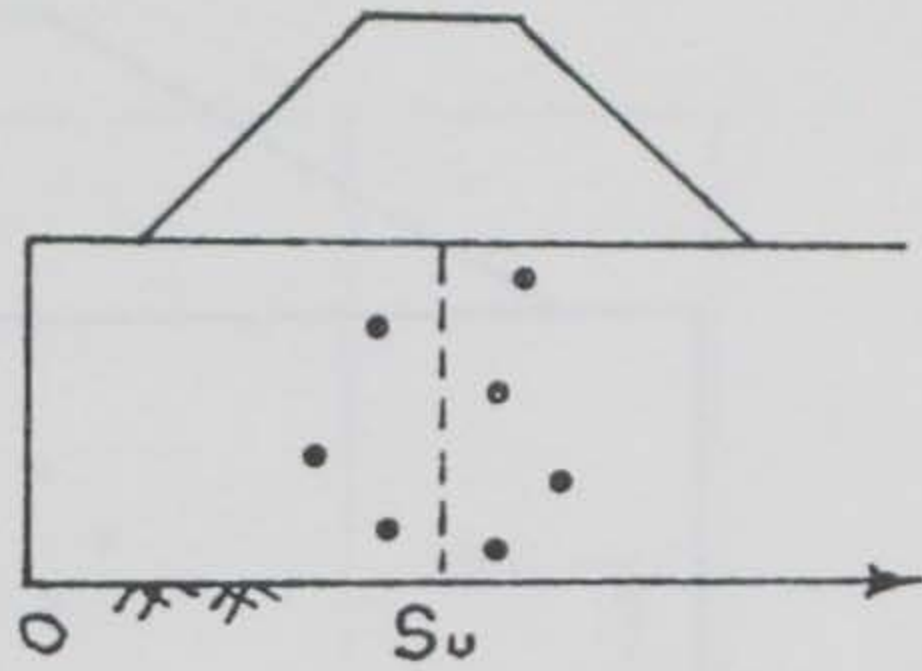
CIRCULAR ARC ANALYSIS

SAFETY FACTOR DEFINITIONS

FIGURE 1-1



TEST METHOD A

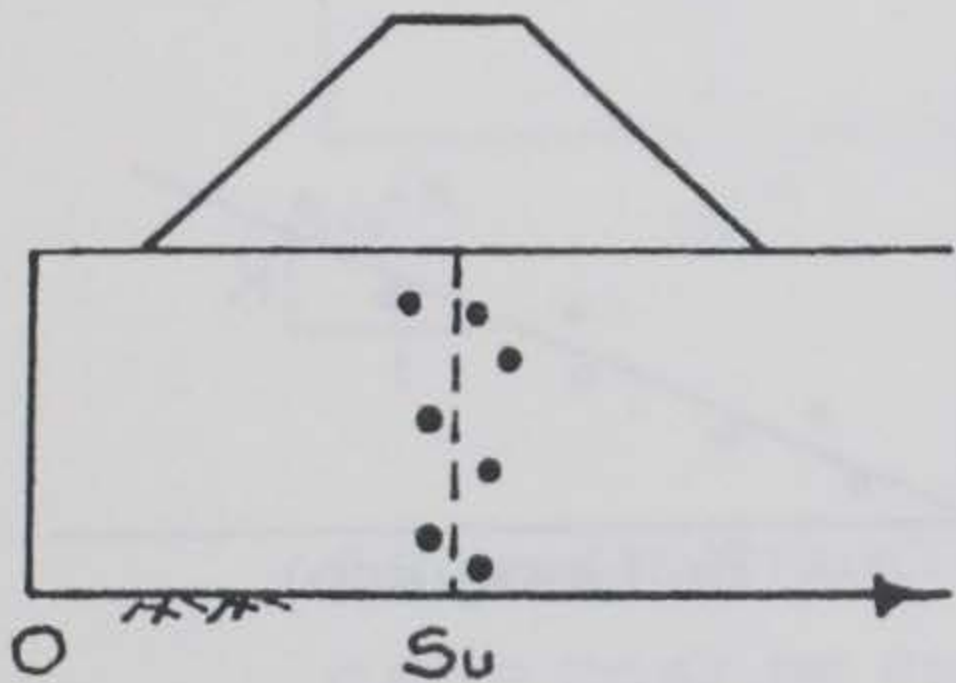


TEST METHOD B

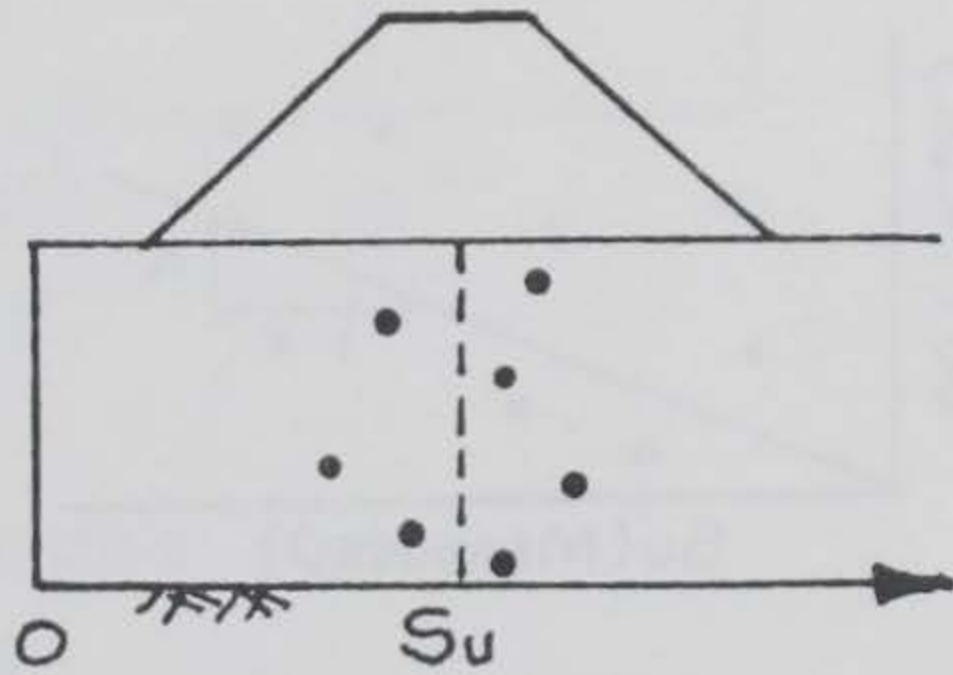
$$FSA = FSB$$

$$pfa < pfb$$

CASE 1 SAME SUBSOIL



SUBSOIL A



SUBSOIL B

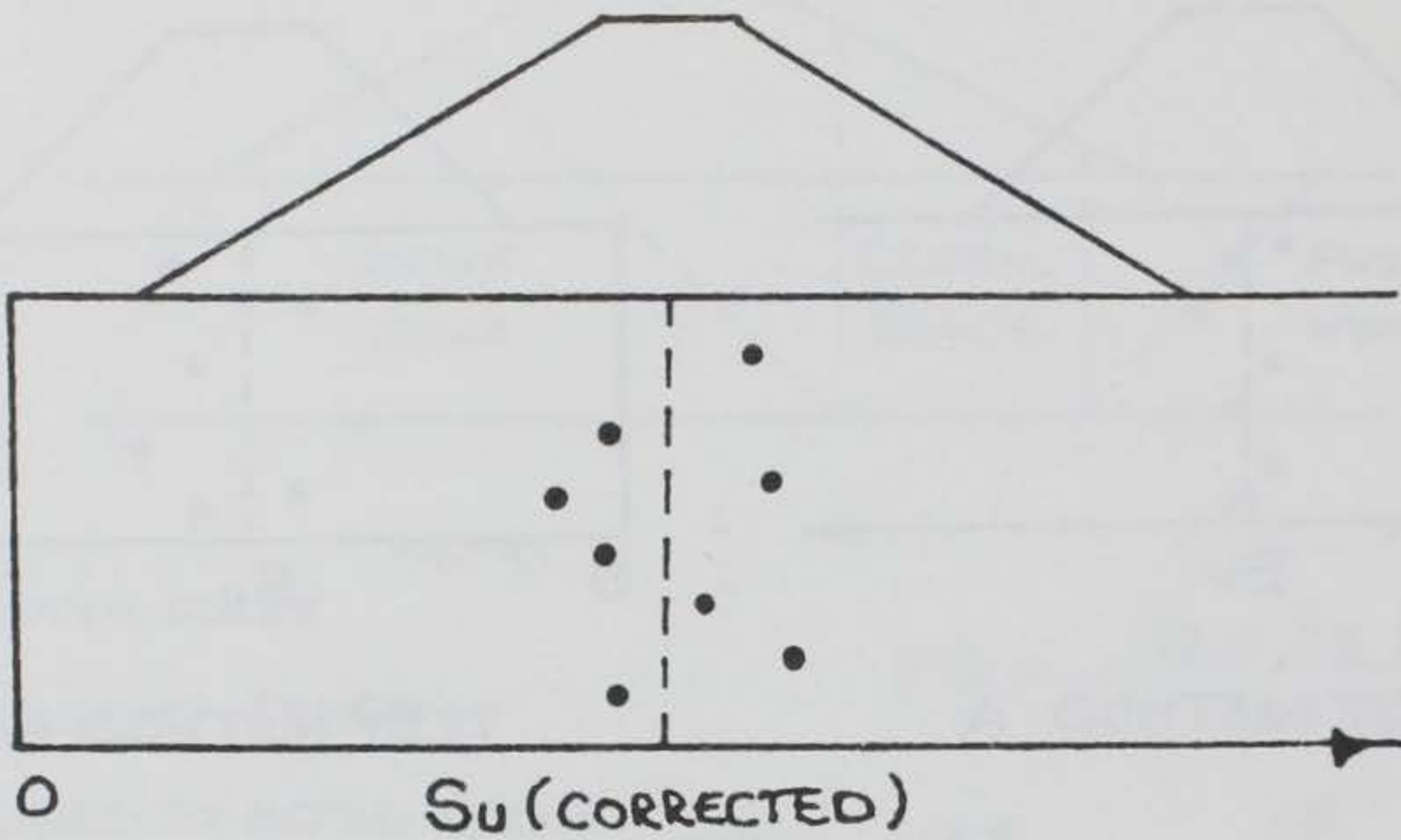
$$FSA = FSB$$

$$pfa < pfb$$

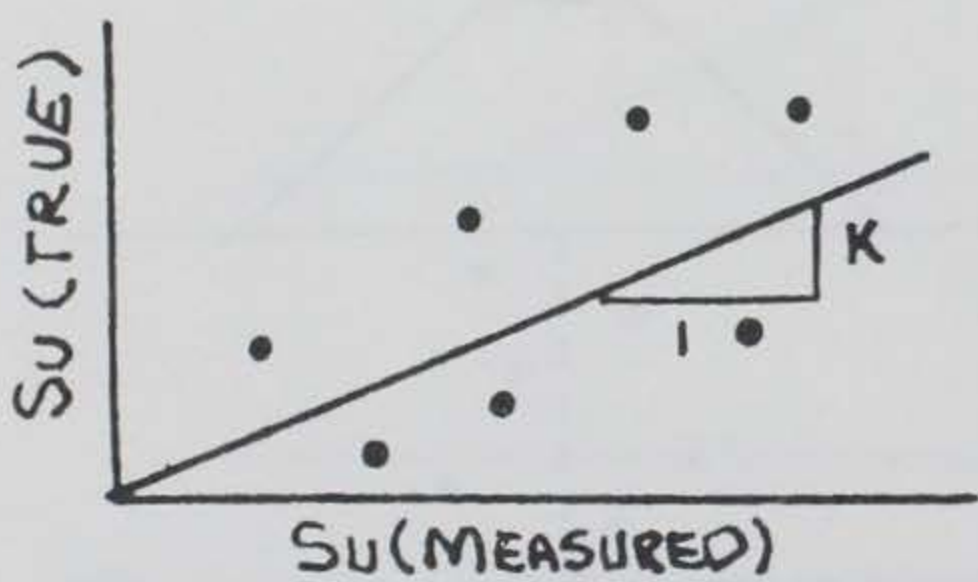
CASE 2 SAME TESTING METHOD

UNCERTAINTY DUE TO RANDOM TESTING ERROR
AND SOIL VARIABILITY

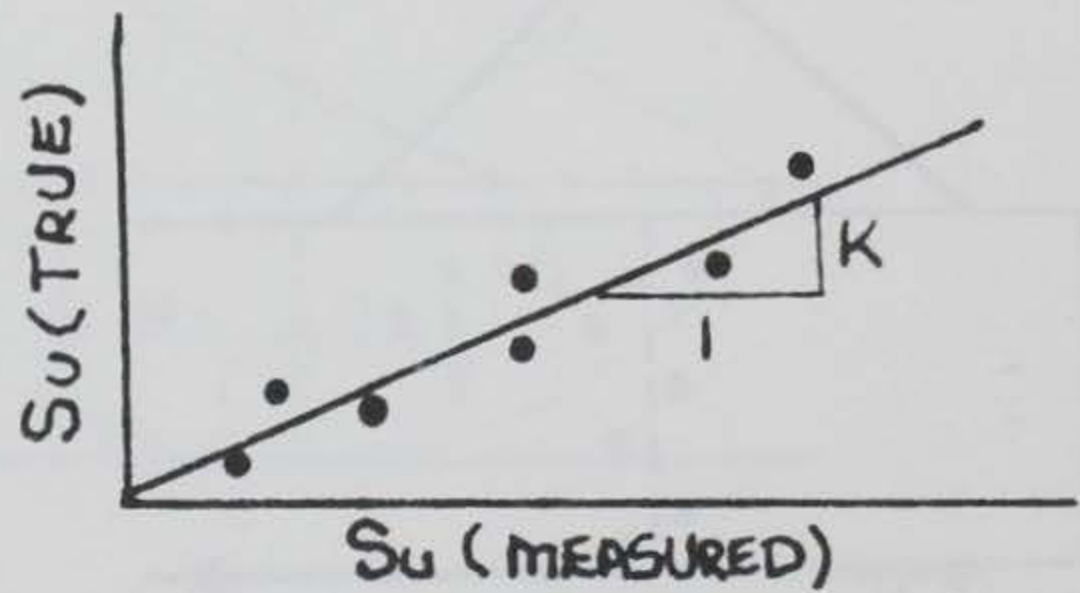
FIGURE 1-2



EMBANKMENT ON BOSTON BLUE CLAY



CORRECTION A



CORRECTION B

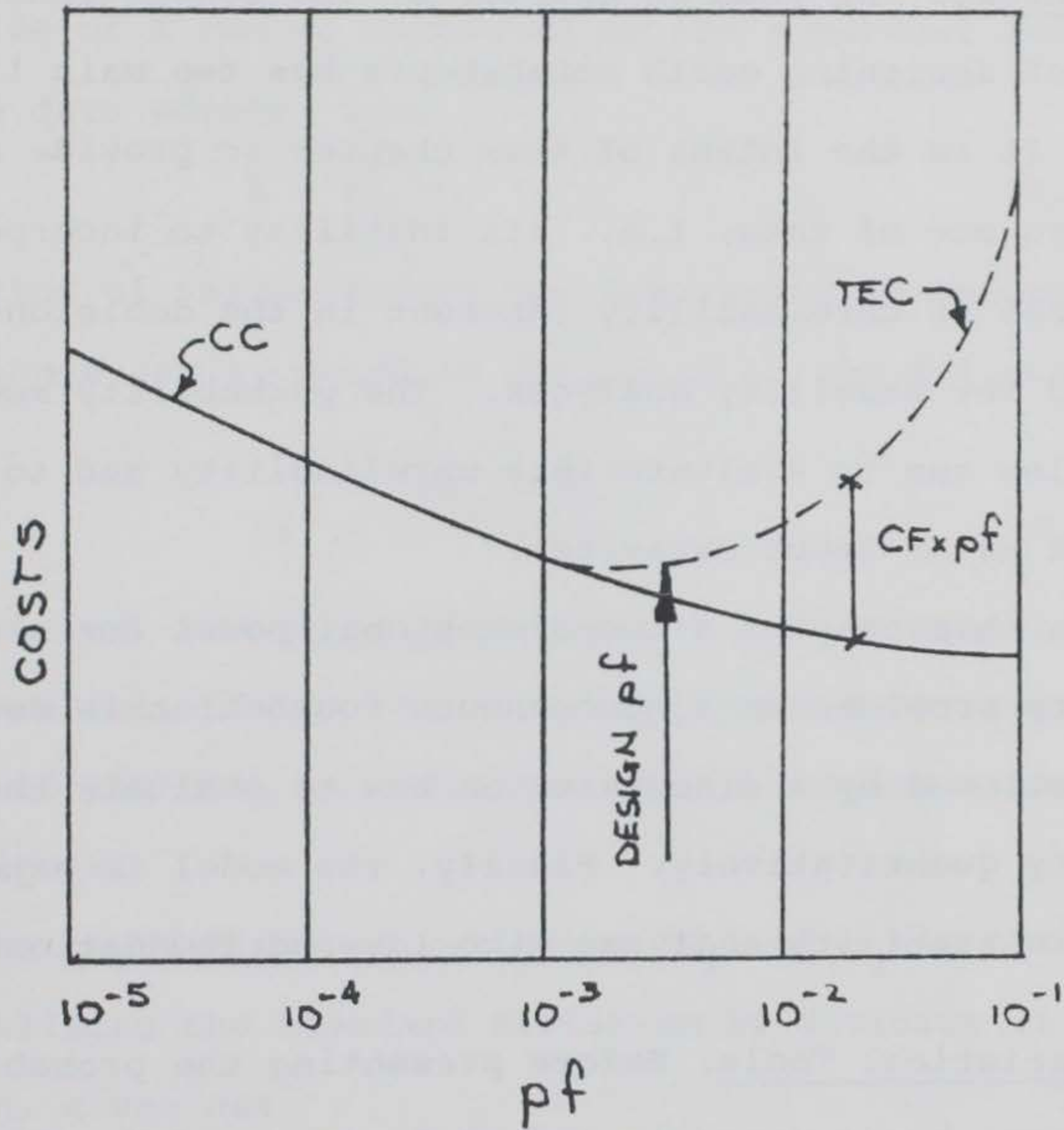
$$Su(\text{TRUE}) = k Su(\text{MEASURED})$$

$$FS_A = FS_B$$

$$pf_A > pf_B$$

UNCERTAINTY IN BIAS CORRECTION FACTOR

FIGURE 1-3



- CC = CONSTRUCTION COSTS
- CF = COST OF FAILURE
- pf = PROBABILITY OF FAILURE
- TEC = TOTAL EXPECTED COSTS
- DESIGN pf = pf @ MINIMUM TEC

DESIGN OPTIMIZATION

Chapter 2 The Probability Model

2.1 General. As seen in Chapter 1, the conventional method of designing earth embankments has two main limitations. It is the intent of this chapter to provide an answer to one of them, i.e., its inability to incorporate the degree of unreliability inherent in the decision-making required for stability analyses. The probability model will allow one to evaluate this unreliability and to include it as an input parameter.

In this chapter a two-dimensional model for slope stability problems on a homogeneous foundation is developed. It is followed by a discussion on how to evaluate the uncertainty quantitatively. Finally, the model is extended to handle stability analyses with layered foundations.

2.2 Statistical Tools. Before presenting the probability model, some basic concepts and tools are needed. First, it will be assumed that the soil properties used in the model are normally distributed. A normal distribution is a bell-shaped curve giving the distribution of the probability associated with the different values of the data. The normal distribution of soil properties of interest for slope stability problems has been suggested by Lumb (1966).

Any random quantity x can be represented by two parameters -- its mean value (\bar{X}) and its standard deviation (σ_x) or coefficient of variation (V_x). Assume that a set

of observations of x are denoted by $x_1, x_2, x_i, \dots, x_n$. The mean value of X can be estimated by the numerical average of the n data points, i.e., (*)

$$\bar{X} = \sum x_i / n \quad (2.2-1)$$

The scatter of values around the mean value is measured by the variance (σ_x^2), which is estimated in the following way: (*)

$$\sigma_x^2 = \sum \frac{(x_i - \bar{X})^2}{n} \quad (2.2-2)$$

By definition, the standard deviation (σ_x) is equalled to the square root of the variance. Approximately seventy percent of all data is contained within the one sigma bounds ($\pm\sigma_x$).

The coefficient of variation (V_x) of x_i is obtained by normalizing the standard deviation by dividing it by the mean, given as:

$$V_x = \frac{\sigma_x}{\bar{X}} \quad (2.2-3)$$

The coefficient of variation and the standard deviation would both equal zero for data having no scatter and would increase with increasing scatter about the mean. Examples of the above definitions are shown in Figure 2-1.

*Representing the estimated variance of X with the notation s_x^2 has been proposed by Benjamin and Connell (1970). Their proposed notation for "true" or theoretical variance (σ_x^2) was used in this report for estimated values. This notation was selected to avoid notational difficulties, since soil strength is also expressed by the letter S .

If paired data are available the correlation between them can be measured by calculating the co-variance, $COV(x,y)$, estimated as follows:

$$COV(x,y) = \frac{1}{n} \sum_{i=1}^n (x_i - \bar{X})(y_i - \bar{Y}) \quad (2.2-4)$$

Normalizing the co-variance by dividing it by the product of the standard deviations of the two data (X and Y) yields the correlation coefficient, (ρ_{xy}) , given as:

$$\rho_{x,y} = \frac{COV(x,y)}{\sigma_x \sigma_y} \quad (2.2-5)$$

The correlation coefficient can vary between +1 and -1. Both extreme values indicate perfect correlation, positive and negative respectively, between the sets of data (Benjamin and Cornell, 1970). That is, the data will plot as a straight line on a natural scale plot. A correlation coefficient equalled to one means that high values of x imply high values of y, and vice versa. A correlation coefficient equalled to negative one means high values of x imply low values of y, and vice versa. A correlation coefficient equalled to zero indicates the data are uncorrelated linearly. There might, however, exist some higher order correlation between the data that is undetected by the correlation coefficient.

The correlation distance of a property (δs) is a measure of how rapid the property changes in space. This requires calculating the coefficient of correlation as a

function of distance apart. Plotting the coefficient of correlation versus distance apart, the correlation distance is defined as that distance having a correlation coefficient equalled to e^{-1} (Vanmarcke, 1974). Examples of these definitions are illustrated in Figure 2-2.

2.3 Basic Probability Model

The probability model presented in this thesis was developed for the circular arc analysis of slope stability. Assuming a circular failure mechanism, the safety of an earth slope against a shear failure can be defined by a safety factor:

$$FS = \frac{\text{Resisting Moment}}{\text{Overturning Moment}} = \frac{M_R}{M_O} = \frac{s\hat{L}r}{Wa} \quad (2.3-1)$$

where:

s = mean shear strength along the assumed failure arc.

\hat{L} = arc length of assumed failure arc.

r = radius of curvature of the failure arc.

W = weight of the material within the assumed failure.

a = horizontal distance from the center of rotation to the center of gravity of the failure mass.

For a description of this expression of safety factor, see Figure 2-3.

The safety of an earth slope against failure can also be defined by its safety margin (M) equalled to the excess resisting moment. Considering M_R and M_O to be random variables, the safety margin is defined as:

$$M = (M_R - M_O) \quad (2.3-2)$$

By expressing safety in terms of net resistance, the problem of handling the passive driving force is eliminated. The safety margin will be the same whether it is considered as a positive resistance or as a negative load.

The probability of failure (pf) of an earth slope is equated to the probability that the safety margin is less than or equalled to zero, expressed as:

$$pf = p (M \leq 0) \quad (2.3-3)$$

By subtracting the mean safety margin from both sides of this equality and dividing both sides by the standard deviation of the safety margin, the probability of failure becomes:

$$pf = p \left[\frac{M - \bar{M}}{\sigma_m} \leq - \frac{\bar{M}}{\sigma_m} \right] \quad (2.3-4)$$

$$\text{or: } pf = p [U \leq -\beta] \quad (2.3-5)$$

$$\text{where: } U = \text{Standardized Safety Margin} = \frac{M - \bar{M}}{\sigma_m}$$

$$\beta = \text{Reliability Index} = \frac{\bar{M}}{\sigma_m}$$

Expanding Equation (2.3-5), the reliability index becomes:

$$\beta = \frac{\bar{M}_R - \bar{M}_O}{(\sigma M_R^2 + \sigma M_O^2)^{1/2}} \quad (2.3-6a)$$

$$\beta = \frac{\bar{M}_R/\bar{M}_O - 1}{\left(\frac{\sigma M_R}{\bar{M}_O}\right)^2 + \left(\frac{\sigma M_O}{\bar{M}_O}\right)^2} \quad (2.3-6b)$$

$$\beta = \frac{\bar{FS} - 1}{(\bar{FS}^2 VM_R^2 + VM_O^2)^{1/2}} \quad (2.3-6c)$$

where \bar{FS} = the mean safety factor

VM_R = the coefficient of variation of
the resisting moment.

VM_O = the coefficient of variation of
the overturning moment.

Assuming the resisting moment and the overturning moment normally distributed, the safety margin is normally distributed. β , then, is a measure of the number of standard deviations between the mean safety margin and the safety margin equal to zero (failure). By evaluating β , the probability of failure can be obtained from a Gaussian or normal distribution table. A graphical representation of the reliability index and a plot of pf versus β are shown in Figure 2-4.

The assumption of normality of the distribution of the standardized safety margin can be critical. The larger the value of β , the more critical the assumption of the distribution type becomes. This is due to the greater importance of the tails of the distributions at greater values of β . Ang (1972) concluded that the distribution sensitivity is not too important for failure probabilities greater than one in one thousand. The assumption of normal distribution can lead to serious error for failure probabilities greater than 10^{-3} .

Inspecting equation (2.3-6c), it can be seen that the probability of failure of an earth embankment is not only dependent on the magnitude of the mean overturning and resisting moments, but also on the uncertainty involved in obtaining them. Figure 2-5 presents how the reliability index, and hence the probability of failure is affected by the magnitudes of the coefficients of variations of the resisting and of the overturning moments.

Figure 2-5a shows the relationship between the reliability index and the mean safety factor for different coefficients of variation of the overturning moment with the coefficient of variation of the resisting moment equalled to zero. Since a straight line relationship exists between the two variables, an embankment can be built to take any unreliability in the overturning moment. This is due to the fact that the magnitude of resistance is certain. The

graph also indicates that variability in the overturning moment can imply large variations in the reliability index for the same value of safety factor.

Figure 2-5b shows the converse plot with VM_0 equalled to zero and VM_R a variable. This plot indicates that the value of the reliability index approaches a maximum value equalled to $1/VM_R$ as a limit. This means that for a given VM_R it may be impossible to design for a specified probability of failure by only increasing the central safety factor. The plot also shows that variability in the resisting moment significantly affects the reliability index.

The above assumption of VM_R as constant for increasing central safety factors is conservative. With an increase in \bar{M}_R associated with an increase in the length of the critical failure arc, VM_R will decrease. The maximum value of the reliability index equalled to $1/VM_R$ is a lower bound.

Since the uncertainty in resistance is usually much larger than the uncertainty in load, the assumption of VM_0 equalled to zero is often made. For this case, the minimum allowable value of the central safety factor can be determined from Figure 2-5b if the failure probability (and hence β) is specified and VM_R is fixed.

It is interesting to note that when the central safety factor is equal to unity, the reliability index is equal to zero. This value of β implies a probability of failure of one-half in the case of the Gaussian probability

distribution. A true safety factor of one does not mean that an earth slope will fail, rather that the slope has a fifty - fifty chance of survival.

2.4 Load and Resistance Uncertainty

As has been previously shown, the uncertainties in determining the resisting moment and the overturning moment are intimately linked to the probability of failure of an earth slope. For the general case, the uncertainty of the overturning moment is due to the scatter in the total unit weight of the soil and to variations in embankment configuration. For this case, the variability of the overturning moment is usually much smaller than that of the resisting moment and will be considered equalled to zero. The equation for the reliability index now becomes:

$$\beta = \frac{\overline{FS} - 1}{\overline{FS} \text{ VM}_R} \quad (2.4-1)$$

This section will present a method for determining the coefficient of variation of the resisting moment that should be used with equation (2.4-1).

Two different concepts of mean strength and variance of strength have to be distinguished from one another. They are the point mean and point variance and the spatial mean and spatial variance. The difference between the two is best illustrated with an example. Consider a "homogeneous"

soil deposit on which twenty-five strength measurements were made. The mean and variance of these data can be calculated by equations (2.2-1) and (2.2-2). Assume that the mean and variance of the data were calculated to be 500 psf and 10,000 psf, respectively. The standard deviation equals 100 psf.

These numbers are the best estimate and uncertainty of the outcome if an additional test were performed. That is, if one additional test were performed, the best estimate of the resulting strength would be 500 psf. Also, there would be a seventy percent chance that the resulting strength would be between 400 and 600 psf.

The spatial mean and spatial variance reflect the best estimate, and the uncertainty in the best estimate, of the average strength of the soil deposit. If the strength tests are uncorrelated, the spatial variance is:

$$\sigma_{(s)}^2 = \frac{\sigma_s^2}{n} = \frac{10,000 \text{psf}}{25} = 400 \text{ psf}$$

and the spatial standard deviation becomes:

$$\sigma_{(s)} = \frac{\sigma_s}{\sqrt{n}} = \frac{100 \text{ psf}}{\sqrt{25}} = 20 \text{ psf}$$

The spatial mean is equal to the point mean. Following up on the example, the best estimate of the average strength of the soil deposit is 500 psf. There is seventy percent confidence that the strength of the deposit is between 480 and 520 psf.

The measured strength at a point in a "homogeneous" soil deposit can be expressed as a sum of contributions:

$$S_{(meas)} = S_{(true)} + \epsilon_r + \epsilon_b \quad (2.4-1)$$

where:

$S_{(meas)}$ = the measured strength at a point.

$S_{(true)}$ = the true in-situ strength at a point.

ϵ_r = the random testing error at a point.

ϵ_b = the bias or systematic error at a point.

The measured strength at the i^{th} point is:

$$S_{(meas)}^{(i)} = S_{(true)}^{(i)} + \epsilon_r^{(i)} + \epsilon_b^{(i)} \quad (2.4-2)$$

The random error term has a zero mean and a variance, $\sigma^2 \epsilon_r$.

The bias error term has a mean equal to $\bar{\epsilon}_b$ and a variance $\sigma^2 \epsilon_b$. The point average or best estimate of strength at a point can be expressed as the average of the contributions to the measured strength:

$$\bar{S}_{(meas)}^{(i)} = \bar{S}_{(true)}^{(i)} + \bar{\epsilon}_b = \bar{S} + \bar{\epsilon}_b \quad (2.4-3)$$

The point variance of the measured strength is equal to the sum of the variances of its contributions, given as:

$$\text{VAR} [S_{(meas)}^{(i)}] = \sigma_s^2 + \sigma \epsilon_r^2 + \sigma \epsilon_b^2 \quad (2.4-4)$$

where: $\text{VAR} [S_{(meas)}^{(i)}]$ = the point variance of the measured strength based on i independent tests.

σ_s^2 = the variance of the true strength, or scatter due to the inherent variability of soil.

The point variance of the measured strength reflects the confidence in the value of strength obtained from a single independent test.

As the number of independent tests increases, the uncertainty in the effect of random testing errors decreases. Since random testing errors fluctuate about the true mean strength, these errors will be self-compensating for large numbers of tests. This is not so for the bias error. Test bias is present when a particular type of testing device consistently measures strength either too high or too low. This source of error cannot be reduced by increasing the number of independent tests, but will be a constant source of error in trying to measure in-situ strength.

The point variance is not the variance of interest for probability models. What are needed are the mean and the variance of the average of all points within the region of interest, or the spatial mean and the spatial variance of n tests performed. This will give a measure of confidence in the value of average strength obtained by testing.

The spatial mean or the mean of the spatial average of all points within the volume of interest is equal to the point mean, i.e.,

$$\langle \bar{S} \rangle_{\text{meas}} = \langle \bar{S} \rangle_{\text{true}} + \bar{\epsilon}_b = \bar{S} + \bar{\epsilon}_b \quad (2.4-5)$$

where:

$$\langle S \rangle_{\text{meas}} = \iiint_{\text{volume}} S(x, y, z) dx dy dz$$

The proper evaluation of the spatial variance, and hence the spatial coefficients of variation, is a critical issue in determining meaningful values of failure probabilities from probabilistic models of slope stability.

The spatial variance is shown in section (2.6-4) equal to:

$$\text{VAR} [\langle S \rangle_{\text{meas}}] = \sigma_b^2 + \frac{\sigma_s^2}{n} + \frac{\sigma_s^2}{N_e} \quad (2.4-6)$$

where: n = the number of independent strength tests performed.

N_e = the equivalent number of independent soil elements within the assumed failure surface. This number is a function of the correlation coefficient of the soil and the area of the failure surface.

The evaluation and implications of this spatial variance is discussed in section (2.6).

2.5 Model Uncertainty. As pointed out in Chapter One, there are two main sources of uncertainty due to the selected method of analysis. The first is the uncertainty of the model (circular arc versus wedge) and the definition of safety factor. The second is the uncertainty due to sim-

plifying assumptions made both for the model and for the problem. This model uncertainty will be handled in these ways:

1. The probability model developed in this thesis is only considered valid for circular arc type failures. Wedge methods of analysis are excluded.
2. The safety of an embankment is defined in terms of safety margin instead of safety factor. This eliminates the problem of the location of the passive moment in safety factor definitions.
3. The bias correction factors used in this thesis are developed from case histories of embankment failures. The bias factor for strength will also include bias (and uncertainty) due to the method of analysis.

The corrected strength need not be the true in-situ strength. It is, however, the value of strength that makes the circular arc method of analysis work -- that is, predict a factor of safety equal to unity for a failed embankment.

2.6 Measurement of Resistance Uncertainty

Measuring the variability of the resisting moment requires evaluating the spatial uncertainty due to bias corrections, random testing errors, and soil variability. These sources of uncertainty will be discussed separately.

2.6.1 Uncertainty Due to Bias

The determination of the means and coefficients of variation of bias correction factors associated with different methods of testing (i.e., field vane and unconfined compression, among others) is difficult to determine. Although embankments are designed for a specific safety factor, the actual safety factor of a satisfactorily performing embankment is unknown. It is only when an embankment fails that the true safety factor is known.

For cases of embankment failures, the true shear strength can be back calculated by assuming the safety factor equal to unity. If soil tests are available at these sites, a bias term can be determined by relating the true strength to the measured strength. Such a bias term will include bias contributions from both testing inaccuracies and model limitations. When a sufficient number of independent bias terms have been developed for the same type strength test, an average or mean correction factor can be calculated. By calculating the coefficient of variation (V_b) about this mean with equation (2.2-3), the uncertainty in applying the mean correction factor is quantified. Such average correction factors have been developed for field vane tests and unconfined compression tests. These will be presented together with the case studies.

In developing a mean correction factor for a particular type of strength test, care must be taken as to the source of data. Ideally, correction factors should be obtained from test embankments purposely constructed to failure, with prior strength tests available. If the correction factors are obtained from embankments that were constructed to a reasonable safety factor based on prior strength information, but failed, an erroneous correction factor would be developed. If the strength test used for the design of the embankment is calibrated to the strength of the failed embankment, the correction factor will equal the inverse of the safety factor, neglecting the strength of the embankment. If the bias correction for a given embankment were greater than the inverse of the safety factor, the embankment would not fail and no data on the magnitude of the bias correction factor would be obtained.

The uncertainty due to only bias cannot be decreased by increasing the number of independent strength tests at an embankment site. Each individual test will be biased and the average of all tests will also be biased. The coefficient of variation of the correction factor data (correction factors obtained from a number of independent case studies of failures) about its mean value will be a measure of the uncertainty in applying that correction factor.

If the coefficient of variation of the bias correction is large and if a large number of tests is performed for a given embankment on a "homogeneous" foundation, the unreliability of the bias correction will probably be the dominant source of uncertainty. for this reason it seems essential that such correction factors should be updated whenever possible. This can be done by performing strength tests at sites of embankment failures after the failure has occurred. Each observed failure will result in another point for calibrating the different types of tests.

Although bias error cannot be eliminated by increased testing, it can be reduced by restricting the applicability of the bias correction. Attempts should be made to develop local correction factors and to evaluate their uncertainty. For similar type sampling and testing on the same type soil, the coefficients of variation of the correction factors should decrease. Such an effort to calibrate a test like the field vane at a local level will result in an increased reliability of that test for design.

2.6.2 Uncertainty Due to Random Testing Error.

This error term is needed to allow for the error in predicting the spatial average strength caused by limited soil testing. If all of the strength tests performed are far enough apart so that they can be considered uncorrelated and if the sum of random errors is expressed as:

$$E_R = \epsilon_{r_1} + \epsilon_{r_2} + \dots + \epsilon_{r_n} \quad (2.6-1)$$

with the mean and variance given below:

$$\bar{E}_R = n\bar{\epsilon}_r \quad (2.6-2a)$$

$$\sigma_{E_R}^2 = n\sigma_{\epsilon_r}^2 \quad (2.6-2b)$$

By defining $\langle \epsilon_r \rangle$ by:

$$\langle \epsilon_r \rangle = \frac{E_R}{n} \quad (2.6-3)$$

then the spatial mean and the spatial variance of random testing error becomes:

$$\langle \bar{\epsilon}_r \rangle = \bar{E}_R/n = n\bar{\epsilon}_r/n \quad (2.6-4a)$$

$$\langle \bar{\epsilon}_r \rangle = \bar{\epsilon}_r \quad (2.6-4b)$$

and

$$\sigma \langle \epsilon_r^2 \rangle = \frac{1}{n^2} \sigma_{E_R}^2 = \frac{n\sigma_{\epsilon_r}^2}{n^2} \quad (2.6-5a)$$

$$\sigma \langle \epsilon_r^2 \rangle = \frac{\sigma_{\epsilon_r}^2}{n} \quad (2.6-5b)$$

By taking the point variance due to random testing error equal to that of the measured strength, equation (2.5-5b)

becomes:

$$\sigma \langle \epsilon_r^2 \rangle = \frac{\sigma_s^2}{n} \quad (2.6-6)$$

The coefficient of variation of the spatial mean shear strength available is:

$$V\langle \epsilon_r \rangle = \frac{(\sigma^2 \langle \epsilon_r \rangle)^{1/2}}{\langle \bar{\epsilon}_r \rangle} = \left(\frac{\sigma^2}{n}\right)^{1/2} / \bar{\epsilon}_r \quad (2.6-7a)$$

$$V\langle \epsilon_r \rangle = \frac{V_s}{\sqrt{n}} \quad (2.6-7b)$$

The coefficients of variation of the spatial mean shear strength due to random testing error is proportional to the point coefficient of variation of the individual data about the mean and inversely proportional to the square root of the number of tests performed.

2.6.3 Uncertainty Due to Inherent Soil Variability

Even the most uniform soils have some heterogeneity of strength. The magnitude and rate of this natural variability affects the calculated failure probability of an earth embankment. What is needed is a measure of the uncertainty of encountering a zone of weak material, sufficiently large for a failure to occur or to adversely affect performance. Such a measure is the spatial variance due to soil variability ($\sigma^2 \langle s \rangle$). This spatial variance is a function of the point variance of the true strength, the correlation distance of the soil, and the area of the assumed failure surface.

It can be shown that the spatial variability of strength due to soil heterogeneity is related to its point

variance through "variance functions". First, consider the concept of one-dimensional variation of a soil property, e.g., the variation of strength with depth in a borehole. The spatial variance can be shown equal to

$$\sigma_{\langle s \rangle}^2 = \Gamma_{(h)}^2 \sigma_s^2 \quad (2.6-8)$$

where:

$\sigma_{\langle s \rangle}^2$ = the spatial variance of strength
due to soil variability

$\Gamma_{(h)}^2$ = the variance function

h = the length of the borehole considered

σ_s^2 = the point variance of strength

If the correlation coefficient of strength between two points varies as a function of the distance between points in the following way:

$$\rho_{s_1 s_2} = \rho(h) = e^{-(x_2 - x_1)^2 / \delta s^2} = e^{-h^2 / \delta s^2} \quad (2.5-9)$$

where:

δs = the correlation distance of the strength
of soil considered.

Then, the variance function will equal:

$$\Gamma_{(h)}^2 = \frac{\sqrt{\pi} \delta s^2}{h} \left\{ \frac{h}{\delta s} \phi\left(\frac{h}{\delta s}\right) + \frac{e^{-h^2 / \delta s^2} - 1}{\sqrt{\pi}} \right\} \quad (2.6-10)$$

where:

$\phi(x)$ = the "Error Function" = $\frac{2}{\sqrt{\pi}} \int_0^x e^{-u^2/2} du$

A plot of the variance function versus $h/\delta s$ are shown in Figure 2-6. The inverse of the variance function is defined as the equivalent number of independent soil elements (n_e).

$$n_e = \frac{1}{\Gamma^2(h)} \quad (2.6-11)$$

If h is much larger than the correlation distance, Γ^2 reduces to:

$$\Gamma^2(h) = \frac{\sqrt{\pi} \delta s}{h} = \frac{1}{n_e} \quad (2.6-12)$$

If h is much smaller than the correlation distance, $\Gamma^2(h)$ equals unity. This implies that the points within the length h are fully correlated and that the spatial variance is equal to the point variance.

The concept of two dimensional spatial variance of strength over a rectangular area can also be related to the point variance through variance functions. The two-dimensional variance function is equalled to the product of the orthogonal variance functions of the two lengths of the rectangle (h, ℓ). The spatial variance can be expressed as:

$$\sigma^2 \langle s \rangle = \Gamma^2(h, \ell) \sigma_s^2 \quad (2.6-13a)$$

$$\sigma^2 \langle s \rangle = \Gamma^2(h) \Gamma^2(\ell) \sigma_s^2 \quad (2.6-13b)$$

where $\Gamma^2(h)$ and $\Gamma^2(\ell)$ are the variance functions in the h and ℓ directions, respectively. Again, if h and ℓ are much larger than the correlation distances in their respective directions, (δs_h and δs_ℓ), then:

$$\Gamma^2(h, \rho) = \frac{\pi \delta s_h \delta s_\rho}{\rho h} \quad (2.6-14)$$

and:

$$n_e = \frac{\rho h}{\pi \delta s_h \delta s_\rho} \quad (2.6-15)$$

The concept of one and two dimensional strength variability due to soil heterogeneity is illustrated in Figure 2-7.

The equivalent number of independent soil elements in a rectangular area of soil is proportional to the area of the rectangle and inversely proportional to the product of the orthogonal correlation distances. This relationship implies that as the correlation of strength increases, the likelihood of encountering a large, uniformly weak zone of soil also increases. But as the area of the rectangle increases, the likelihood of such a weak zone existing over the whole rectangle decreases.

A simplified approach to estimating the equivalent number of independent soil elements in an assumed failure plane (3-dimensional) begins with an idealization of the failure plane. Such an idealization allows one to deal with the three principal correlation distances in a straight forward manner. The failure plane is modeled as a series of rectangular surfaces as shown in Figure 2-8. Considering the cross sectional view, the length of the failure surface and the depth of the failure are preserved. The length in the third dimension, or length of embankment

along the centerline, is selected as three times the base width, B. This serves as a crude estimate of the third dimension to satisfy the plane strain assumption of the analysis.

The surface areas in the three principal planes are then combined into three rectangular areas. The equivalent number of independent elements is calculated for each area by the equations presented in the previous section. The sum of these calculated elements is an approximation of the number of independent soil elements for a three-dimensional failure plane (N_e). By determining the point variance of strength, the spatial variance will be equalled to:

$$\sigma^2_{\langle s \rangle} = \frac{\sigma_s^2}{N_e} \quad (2.6-16a)$$

with a spatial coefficient of variation equal to:

$$V_{\langle s \rangle} = \frac{V_s^2}{\sqrt{N_e}} \quad (2.6-16b)$$

2.6.4 Combined Uncertainty

The variances of bias correction, random error, and soil variability can be added together to give the total variance in the prediction of strength:

$$\text{VAR}[\langle s \rangle_{\text{meas}}] = \sigma^2_{\langle \epsilon_b \rangle} + \sigma^2_{\langle \epsilon_r \rangle} + \sigma^2_{\langle s \rangle} \quad (2.6-17a)$$

or:

$$\text{VAR}[\langle s \rangle_{\text{meas}}] = \sigma^2 \epsilon_b + \frac{\sigma_s^2}{n} + \frac{\sigma_s^2}{N_e} \quad (2.6-17b)$$

The spatial coefficients of variation of the bias correction factor, random error, and inherent soil variability can be combined by taking the square root of the sum of the squares of the individual coefficient of variation:

$$V\langle S \rangle = (Vb^2 + \frac{Vs^2}{n} + \frac{Vs^2}{N_e})^{1/2} \quad (2.6-18)$$

where:

$V\langle S \rangle$ is the spatial coefficient of variation of strength.

This is a measure of uncertainty equal to the uncertainty in the resisting moment for the case of an embankment on a homogeneous foundation.

2.7 Probability Model for Layered Foundations

Extending the general probability model to handle layered soils introduces a second aspect of soil variability into the problem. That is the variability in the thickness of the different layers encountered through subsurface exploration. The thickness of a layer of soil is measured by a direct observation of samples from boreholes. This type of measurement is assumed to be unbiased and free from random error. The spatial variance of a layer thickness ($\sigma^2_{\langle t \rangle}$) is a function of the point variance of layer

thickness, (σ^2_t) , and the correlation distance of layer thickness, and the assumed area of an embankment failure.

The point variance can be obtained by calculating the variance of observed thicknesses from a series of boreholes. The point variance will give an indication as to what degree the layer thickness will vary along the length of an embankment. The spatial variance of layer thickness also can be related to the point variance through variance functions:

$$\sigma^2_{\langle t \rangle} = \Gamma^2(\ell)\Gamma^2(w)\sigma^2_t = \frac{\sigma^2_t}{N_e} \quad (2.7-1)$$

where:

$$N_e = \frac{1}{\Gamma^2(\ell)\Gamma^2(w)}$$

ℓ = the length of the layer parallel to the embankment centerline included in the assumed failure surface;

w = the width of the layer contained within the assumed failure arc.

$\Gamma^2(\ell), \Gamma^2(w)$ = the horizontal variance functions parallel to and perpendicular to the embankment centerline, respectively,

N_e = the equivalent number of independent layer thicknesses within an assumed failure plane.

These variance functions will be assumed to be of the form:

$$\Gamma^2_{(\ell)} = \frac{\sqrt{\pi} \delta T_{\ell}^2}{\ell} \left\{ \frac{\ell}{\delta T_r} \phi \left(\frac{\ell}{\delta T_r} \right) + \frac{e^{-\ell^2 / \delta T_r^2} - 1}{\sqrt{\pi}} \right\} \quad (2.7-2a)$$

$$\Gamma^2_{(w)} = \frac{\sqrt{\pi} \delta T_w^2}{w} \left\{ \frac{w}{\delta T_w} \phi \left(\frac{w}{\delta T_w} \right) + \frac{e^{-w^2 / \delta T_w^2} - 1}{\sqrt{\pi}} \right\} \quad (2.7-2b)$$

where:

δT_{ℓ} , δT_w are the correlation distances of layer thickness parallel to and perpendicular to the embankment centerline, respectively.

As the ratio of $(\frac{\delta T_w}{w})$ and $(\frac{\delta T_{\ell}}{\ell})$ becomes large, $\Gamma^2_{(w)}$ and $\Gamma^2_{(\ell)}$ approaches unity and the spatial variance approaches the point variance as a limit.

As the ratios become small:

$$\Gamma^2_{(w)} = \frac{\sqrt{\pi} \delta T_w}{w} \quad (2.7-3a)$$

$$\Gamma^2_{(\ell)} = \frac{\sqrt{\pi} \delta T_{\ell}}{\ell} \quad (2.7-3b)$$

With the spatial variance of layer thickness expressed as:

$$\sigma^2_{\langle t \rangle} = \Gamma^2_{(\ell)} \Gamma^2_{(w)} \sigma^2_t = \frac{\sigma^2_t}{N_e} \quad (2.7-4)$$

the spatial coefficient of variation of layer thickness becomes:

$$V_{\langle t \rangle} = V_T / \sqrt{N_e} \quad (2.7-5)$$

The implication of spatial variability of layer thickness are illustrated in Figure 2-9. Both embankment foundation A and B contain a layer of weak soil. The mean

layer thickness and the point coefficient of variation of layer thickness are the same for both cases. The correlation distances for case A are much greater than those for case B. The extent of the assumed failure surface is also shown in Figure 2-9. For case A, the spatial coefficient of variation will be approximately equalled to the point coefficient of variation. For case B, the spatial coefficient of variation will approach zero.

These results are reasonable. As the correlation distances increase or as the area of the failure decreases, the probability of encountering a thick, weak layer over the entire failure area increases. As the correlation distances of layer thickness decreases or as the area of the failure increases, the chances of encountering such a thick weak layer over the entire failure area decreases. If the layer thickness fluctuates rapidly compared to the failure area, an averaging effect takes place.

Once the spatial coefficient of variation of soil strength and layer thickness are measured, the coefficient of variation of the resisting moment can be determined. Based on the section in Figure 2-10, the mean resisting moment of a failure arc passing through n layers of soil is:

$$\bar{M}_R = r \sum_i \bar{\ell}_i \bar{s}_i \quad (2.7-6)$$

The variance of the resisting moment depends on the variances of and the correlations among the products, $\ell_i s_i$. Assuming that strength and length are both perfectly correlated within the i^{th} layer (which would be reasonable if the horizontal correlation distances are relatively large) and that they are both uncorrelated from layer to layer, the variance of the resisting moment can be expressed as:

$$\sigma_{M_R}^2 = \sum (V\langle t_i \rangle^2 + V\langle s_i \rangle^2) (\bar{\ell}_i^2 \bar{s}_i^2) + 2\sum (V\langle t_i \rangle^2 + V\langle s_i \rangle^2)^{\frac{1}{2}} \cdot \bar{\ell}_i \bar{s}_i \quad (2.7-7)$$

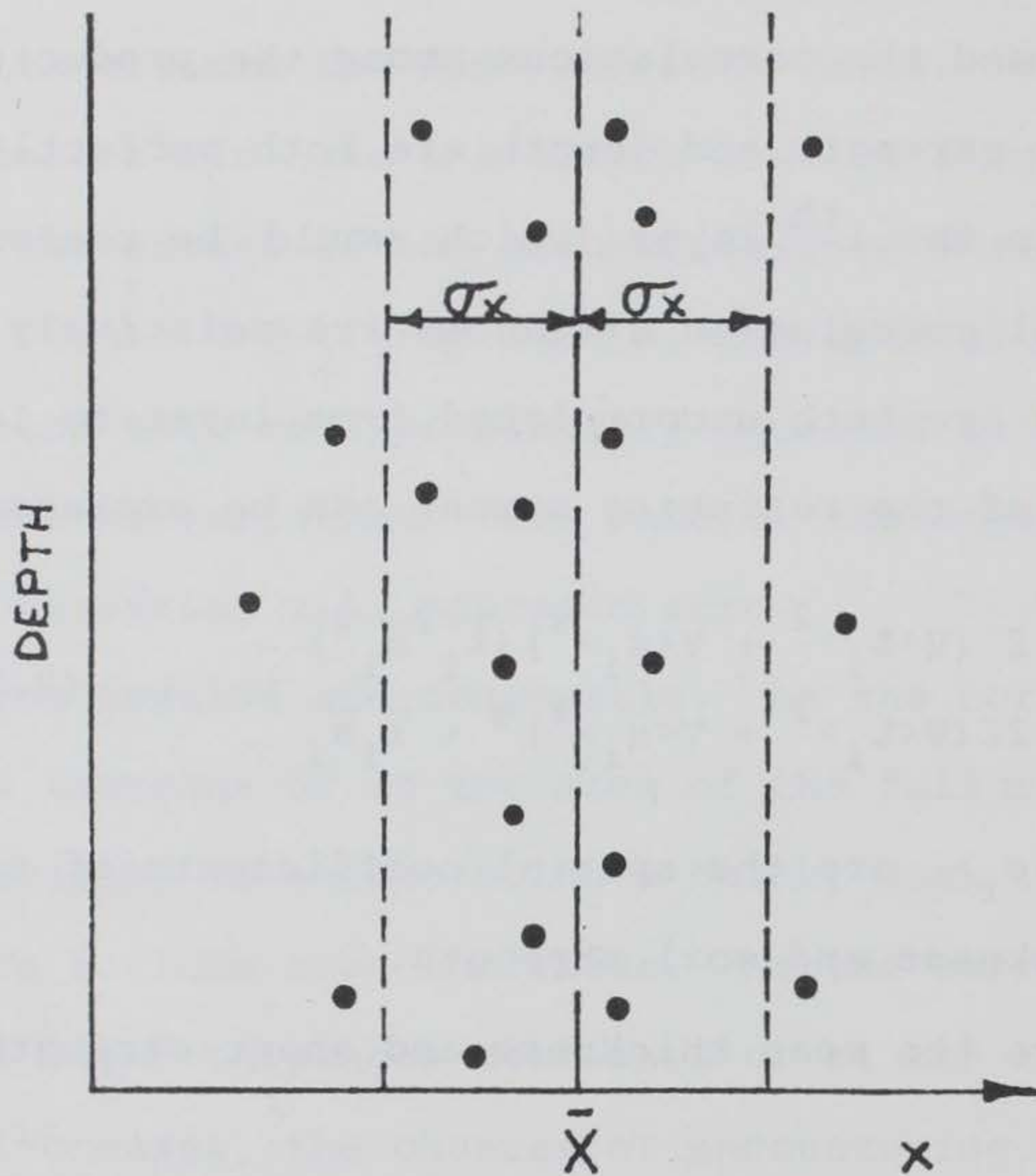
$V\langle \ell_i \rangle$ and $V\langle s_i \rangle$ are the spatial coefficients of variation of layer thickness and soil strength.

$\bar{\ell}_i$ and \bar{s}_i are the mean thickness and shear strength of the i^{th} layer.

The coefficient of variation of the resisting moment is obtained by dividing both sides of equation (2.7-7) by the mean resisting moment squared, or:

$$VM_R = \sum (V\langle t_i \rangle^2 + V\langle s_i \rangle^2) \frac{(\bar{\ell}_i^2 \bar{s}_i^2)}{(\sum \bar{\ell}_i \bar{s}_i)^2} + 2\sum (V\langle t_i \rangle^2 + V\langle s_i \rangle^2)^{\frac{1}{2}} \cdot \frac{(\bar{\ell}_i \bar{s}_i)}{(\sum \bar{\ell}_i \bar{s}_i)^2} \quad (2.7-8)$$

The derivation of this equation is presented in Appendix A .



$$\bar{X} = \text{MEAN} = \sum x_i / n$$

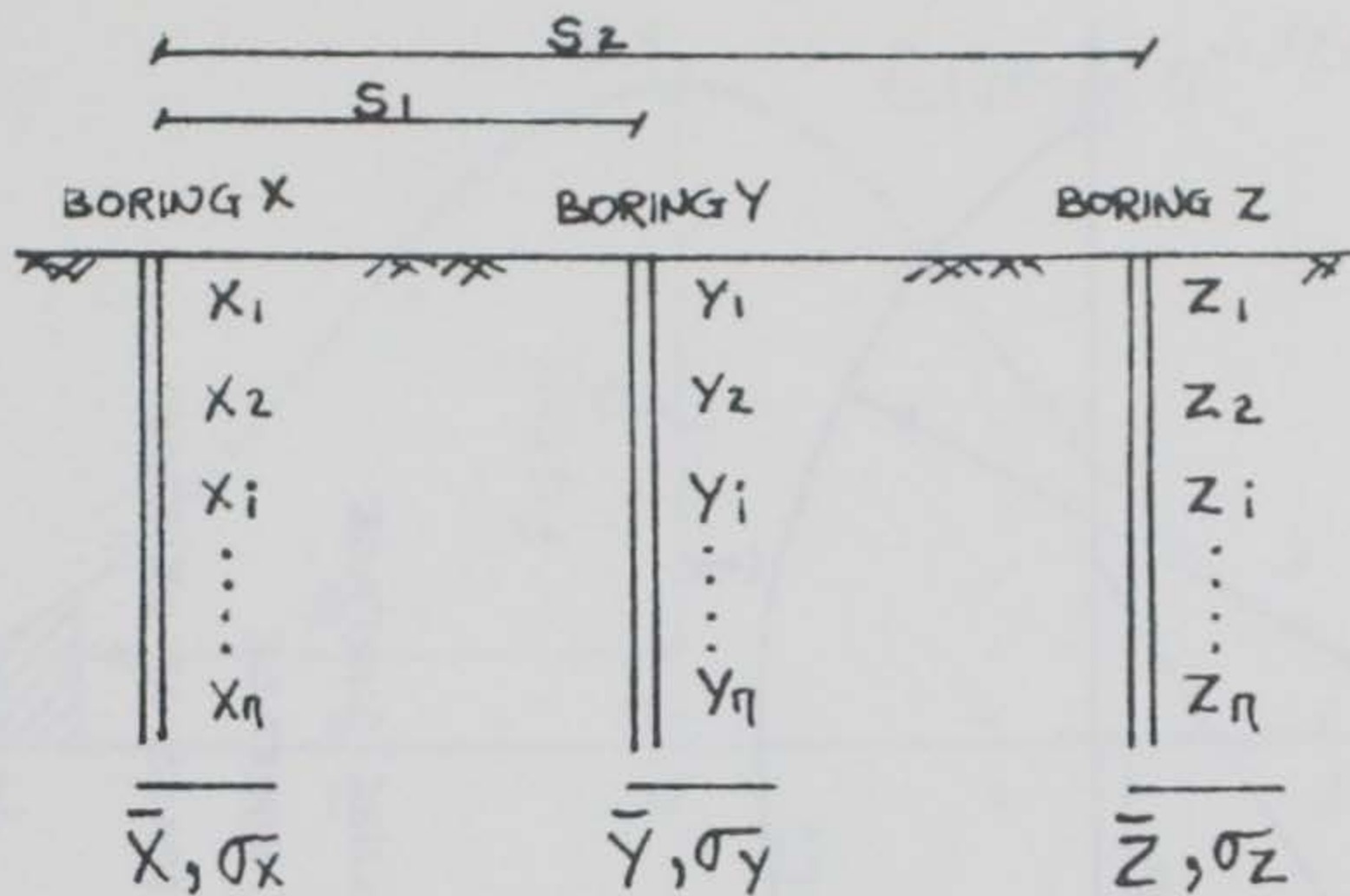
$$\sigma_x^2 = \text{VARIANCE} = \sum (x_i - \bar{x})^2 / n$$

$$\sigma_x = \text{STANDARD DEVIATION} = \sqrt{\sigma_x^2}$$

$$V_x = \text{COEFFICIENT OF VARIATION} = \sigma_x / \bar{x}$$

BASIC STATISTICAL TERMS

FIGURE 2-1

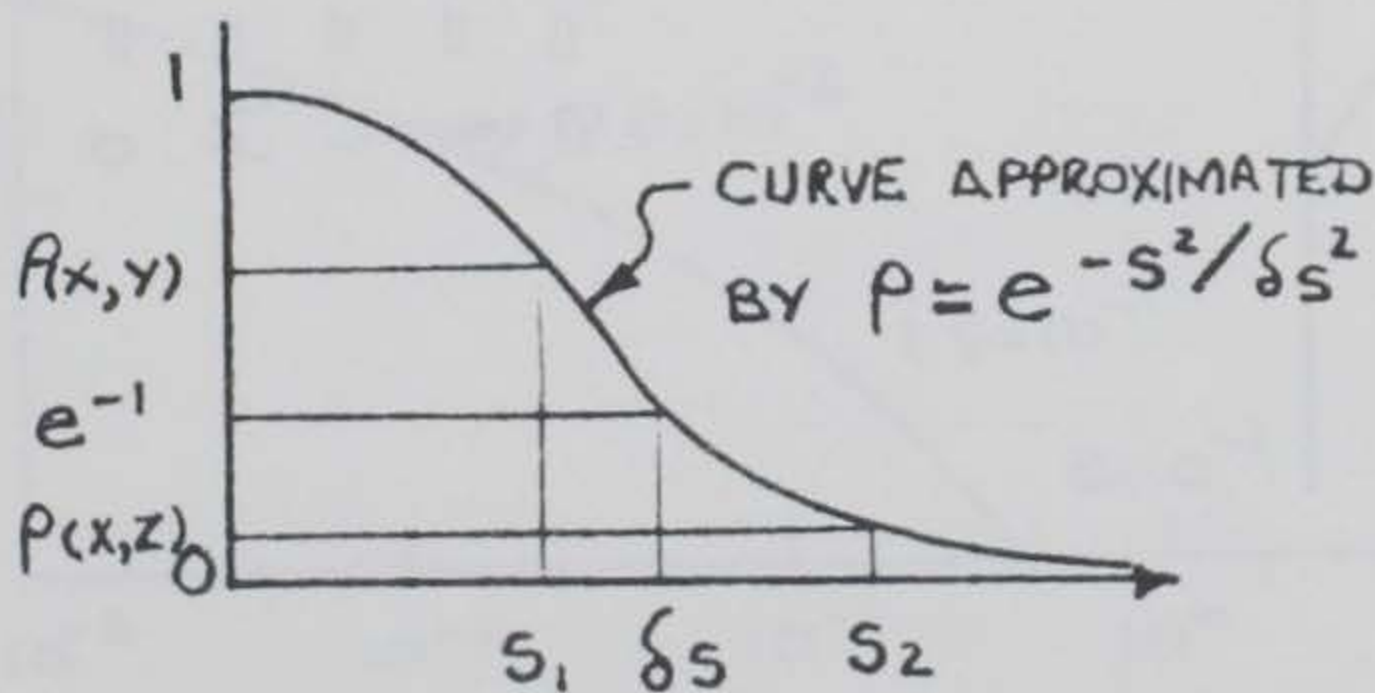


$$\text{COV}(X, Y) = \frac{1}{n} \sum (x_i - \bar{X})(y_i - \bar{Y}) = \text{COVARIANCE OF X AND Y}$$

$$\rho(X, Y) = \text{COV}(X, Y) / \sigma_X \sigma_Y = \text{CORRELATION COEFFICIENT}$$

$$\text{COV}(X, Z) = \frac{1}{n} \sum (x_i - \bar{X})(z_i - \bar{Z})$$

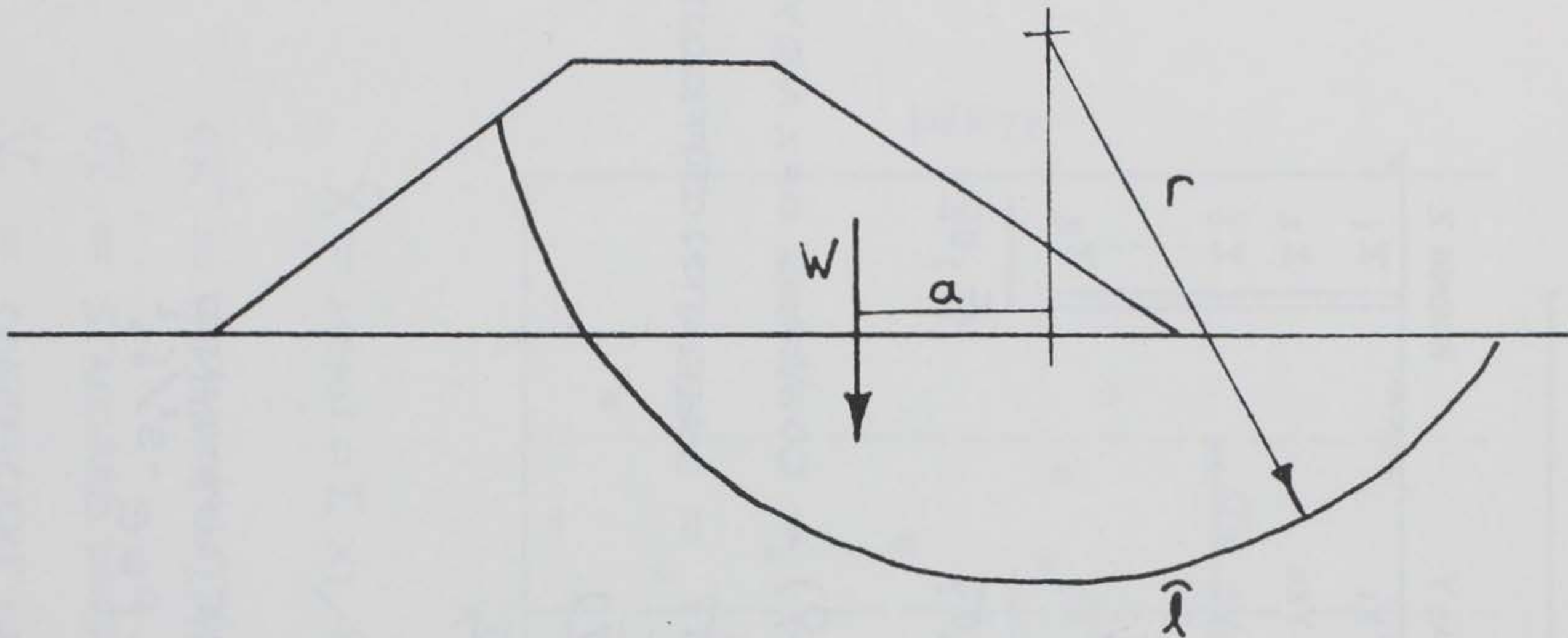
$$\rho(X, Z) = \text{COV}(X, Z) / \sigma_X \sigma_Z$$



$$\delta_s = s \text{ AT } e^{-1} = \text{CORRELATION DISTANCE}$$

COVARIANCE, CORRELATION COEFFICIENT
AND CORRELATION DISTANCE

FIGURE 2-2



S = SHEAR STRENGTH OF SOIL

\hat{l} = ARC LENGTH OF ASSUMED FAILURE SURFACE

r = RADIUS OF ASSUMED FAILURE SURFACE

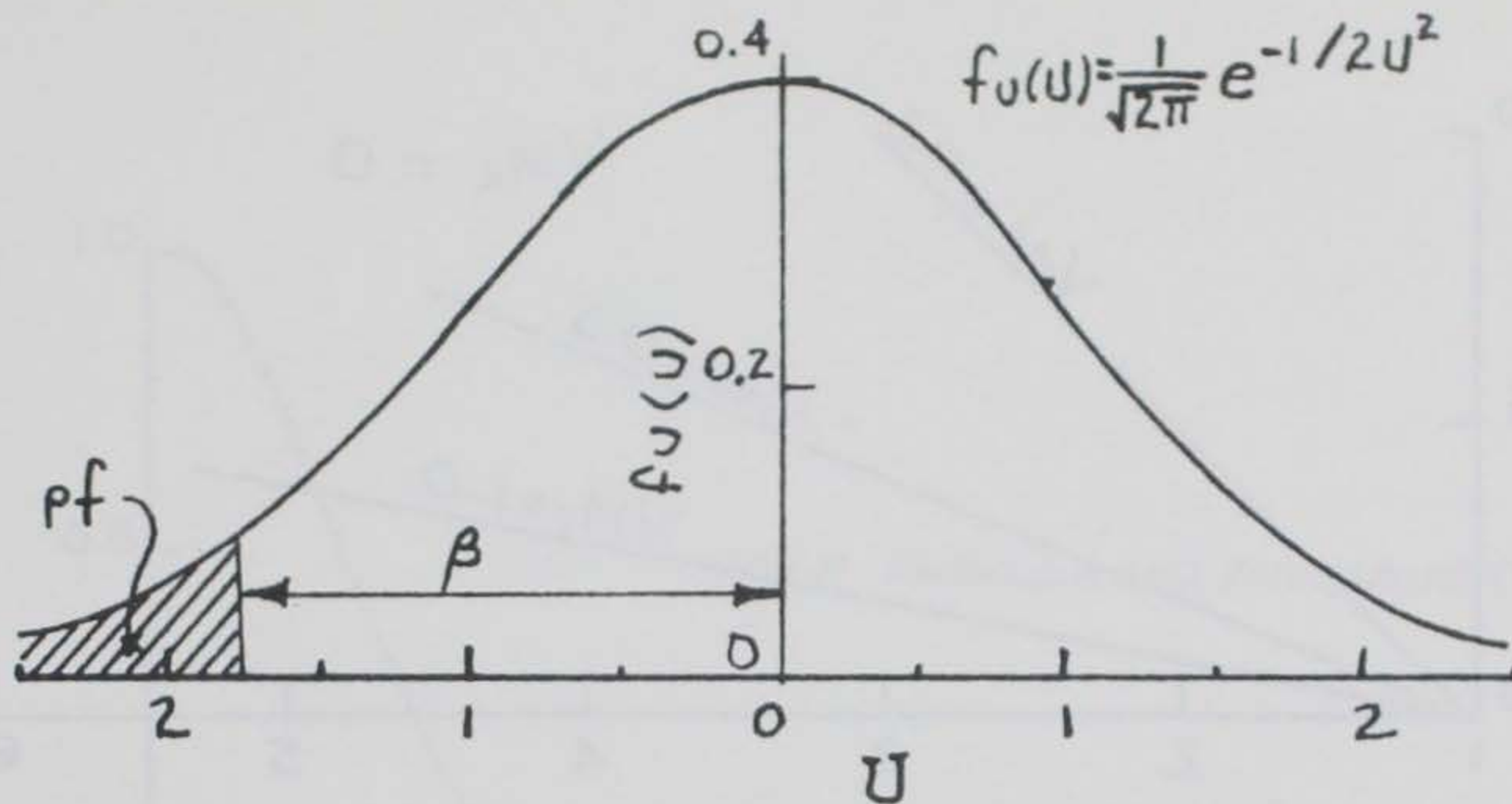
W = WEIGHT OF ASSUMED FAILURE MASS AT CENTROID

a = MOMENT ARM

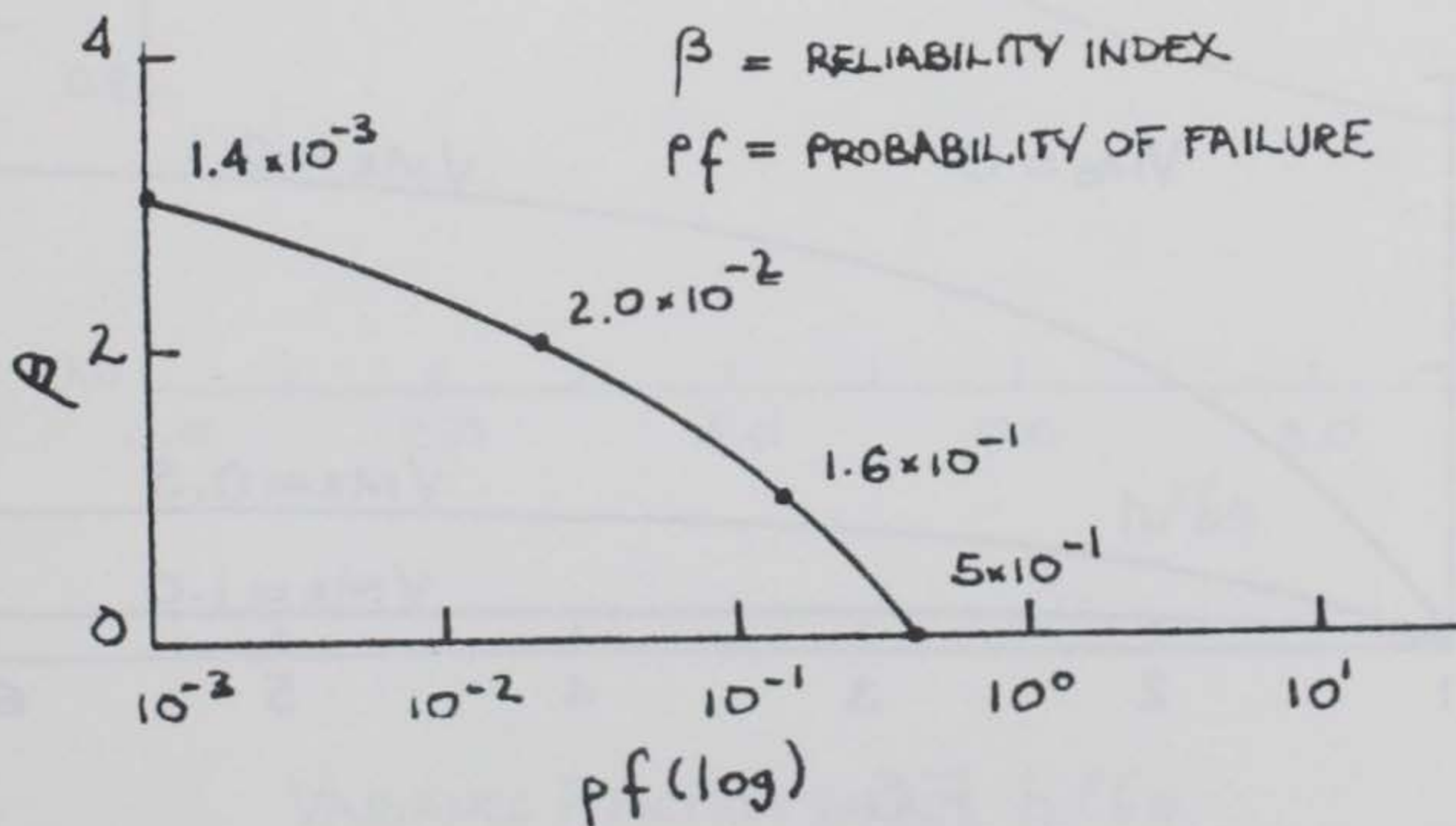
$$FS = \text{SAFETY FACTOR} = \frac{S \hat{l} r}{W a} = \frac{M_R}{M_o}$$

DEFINITION OF SAFETY FACTOR
CIRCULAR ARC ANALYSIS

FIGURE 2-3



STANDARDIZED NORMAL DISTRIBUTION



β vs pf

STANDARDIZED NORMAL DISTRIBUTION AND β vs pf

FIGURE 2-4

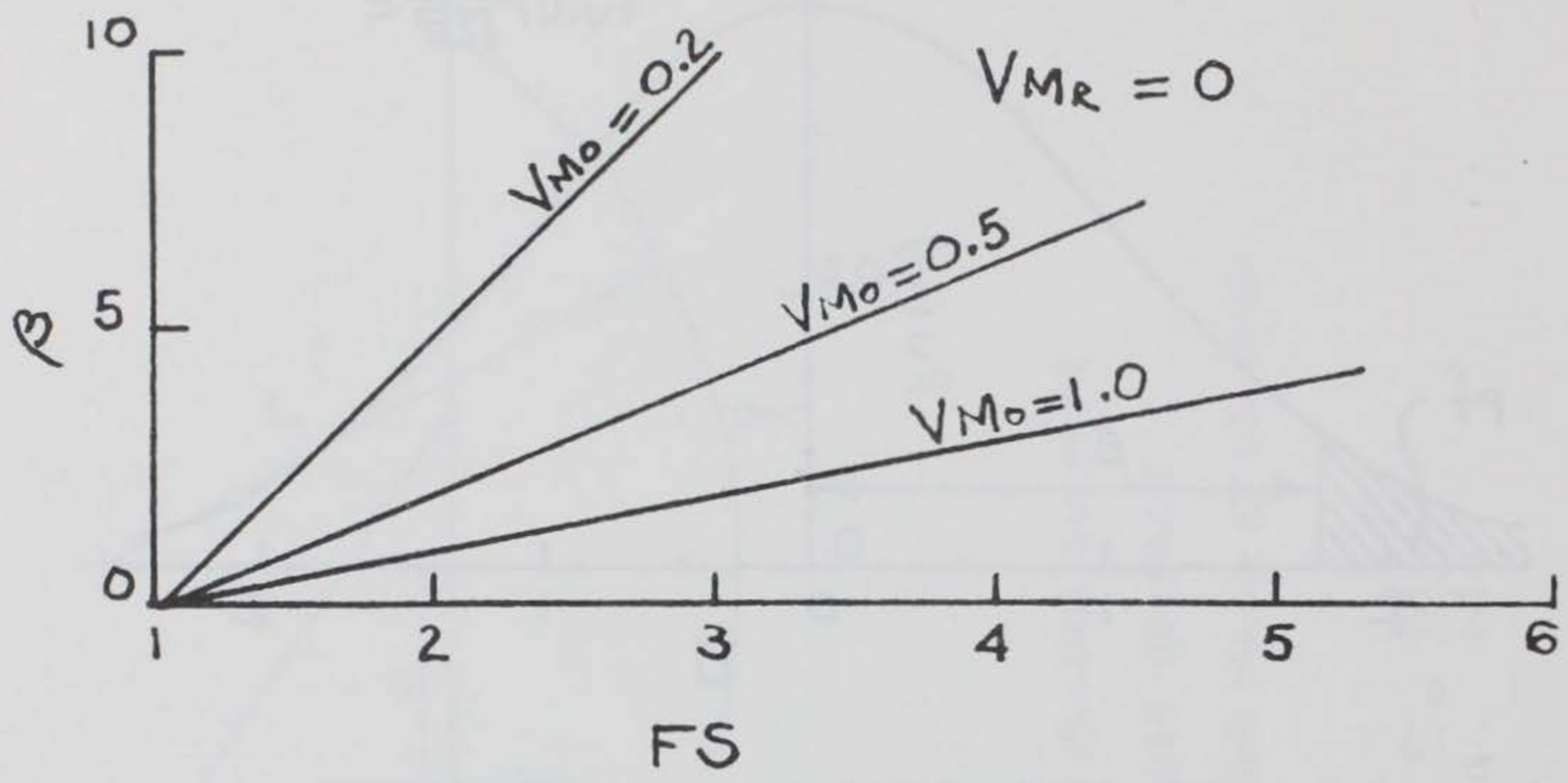


FIGURE 5a β vs FS - $V_{MR} = 0$

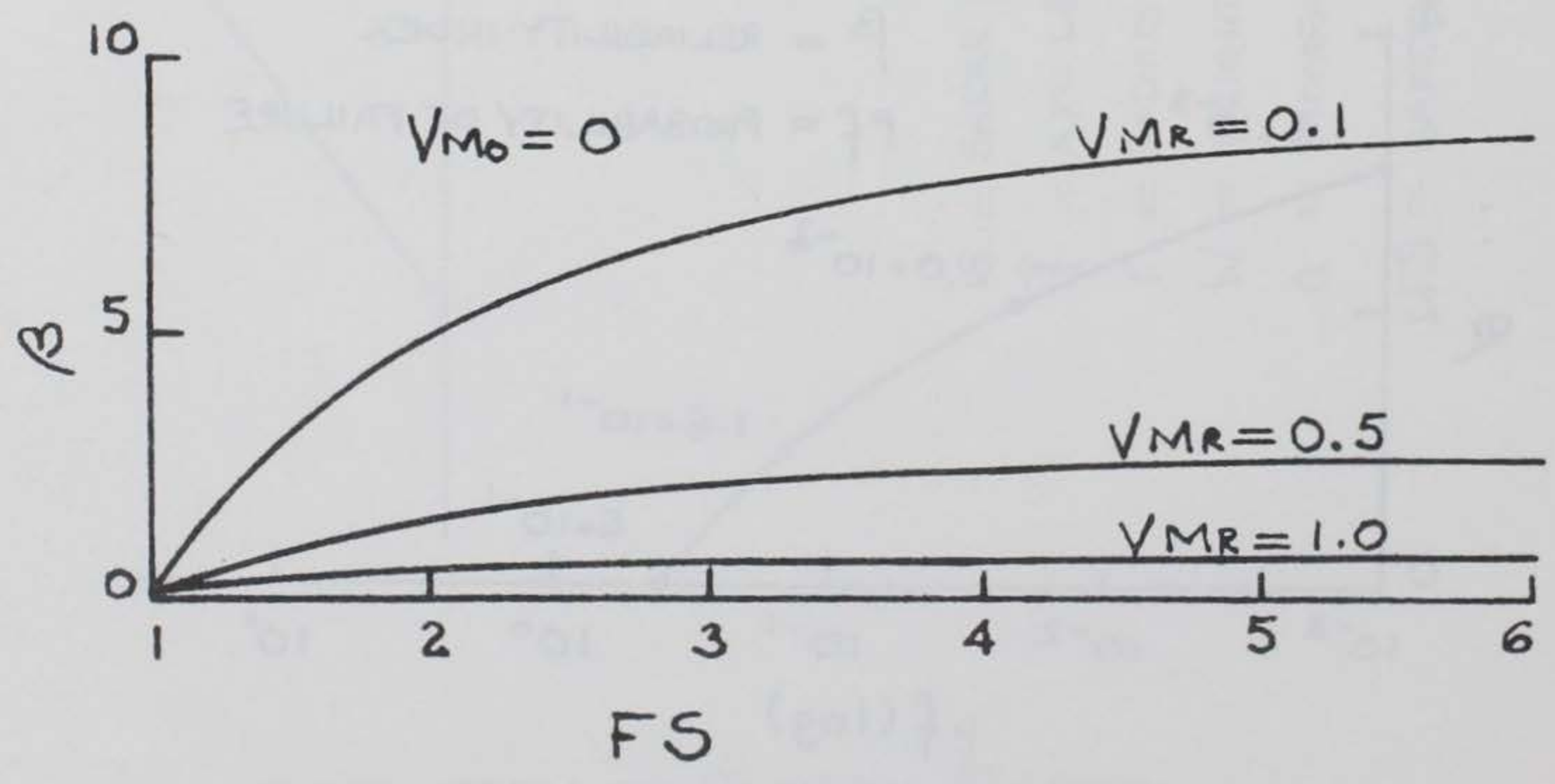
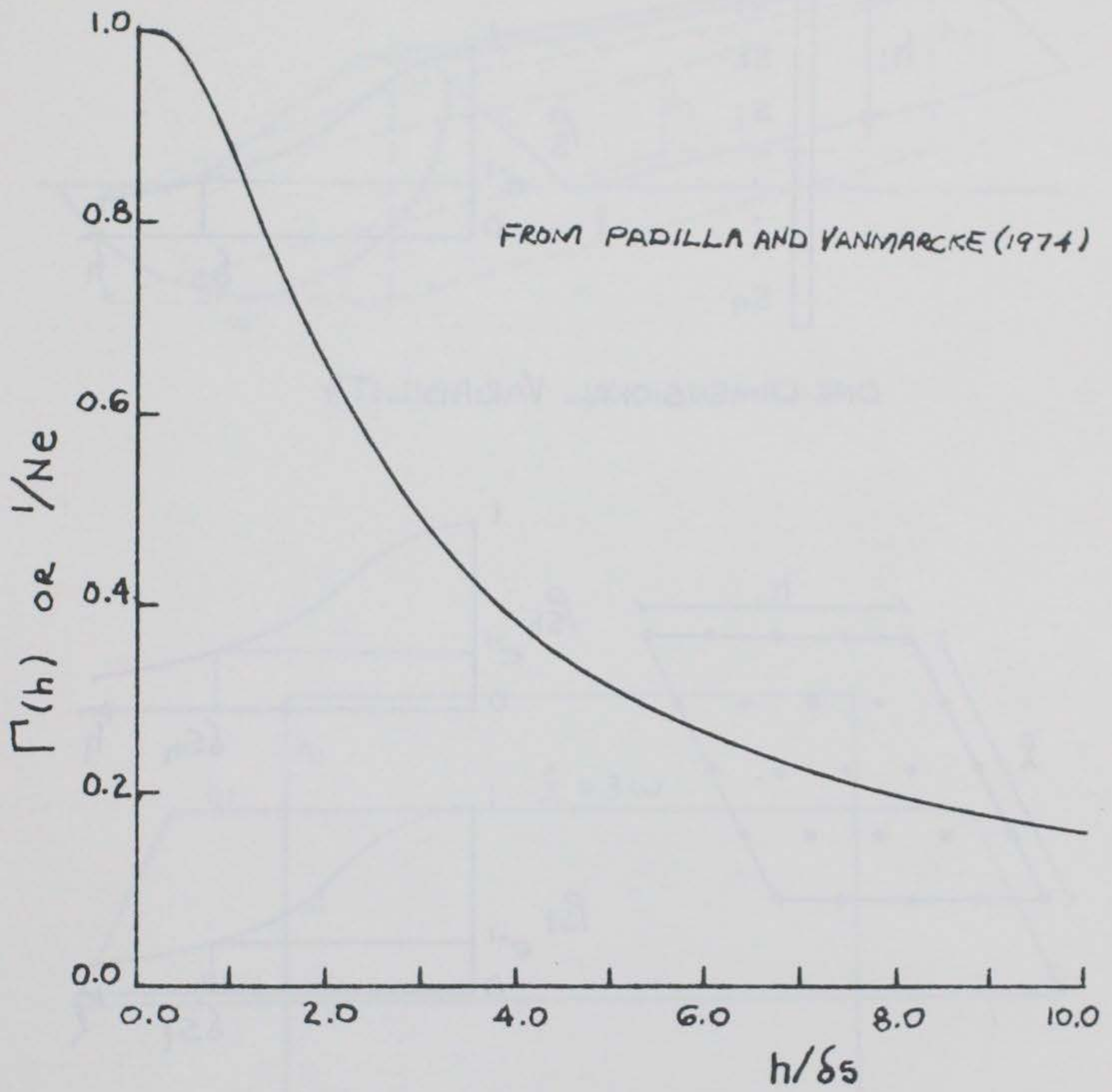


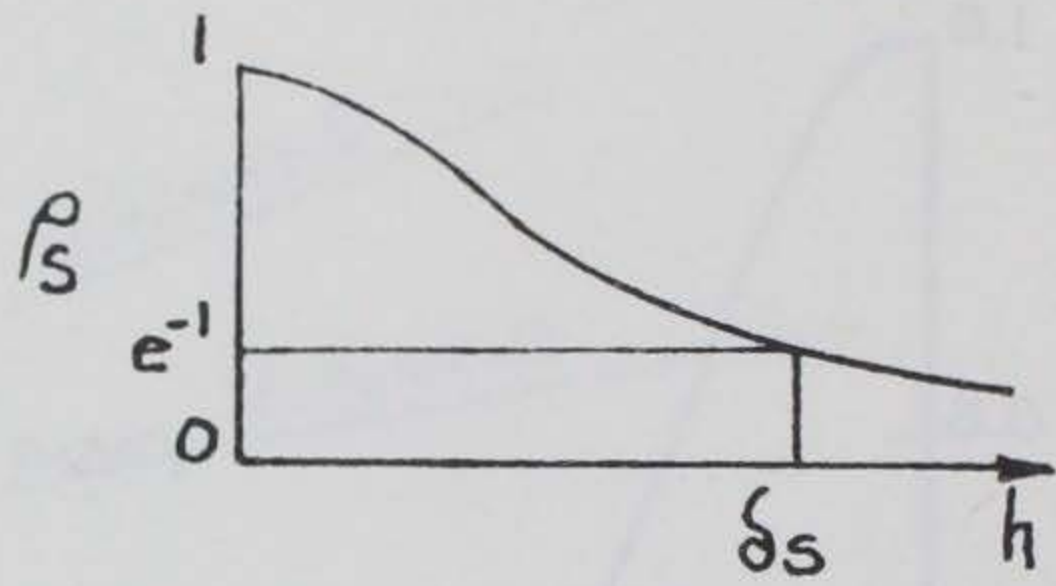
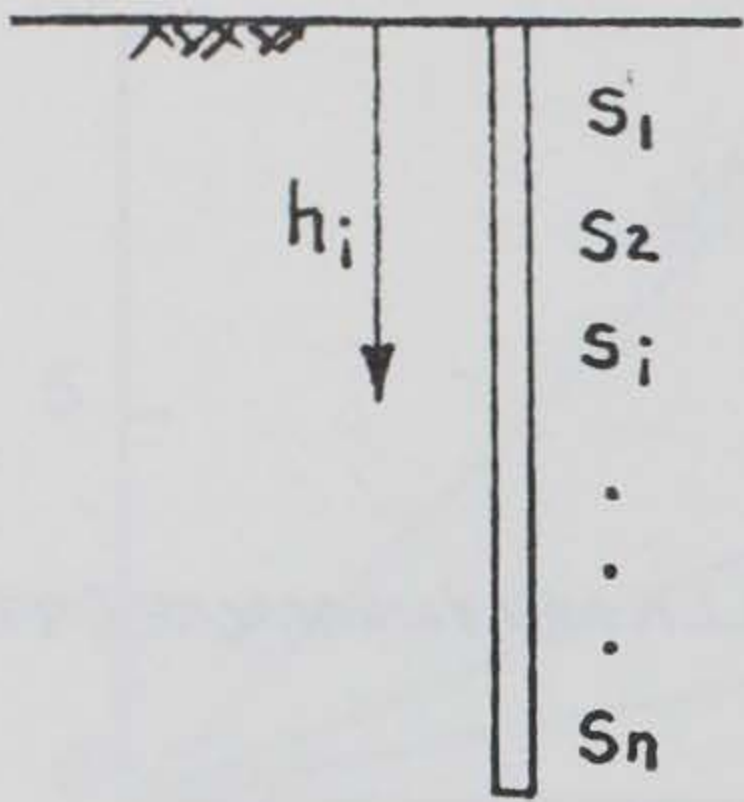
FIGURE 5b β vs FS - $V_{Mo} = 0$

RELIABILITY INDEX vs SAFETY FACTOR

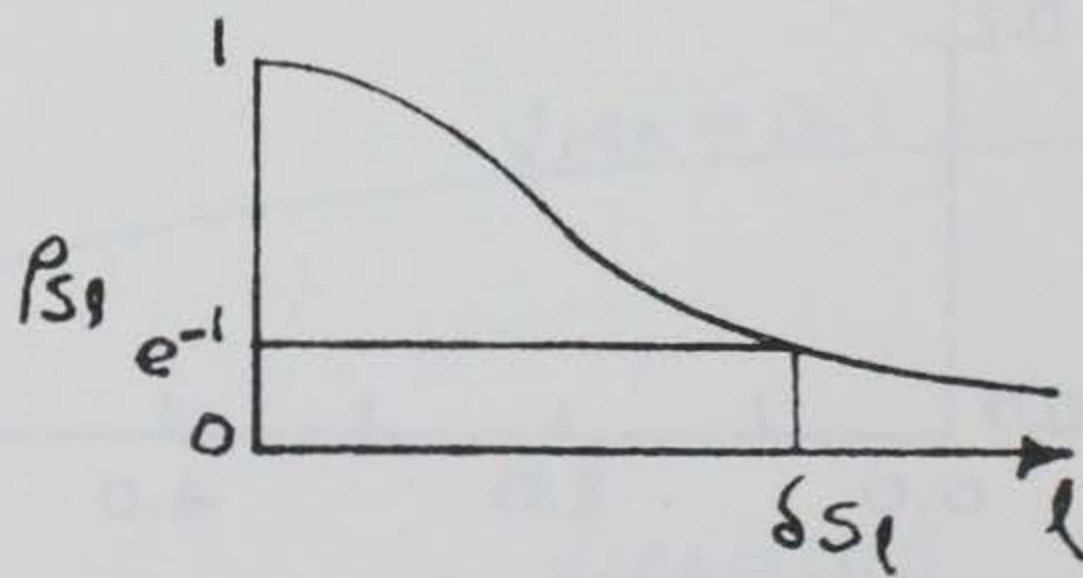
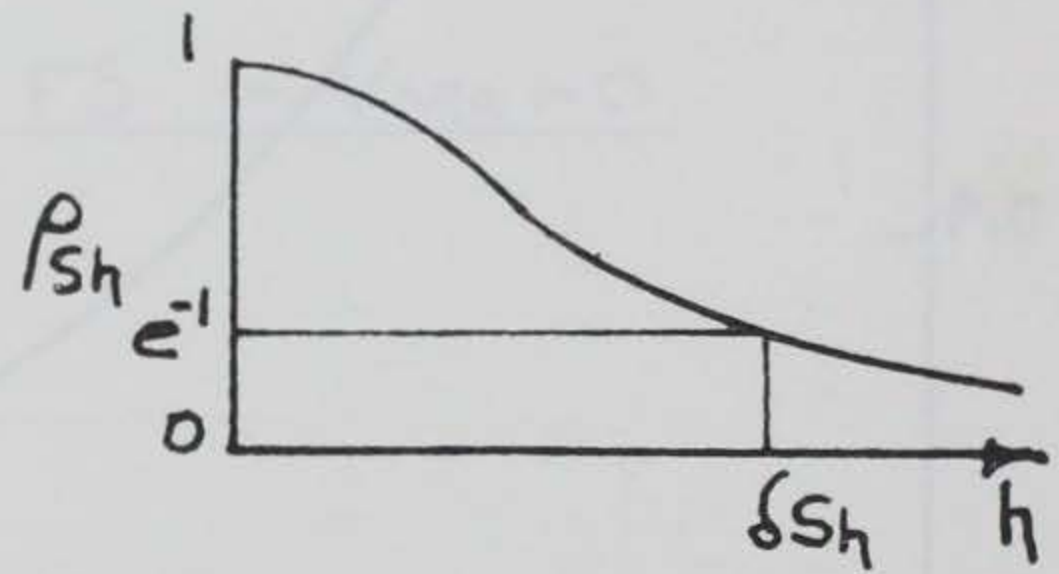
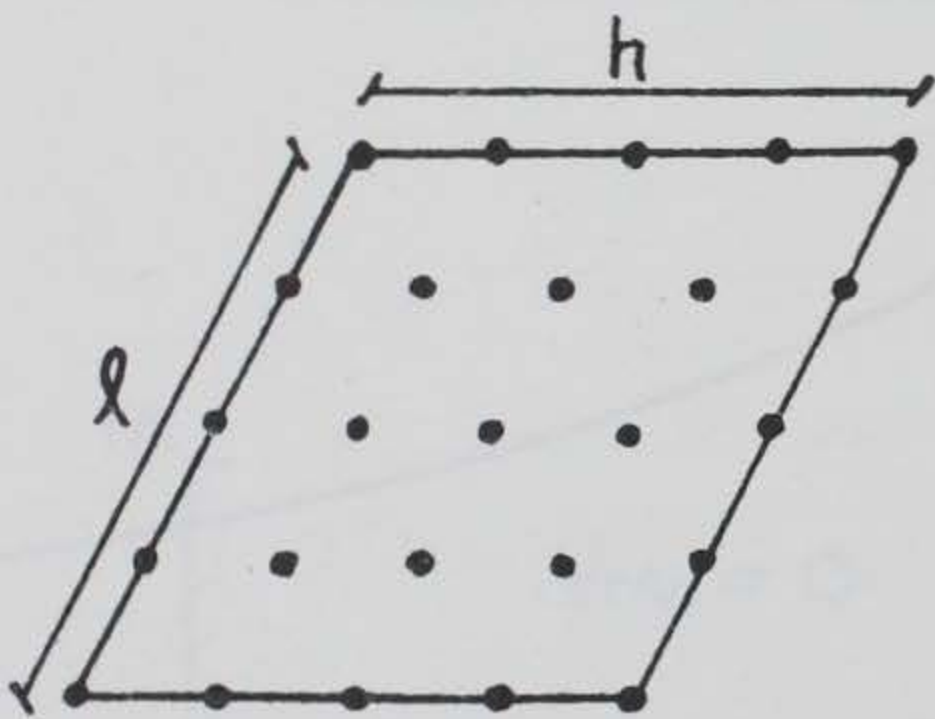


VARIANCE FUNCTION VERSUS h/δ_s

FIGURE 2-6

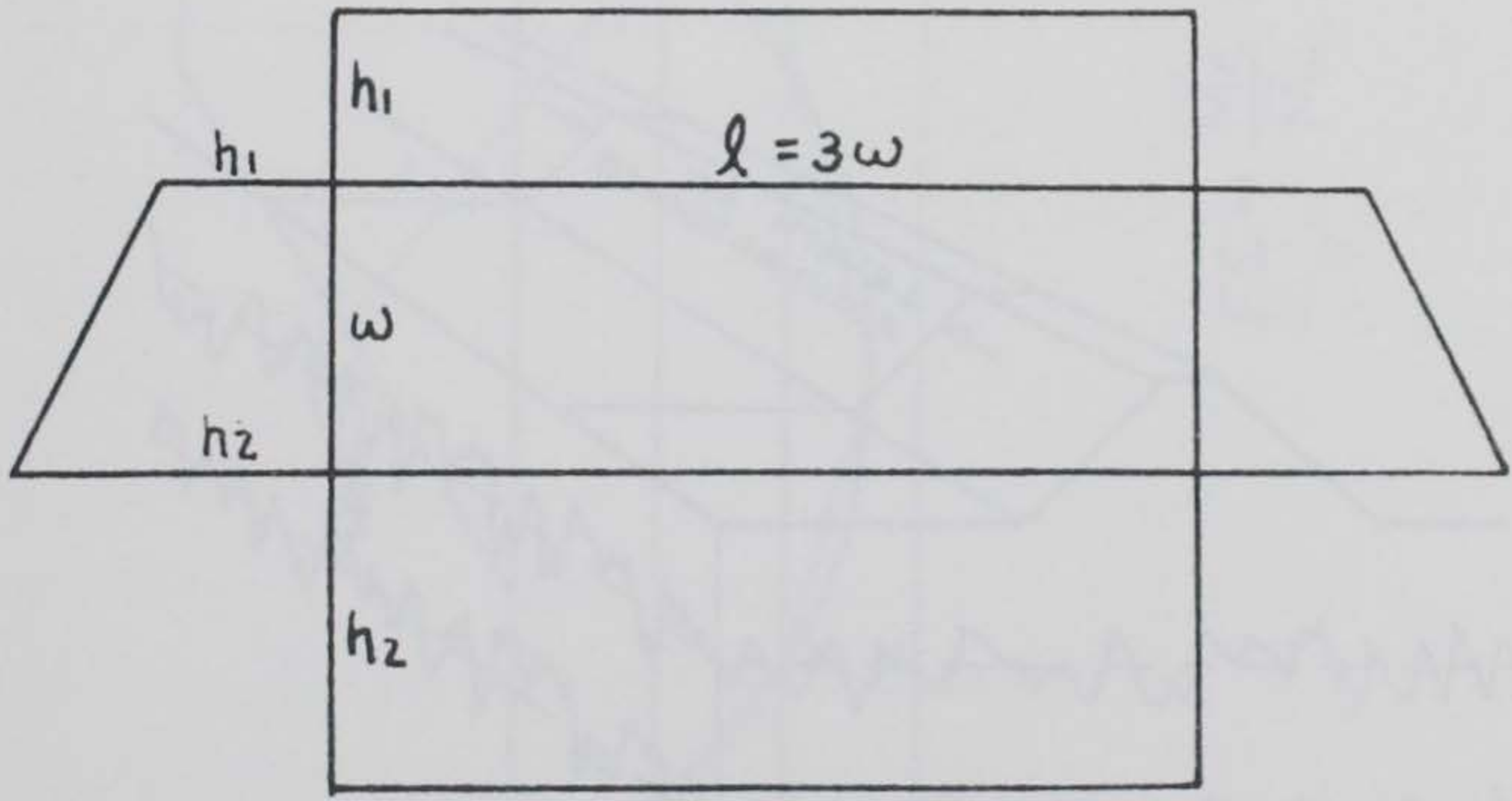
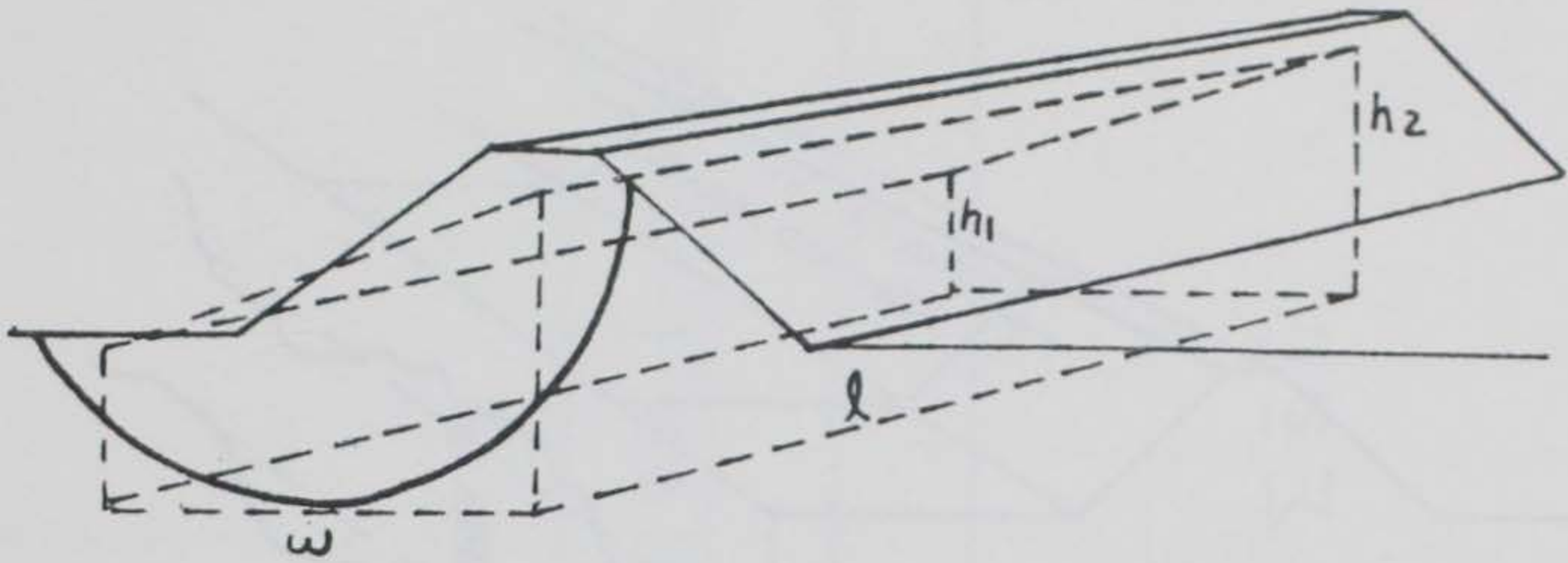


ONE DIMENSIONAL VARIABILITY

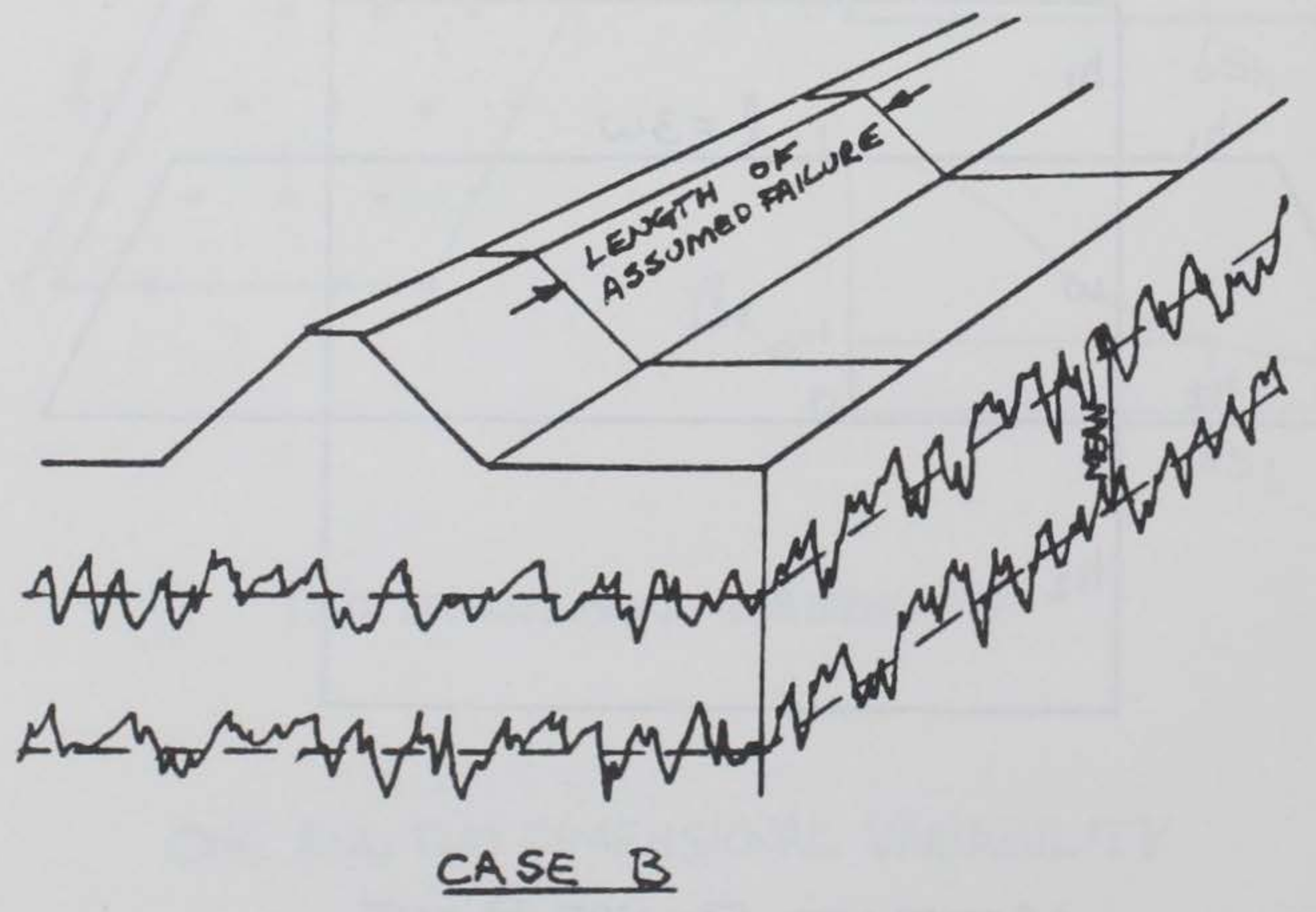
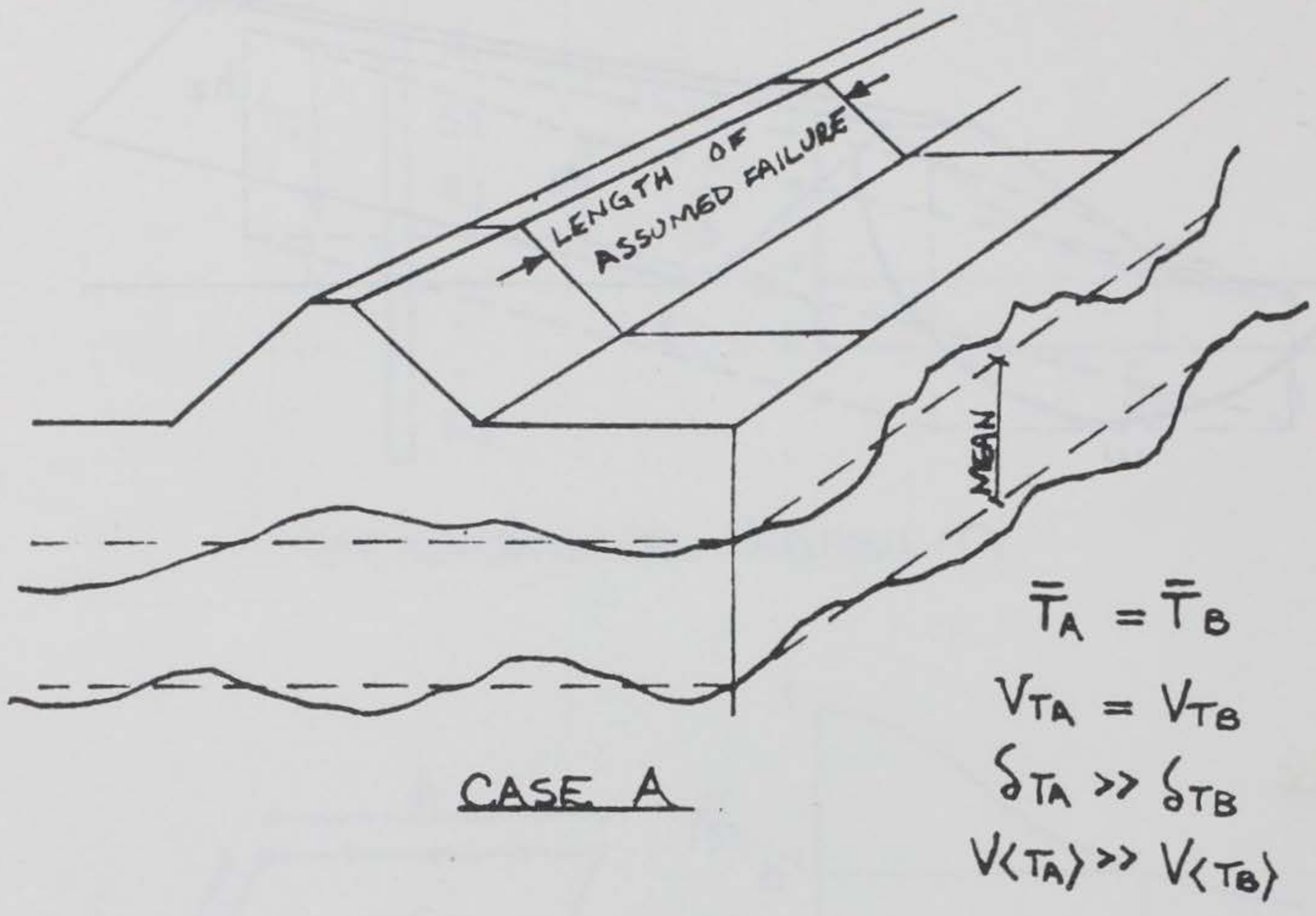


TWO DIMENSIONAL VARIABILITY

ONE AND TWO DIMENSIONAL VARIABILITY



MODELLED FAILURE PLANE



SPATIAL VARIABILITY OF LAYER THICKNESS

FIGURE 2-9

Chapter 3 Case Studies

3.1 General

The application of the probability model presented in the previous chapter is illustrated with two examples. In this chapter, a probabalistic analysis is made for two different embankment case studies. The results obtained from the probabalistic analysis are compared to those from a conventional stability analysis.

3.2 Fore River Test Section

3.2.1 Conventicral Analysis

The embankment analyzed in this chapter was a test section constructed for the Maine State Highway Commission. The Fore River Test Section (FRT) was designed in order to evaluate the efficiency of sand drains for the proposed I-295 highway (Haley and Aldrich, 1967). A plan map for this test section is shown in Figure 3-1.

The 240 foot square test section was constructed at Portland, Maine, over a tidal mud flat. The natural ground surface at the site of the test section was approximately horizontal and at El. -3 feet, msl. The first phase of construction required placing granular fill to the section shown on Figure 3-2.

Sand drains then were to be installed through the

first phase of construction into the foundation clay. This was to be followed by additional granular fill to El. +20 ft. However, shortly after construction of the first lift, an undrained shear failure occurred on the North slope of the test section.

The foundation for the test section consisted of a layer of soft gray organic silty clay with shells, sand lenses and pockets, and wood chips. This clay layer extended to El. -30ft, where silty sand and gravel was encountered.

The underlying sand deposit had a 5 foot artesian head. The top of the sand was considered to be the limiting depth of failure.

The organic clay was tested both before and after the slide occurred. Before the failure, a number of borings were made and field vane tests were performed. Four undisturbed borings also were made with undisturbed samples taken at regular intervals. Laboratory testing of these samples included visual classification, moisture content determination, Atterberg limits, and unconfined compression strength tests (UC).

Within two weeks after the slide occurred, six additional borings were made through the failed embankment. Field vane tests were performed in three of these borings. Unconfined compression tests (UC) and unconsolidated,

undrained triaxial tests (UUC) were performed on undisturbed samples recovered from the other three borings. Since the failure occurred in an essentially undrained state, these strength tests will be considered as measures of the undisturbed strength prior to construction, supplementing the original strength data.

The field vane strength data from tests performed both before and after the slide are plotted in Figure 3-3. Similar plots for the unconfined compression test data are shown in Figure 3-4. None of these plots indicate a definite change in strength with depth; therefore, it was assumed that the strength in the organic clay layer was constant with depth. For the cases of field vane tests and unconfined compression tests, the additional testing subsequent to failure did not change the mean strength significantly.

Conventional circular arc and sliding wedge slope stability analyses were performed on the test section, constructed to El +10. The four mean strengths from Figures 3-3 and 3-4 were used for comparison. The critical failure arc for the test section is shown in Figure 3-2. The calculated safety factors based on field vane data and unconfined compression data were then corrected for testing and modeling bias. This was done by multiplying them by correction factors proposed for the respective type of strength

test.

By back calculating the in situ shear strength at sites of embankment failures and by comparing it to the measured vane strength, Bjerrum developed a correction factor, μ :

$$\mu = \frac{s_u(\text{in situ})}{s_u(\text{FV})} \quad (3.2-1)$$

which is a factor of the plasticity index (PI) of the soil. This correction factor has been updated based on additional case studies by Milligan (1972), Ladd(1973), and Flaate and Preber(1974). The in situ strength is calculated as the product of the measured strength and μ , knowing the plasticity index of the soil.

The resisting moment for the FRT test section is almost directly proportional to the shear strength of the organic clay layer. Then, multiplying the safety factor based on the measured strength by the revised Bjerrum factor yields the best estimate of the true (FV) safety factor. The revised Bjerrum correction factor is shown in Figure 3-5.

A similar correction factor was proposed by Wu(1974) for soft to medium clays. By relating the in situ shear strength obtained from embankment failures to the shear strength measured by unconfined compression tests, the Wu correction factor is defined as:

$$v = \frac{s_u(\text{in situ})}{s_u(\text{UC})} \quad (3.2-2)$$

Again, the best estimate of the true (UC) safety factor at the FRT test section is the product of the measured safety factor and the W_u correction factor. This correction factor developed from 18 case studies has a mean value of 1.10. The W_u correction factor is shown in Figure 3-6.

The calculated and the corrected safety factors of the FRT test section for the four mean strengths are shown in Table 3-1.

CASE	\bar{s}_u	FS	CF (@PI=35)	FS x CF
FV (before failure)	520	2.04	0.85	1.73
FV (before & after failure)	520	2.04	0.85	1.73
UC (before failure)	210	0.82	1.10	0.90
UC (before & after failure)	205	0.80	1.10	0.88

STABILITY OF FRT TEST EMBANKMENT

Table 3-1

The resulting safety factors indicate that the testing after failure measured the same undrained strength as those performed before the failure; therefore, the additional testing did not change the computed safety factor. Also, the correction factors brought the safety factors based on field vane and on unconfined compression data closer together. However, the corrected results based on field vane data indicate satisfactory performance (FS = 73 percent high); the corrected results based on unconfined compres-

sion data still show the safety factor about 10 percent too low.

Before the occurrence of the failure, it was difficult to decide what type of strength was more reliable for this test section. A number of sources of bias control the reliability of the measured strength from both types of tests (Haley and Aldrich, 1967). For the unconfined compression test, sample disturbance and inhomogeneity due to sand lenses and shells would cause the measured strength to be too low. On the other hand, the applied stress system and the rate of strain to failure would cause the measured strength to be too high. The net result would probably be strengths a little too low. This trend is reflected by the Wu correction factor.

For the field vane test, sample disturbance would result in too low strength measurements - but not as low as for unconfined compression tests. This would be expected, since the vane test is performed in situ, minimizing sample disturbance. The effects of the applied stress system are generally unknown. Both the applied rate of strain (10% per second) and the presence of shells, peat fibers and wood chips would cause the measured strength to be too high. The net result for the field vane test would probably be strengths too high. This trend is reflected in the revised Bjerrum correction factor.

The design engineer is faced with the decision of what safety factor to select. Such a decision is conventionally based on experience and "engineering judgement". The following section will examine the implications of these safety factors, considering the uncertainty involved in their determination.

3.2.2 Probabalistic Analysis

The corrected safety factors presented in Table 3-1 are the mean or central safety factors for the four cases based on the available strength information. In order to assess the failure probability based on these different states of knowledge, it is necessary to evaluate the uncertainty associated with the number and types of test made for each case. As previously described, the sources of uncertainty are in the bias correction factor, random testing error, and inherent soil variability. These sources will be looked at seperately.

BIAS Figures 3-5 and 3-6 present the revised Bjerrum correction factor and the Wu correction factor, repsectively. The revised Bjerrum correction factor is the best fit or mean of the twenty-eight available case studies. The assumption was made that the standard deviation about this mean is a constant. This implies that the coefficient of variation of the correction factor is a variable and is a func-

tion of the plasticity index of the soil. The standard deviation of the revised Bjerrum correction factor is estimated at 0.15. This correction factor and its estimated one sigma bounds are shown in Figure 3-5.

The organic clay foundation for the FRT test section had an average plasticity index equal to 35 percent. This plasticity index implies that a mean correction factor of 0.85 and a coefficient of variation (V_b) due to bias of $0.15/0.85$ or 0.18 for the field vane test results.

The Wu correction factor for unconfined compression tests is not considered to be a function of soil property. The mean correction factor is a numerical average of the correction factors of the eighteen available case studies and is equal to 1.10. The coefficient of variation (V_b), of the Wu correction factor is equal to 0.30.

RANDOM TESTING ERROR The coefficient of variation due to random error was shown to be proportional to the point coefficient of variation, V_s , of strength and inversely proportional to the square root of the number of independent strength tests. The point coefficient of variation and number of tests performed for the four mean strengths used in analyzing the FRT test section are shown in Table 3-2. Also shown in this table are the spatial coefficients of variation (V_s/\sqrt{n}), for the four cases analyzed.

The resulting coefficients of variation indicate that the number of tests performed prior to failure was sufficient for both field vane and unconfined compression tests. Increasing the number of independent test neither changed the mean strength significantly nor reduced the uncertainty related to random testing error measurably.

The results also show that although the standard deviation of strength based on field vane testing is more than twice that based on unconfined compression tests, the normalized standard deviations or the point coefficients of variation are approximately equal. The spatial coefficients of variation, (V_s/\sqrt{n}) , due to random testing error are twice as high for the unconfined compression tests as for the field vane tests. This is a result of the greater number of field vane tests performed.

INHERENT SOIL VARIABILITY The coefficient of variation due to inherent soil variability was shown to be proportional to the point coefficient of variation of strength and inversely proportional to the square root of the equivalent number of independent soil elements. The point coefficient of variation of strength, (V_s) is shown on Table 3-2 for the four mean strengths used.

The number of equivalent soil elements was obtained by first approximating the surface area of the failure sur-

face with perpendicular rectangles. The critical failure arc was simplified into a rectangle, 30 feet high and 80 feet along the base. The height was selected equal to the maximum depth that the critical failure arc passed into the organic clay layer. The base width was selected equal to the difference in the failure arc length and twice the rectangle height.

The axial length of the critical failure surface was set equal to three times the base width, or 240 feet. This length was selected to preserve the assumption of "plane strain". The rectangles in the three principal planes that comprise the simplified failure surface are unfolded and shown in Figure 3-7.

The number of equivalent soil elements are a function of the dimensions of these rectangles and also of the correlation distance in the three principal directions. A detailed study of the correlation of soil properties is currently underway at M.I.T. Although correlation distances of soil strength have not been investigated to date, those of related material properties have been measured.

Based on results of studies on total unit weight, moisture content, and maximum past pressure, correlation distances of strength equal to 5 feet vertically and 100 feet horizontally were selected. Using these typical values as estimates of the correlation distances of soil

strength at the FRT test section, the number of equivalent soil elements contained within the simplified failure surface is determined from Figure 2-6.

The number of equivalent soil elements is 2 for the base ($L \times B$) and 11 for the four sides ($2LH + 2HB$). The total number of equivalent elements (N_e) is 13. This number is independent both of the number of tests and the type of tests performed. Using an average point coefficient of variation for the four cases equal to 0.21, the spatial coefficients of variation due to soil heterogeneity is equal to 0.06.

A summary of the data pertinent to a probabilistic study of the FRT test section is presented in Table 3-2. An important result is that the uncertainty of the bias correction factor (V_b), as measured by the coefficient of variation of the bias correction, is the dominant source of uncertainty. This reflects the dilemma of the design engineer.

As a result of the quantity of strength tests performed, the design engineer is not much concerned with the question of what is the average measured strength. However, he is more concerned with the bias correction factor, or which test, if either, is measuring the in situ strength correctly after applying a mean bias correction factor.

The total uncertainty in predicting the spatial

average shear strength for the FRT test section can be calculated with the equation (2.6-18). For the field vane method of testing:

$$V_S = V_{Mr} = \sqrt{0.15^2 + 0.06^2 + 0.02^2} = 0.16$$

and for the unconfined compression testing method:

$$V_S = V_{Mr} = \sqrt{0.30^2 + 0.06^2 + 0.04^2} = 0.31$$

The fractional contribution of the bias term to the total variance is 88 percent and 94 percent for the field vane test and the unconfined compression test, respectively.

Now that both the mean safety factors and the uncertainties in the resisting moment are known, the reliability index, β , can be calculated from equation (2.4-1). For the field vane method of testing, β equals 2.64 regardless of which amount of tests is performed. This value of β suggests a failure probability of 0.4 percent. For the unconfined compression testing method and a mean safety factor of 0.89, β equals 0.40. This value of β leads to an estimated failure probability of 65 percent. The graphical representations of the reliability indices and failure probabilities of both methods of testing are shown in Figure 3-8.

The calculated failure probability for the unconfined testing method is high and would generally be considered unacceptable. On the other hand, the probability of failure based on field vane testing is relatively small

and may be considered as an acceptable risk. The fact that the test section actually did fail illustrates that even with a high safety factor, an embankment is still susceptible to failure.

Also shown in Figure 3-8 are plots of failure probability versus safety factor, assuming that the uncertainty in the resisting moment is constant.

3.3 Atchafalaya Basin Test Section

3.3.1 Conventional Analysis

In order to further illustrate the probability model, the stability of a flood levee is studied. The levee in question is part of the Atchafalaya Basin protection system. A pair of guide levees, each approximately 100 miles in length were erected from Morganza, Louisiana to the Gulf of Mexico to help channel flood waters of the Mississippi River. By diverting the excess flood waters down the Atchafalaya Basin Floodway, the area surrounding the lower 280 miles of the Mississippi River is protected from flooding.

The construction of these levees began in the 1930's. Due to stability and deformation problems, large sections of the levees are presently below design grade. For this reason and because the design flowline had been increased to allow for siltation in the Basin, several test embank-

ments were constructed. These test sections straddled the existing embankments and were built to investigate design alternatives for future construction. Two 1500 ft long test embankments, Test Sections II and III, were adjacent sections that only differed in their design safety factors. Test Section II was designed for a safety factor equal to 1.1; Test Section III for a safety factor equal to 1.3 (USCE, 1968). Test Section III (TS III) is analyzed in this report.

Before construction of the existing levee began, the original ground surface was approximately horizontal and at El. +1msl. The foundation materials were very soft to medium clays to El. -120msl. This thick clay layer was underlain with sand. Geologically, the clay is divided into three main deposits. From ground surface to El. -25msl is a poorly drained swamp deposit. Very high moisture content is encountered between El. -5 and -25ft. Below El. -25ft, the clay consists of lake deposits with a layer of well drained swamp deposit between El. -75 and -90ft.

The existing levee was initially constructed with material excavated from an adjacent borrow pit. The pit was located approximately 300ft to the floodway side of the levee centerline. Additional lifts ensued until by 1965 the levee was at El +17ft and the borrow pit at El. -20ft. Approximately 6 ft of settlement under the exis-

ting levee centerline has been observed from the centerline soil borings made in 1964.

The sequence of construction of TS III is shown in Figure 3-9. Enlarging the existing levee involved five basic steps:

1. Construct cast fill dikes on both sides of the existing levee to serve as retaining dikes for the hydraulically placed berms.
2. Place semi-compacted, hauled fill within the main levee section to El. +17msl.
3. Pump in the hydraulic fill berms.
4. Place semi-compacted, hauled fill to the interim gross grade.
5. At a later date, place semi-compacted, hauled fill to the final gross grade.

The construction operations were monitored by a detailed instrumentation program including piezometers, slope inclinometers and settlement plates and plugs. Piezometric measurements taken during construction indicate that little pore pressure dissipation occurred. For this case, the undrained slope stability analysis is appropriate.

Prior to construction of Test Section III, 30 undisturbed soil borings were made to El. -120msl. Borings were located at the levee centerline and at 105 and 180ft offsets to both sides of the centerline at each of six

stations. Continuous samples were taken with a 5-inch diameter steel tube piston type sampler. The laboratory testing program included visual classification, Atterberg limits; unconfined compression tests (UC), unconsolidated undrained (UUC) and isotropically consolidated undrained (CIU) triaxial compression tests; consolidated drained (CD) direct shear tests; lab vane tests; undrained creep tests; and consolidation tests. The undrained shear strength was also measured in the field with a 2-inch diameter hand cranked vane test. Test holes were drilled adjacent to each undisturbed boring. The vane strength tests were performed at 5-foot increments of depth. Boring locations are shown in Figure 3-10.

Due to the proximity of the adjacent borrow pit, floodwayside stability is more critical than landside stability. Therefore, this case study will focus on the floodwayside stability of the main embankment at TS III. A sharp increase in strength at El. -45msl was detected with the field vane. This increase was found to be the result of an overconsolidated layer beginning at that elevation (Foott and Ladd, 1973). El. -45msl will serve as a limiting depth of assumed failure arcs. Only strength measurements above this elevation will be used.

The analyses of Test Section III is subdivided into two groups. One group will be based solely on field vane

data, the other on only unconfined compression data. The reliability of the main embankment of Test Section III will be expressed in terms of safety factors and failure probabilities.

Figures 3-11 through 3-16 present the results of strength tests performed on samples from the centerline, 105ft floodwayside, and 180ft floodwayside borings. Figures 3-11 through 3-13 show the average results of field vane testing; Figures 3-14 through 3-16 show the average results of unconfined compression testing. The strength lines presented are the average of results over 5ft layers from the six borings at each respective offset.

Based on these average undrained strengths, the stability of the main (floodwayside) embankment was checked with a circular arc method of analysis. The critical mean safety factors for field vane and for unconfined compression strength measurements are shown in Table 3-3. Also shown in Table 3-3 are the critical mean safety factors corrected for bias by the revised Bjerrum and the Wu correction factors.

<u>CASE</u>	<u>FS</u>	<u>CF (PI=70)</u>	<u>FS x CF</u>
FV	2.08	0.69	1.43
UC	1.42	1.10	1.56

STABILITY OF TS III MAIN (FLOODWAYSIDE)
EMBANKMENT (Foott and Ladd, 1973)

Table 3-3

From the results of conventional stability analyses, both methods of measuring strength predict satisfactory performance. The corrected safety factors using field vane tests and unconfined compression tests to measure strength were within fifteen percent of each other. The critical mean safety factor based on the unconfined compression test, when corrected, was higher than that based on a field vane tests. The critical failure arcs for Test Section III are shown in Figure 3-17 and 3-18.

3.3.2 Probabalistic Analysis

The corrected safety factors presented in Table 3-3 are the mean safety factors of the main (floodwayside) embankment using two different methods of strength determination. The failure probabilities of this embankment, calculated with the different strength measurements, are dependent on the uncertainty of bias, random error and inherent variability.

BIAS The uncertainty of strength bias is measured by the coefficient of variation of the two bias correction factors. For the unconfined compression tests, the Wu correction factor was used. This correction factor has a coefficient of variation V_b , equal to 0.30, see Figure 3-6.

The clay foundation for Test Section III had an average plasticity index equal to 70 percent. From Figure 3-5,

the revised Bjerrum correction factor for this type soil is 0.69. The coefficient of variation due to this bias is equal to 0.22 for the field vane test results.

RANDOM TESTING ERROR The spatial coefficient of variation due to random testing error is calculated by equation (2.6-7b). The average point coefficient of variation of strength, V_s , is equal to 0.32 and 0.28 as measured by unconfined compression tests and field vane tests, respectively. The mean strength from unconfined compression tests reflect the average of 239 tests; the mean strength from field vane tests was determined from 178 tests.

The spatial coefficients for variation, V_s/\sqrt{n} , due to random testing error are equal to 0.02 for both methods of testing. This source of uncertainty is small relative to the uncertainty of the bias correction.

INHERENT SOIL VARIABILITY The spatial coefficient of variation due to inherent soil variability is calculated by equation (2.6-16b). The critical failure arc using field vane strengths was approximated with three perpendicular lines as shown in Figure 3-20. The lines were selected to preserve both the depth of failure and the length of the failure arc. The axial length of the critical failure surface was set equal to three times the base width.

Based on the surface area of the simplified failure plane and on correlation distances selected equal to 5

feet vertically and 100 feet horizontally, the number of equivalent soil elements is determined from Figure 2-6. The total number of equivalent elements is 82. For this number of elements, the spatial coefficient of variation, V_s/\sqrt{Ne} , due to soil heterogeneity is equal to 0.03. Through similar calculations, the spatial coefficients of variation due to soil heterogeneity using unconfined compression strength is also equal to 0.03.

A summary of the data for Test Section III is shown in Table 3-4. Again, the uncertainty of the bias correction is the main source of uncertainty. The total uncertainty in the predicted average shear strength, and hence the resisting moment, is equal to 0.22 and 0.30 for field vane testing and unconfined compression testing, respectively.

Based on the above uncertainties and the safety factors shown in Table 3-3, the failure probability with field vane strength measurements is calculated as 9 percent ($\beta = 1.37$) using equation (2.4-1). The failure probability with unconfined compression tests is 12 percent ($\beta = 1.20$). The graphical representation of these failure probabilities is shown in Figure 3-21. Also shown in this figure are plots of failure probability versus safety factor, assuming that the uncertainty in the resisting moment is constant.

It is interesting to note that the safety factor calculated from field vane data is lower than that from unconfined compression data; however, the probability of failure calculated from field vane data is lower than that from unconfined compression data. This is due to the increased uncertainty in applying the Wu bias correction factor.

To investigate the importance of failure arc length on the calculated failure probability, a smaller failure arc having a higher safety factor based on field vane strengths was checked. The comparative failure arcs are shown in Figure 3-18. The uncertainties due to bias and to random testing error are the same for both failure arcs. However, the spatial uncertainty due to soil variability increases from 0.03 to 0.04 (N_e decreases from 82 to 54 due to the decrease in the failure surface size). This change in uncertainty has a negligible effect on the total uncertainty.

The failure probability for the smaller arc is 7 percent ($\beta = 1.51$). Although the critical failure arc based on minimum safety factor does not necessarily define the arc with the maximum failure probability, it generally does for the above examples due to the significance of the uncertainty in bias. The data for the smaller failure arc are shown in Table 3-4.

Test Section III did not fail. It did undergo large deformations and cracking along the embankment crown. These deformations indicate that the embankment was on the verge of failure. This nearness to failure is not surprising in view of the high failure probabilities based on both methods of strength measurements.

TYPE TEST	Data*	\bar{s}	σ_s	V_s	n	N_e	\overline{CF}	V_b	$\frac{V_s}{\sqrt{n}}$	$\frac{V_s}{\sqrt{N_e}}$	V_S
FV	BV	520	110	0.21	82	13	0.85	0.15	0.02	0.06	0.16
FV	B&AF	520	110	0.21	116	13	0.85	0.15	0.02	0.06	0.16
UC	BF	210	40	0.18	20	13	1.10	0.30	0.04	0.06	0.31
UC	B&AF	205	45	0.23	37	13	1.10	0.30	0.04	0.06	0.31

- 86 -

FORE RIVER TEST SECTION DATA

TABLE 3-2

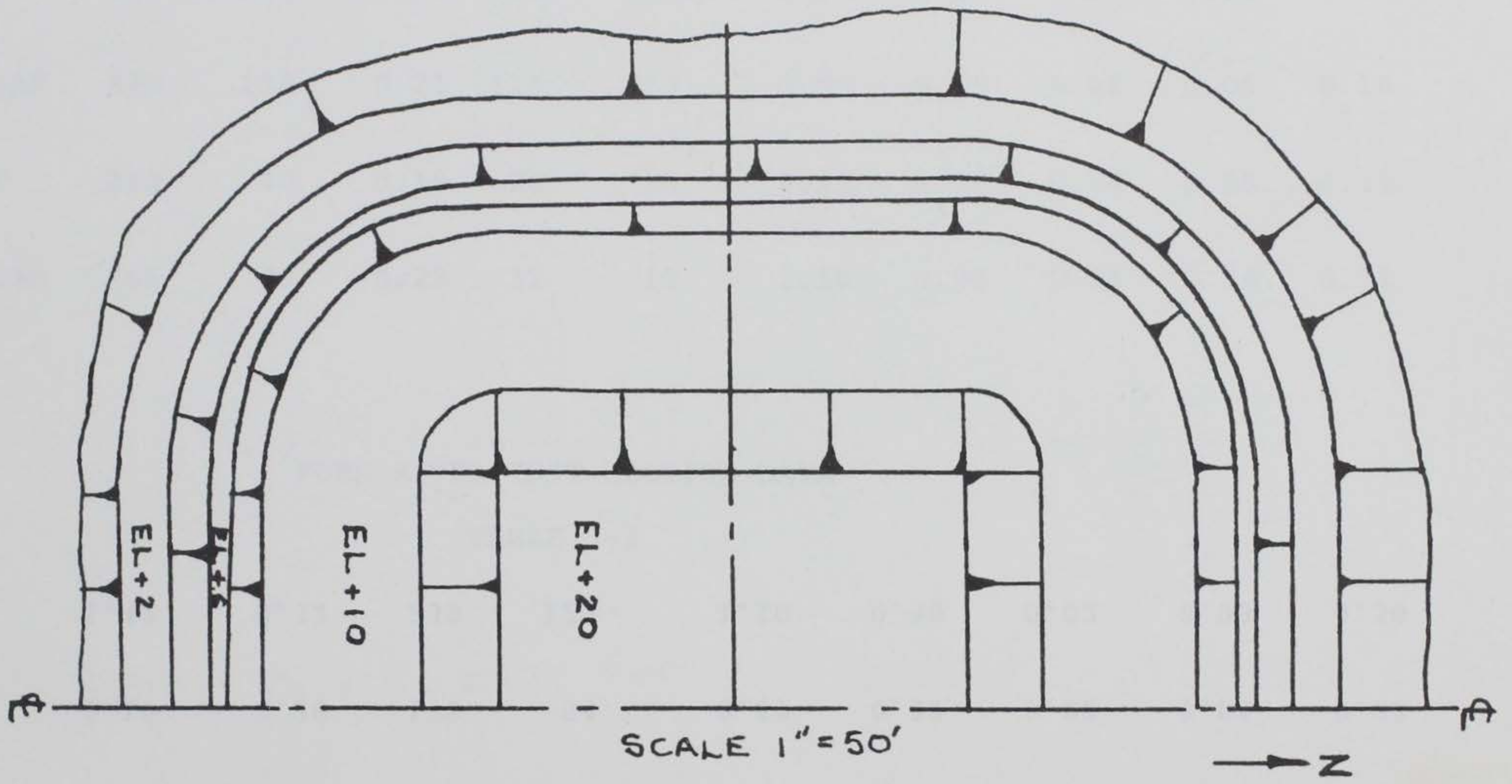
*BF = Before failure data
 B&AF = Before and after failure data

TEST TYPE	\bar{FS}	Vs	n	Ne	\bar{CF}	Vb	$\frac{Vs}{\sqrt{n}}$	$\frac{Vs}{\sqrt{Ne}}$	VS
FV	2.08	0.28	178	82	0.69	0.22	0.02	0.03	0.22
FV	2.19	0.28	178	54	0.69	0.22	0.02	0.04	0.22
UC	1.42	0.32	239	123	1.10	0.30	0.02	0.03	0.30

ATCHAFALAYA BASIN TEST SECTION III DATA

Table 3-4

FORE RIVER TEST SECTION, PLAN

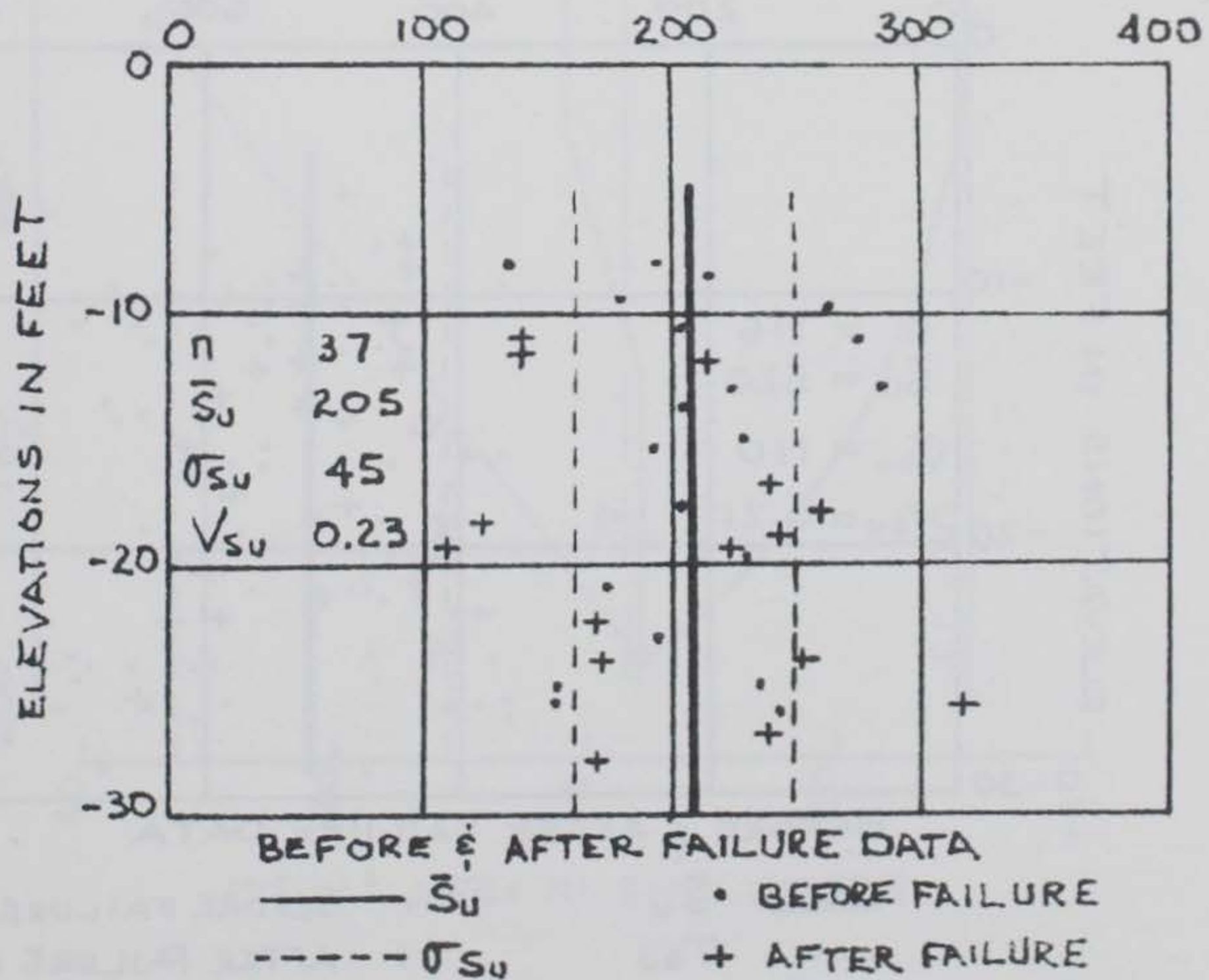
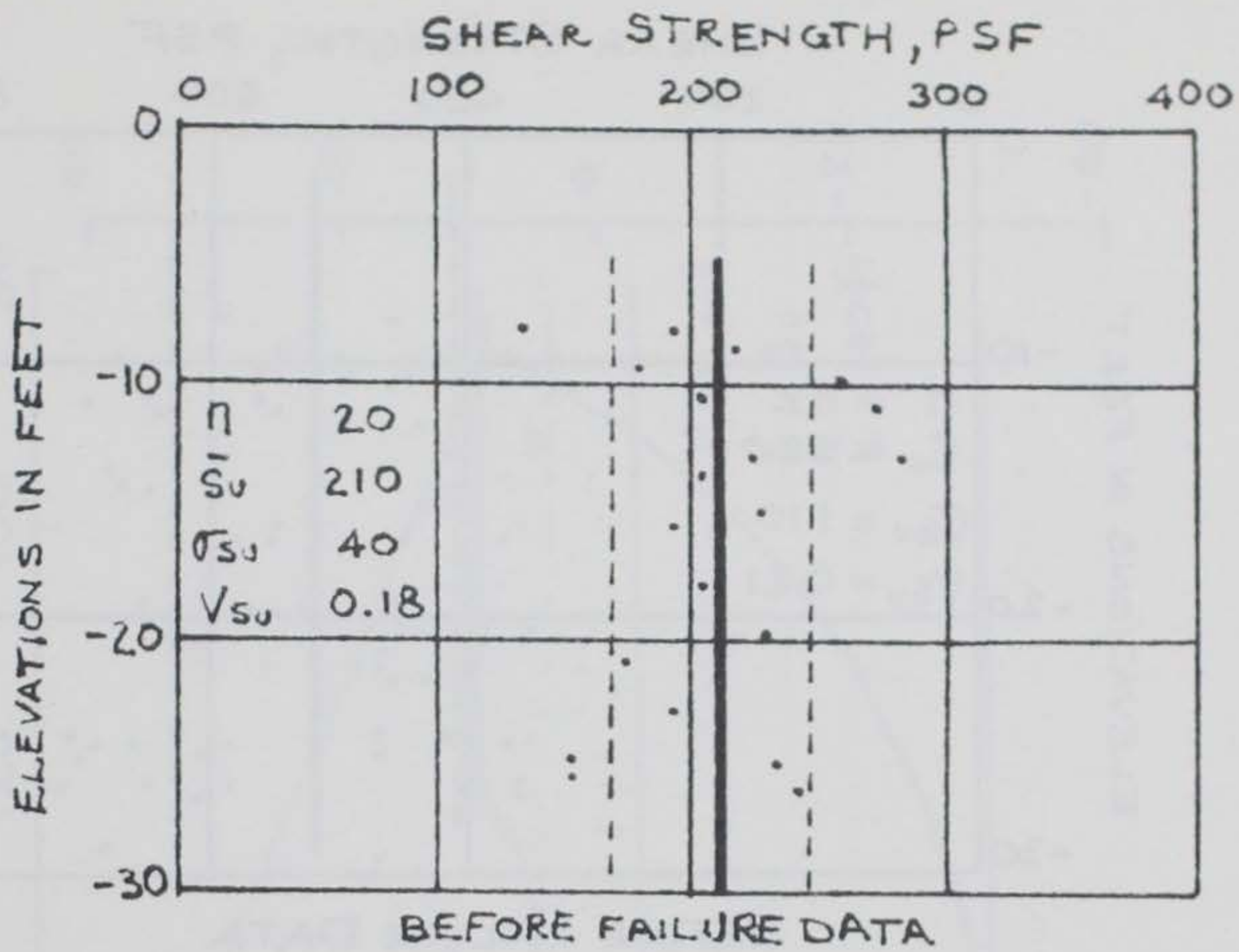


-100-

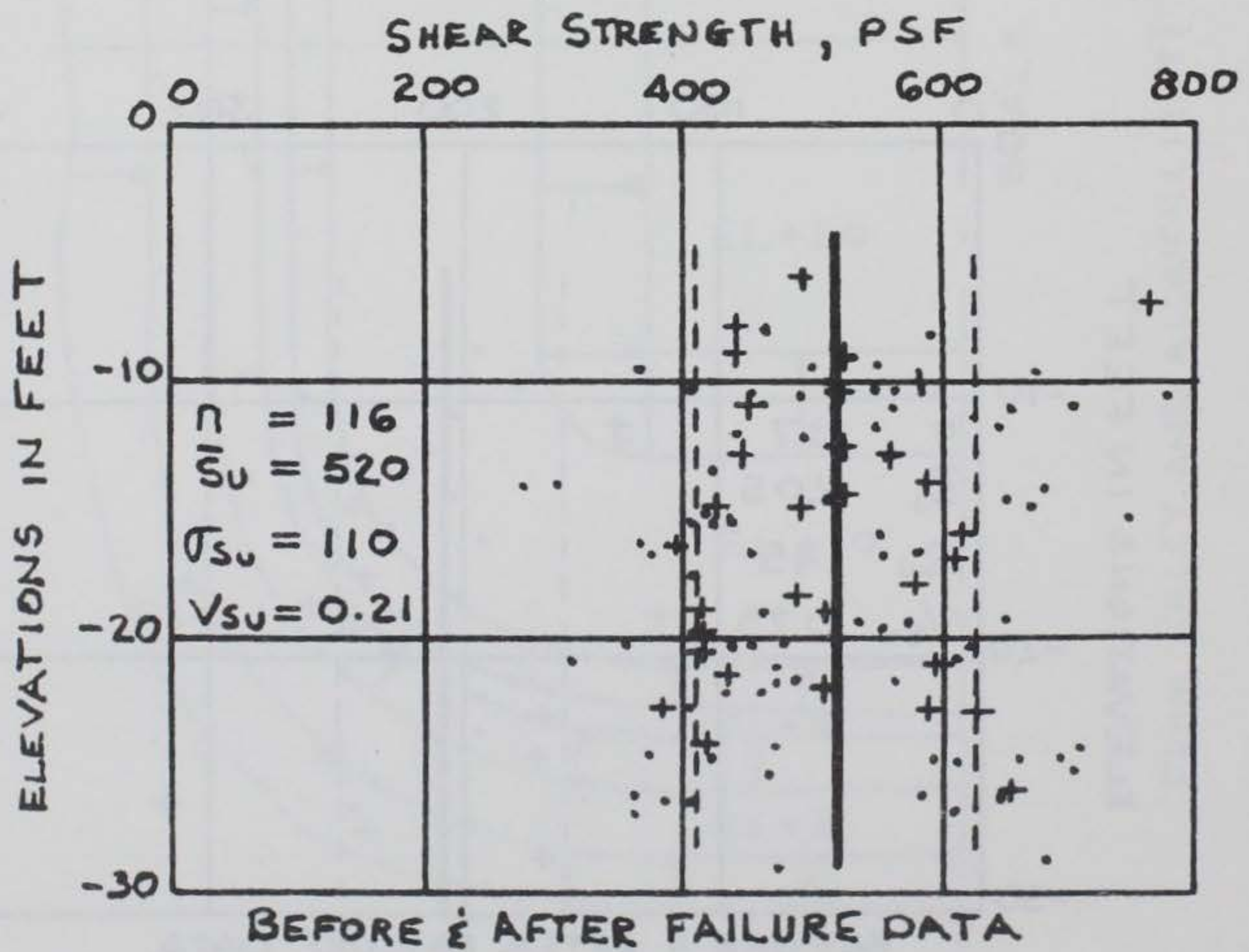
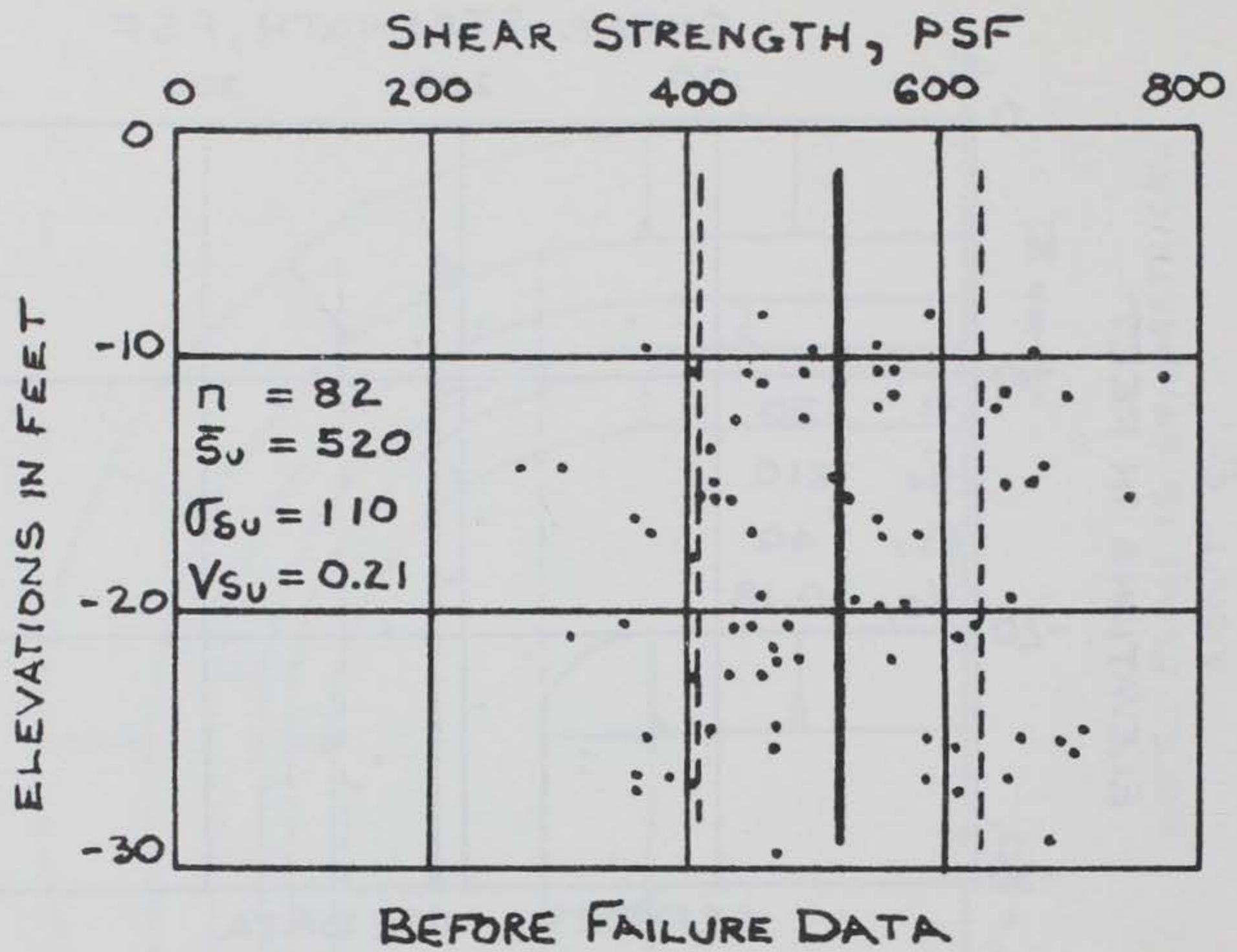
FIGURE 3-1

FROM HALEY AND ALDRICH (1967)

NOTE: PLAN IS SYMMETRICAL ABOUT Φ.



FORE RIVER TEST SECTION UC TEST DATA



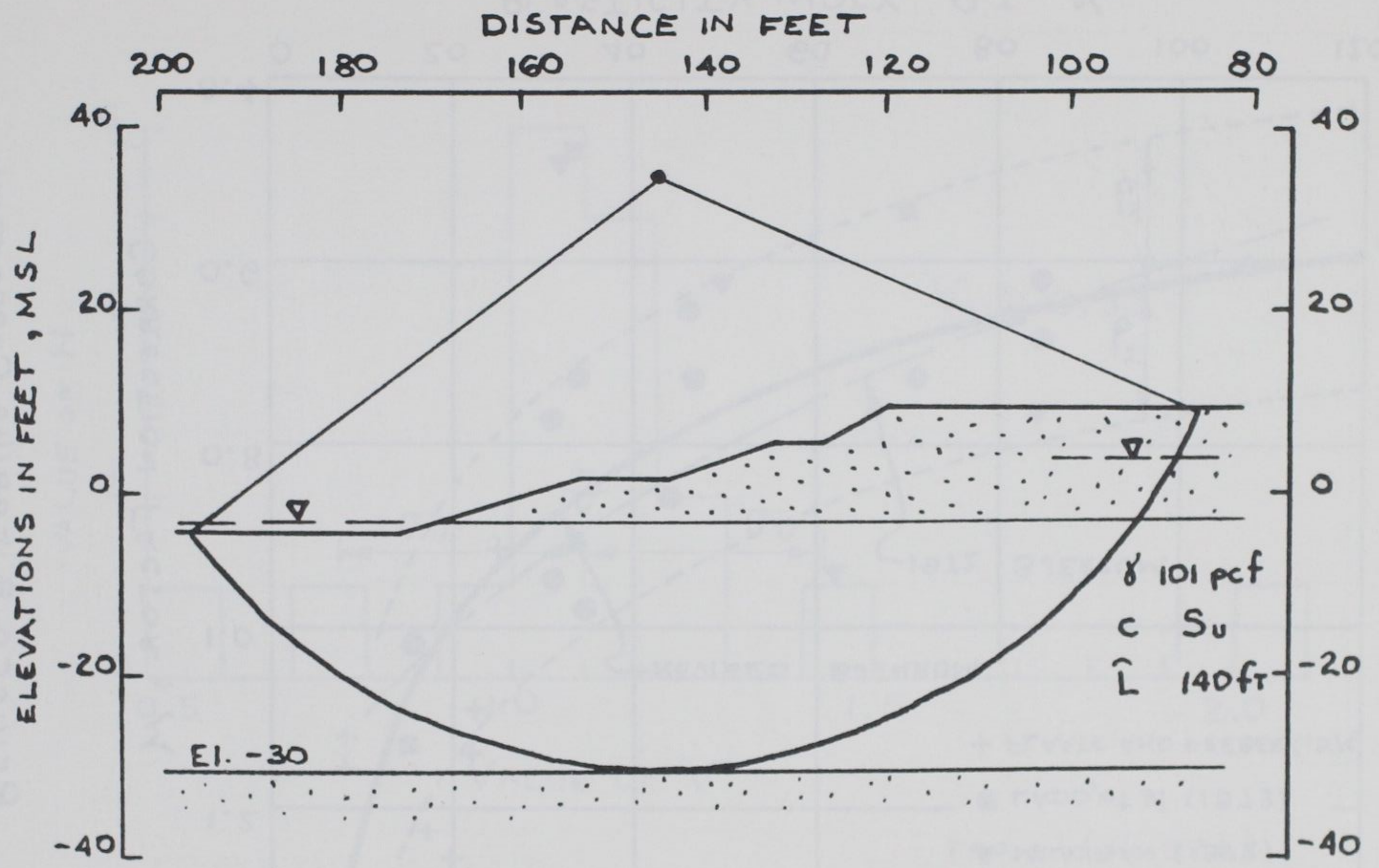
— \bar{S}_u
- - - σ_{Su}

• BEFORE FAILURE FV TEST
+ AFTER FAILURE FV TEST

FRT TEST SECTION

FV TEST DATA

FRT TEST SECTION - CRITICAL ARC



-103-

FIGURE 3-4

REVISED BJERRUM CORRECTION

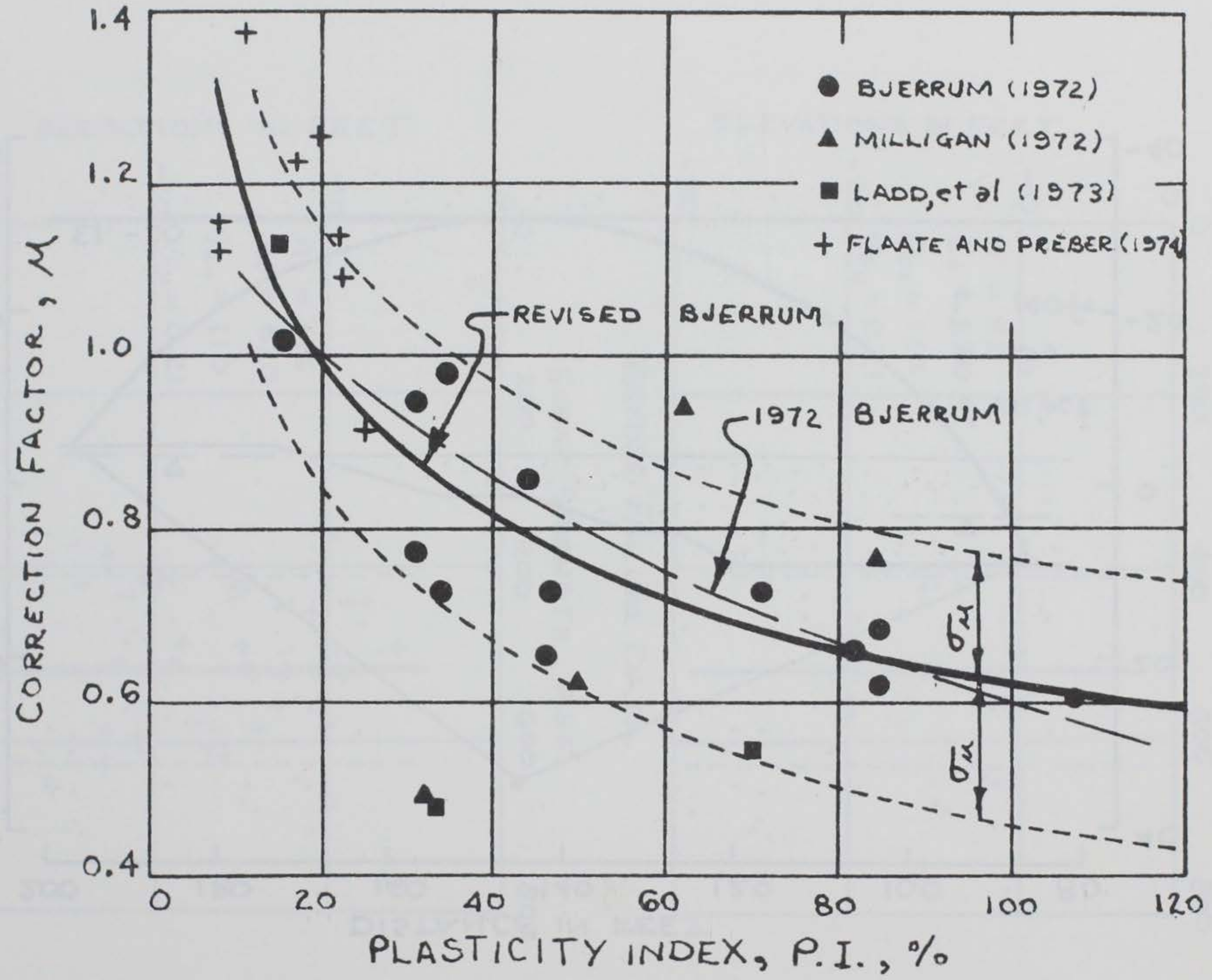
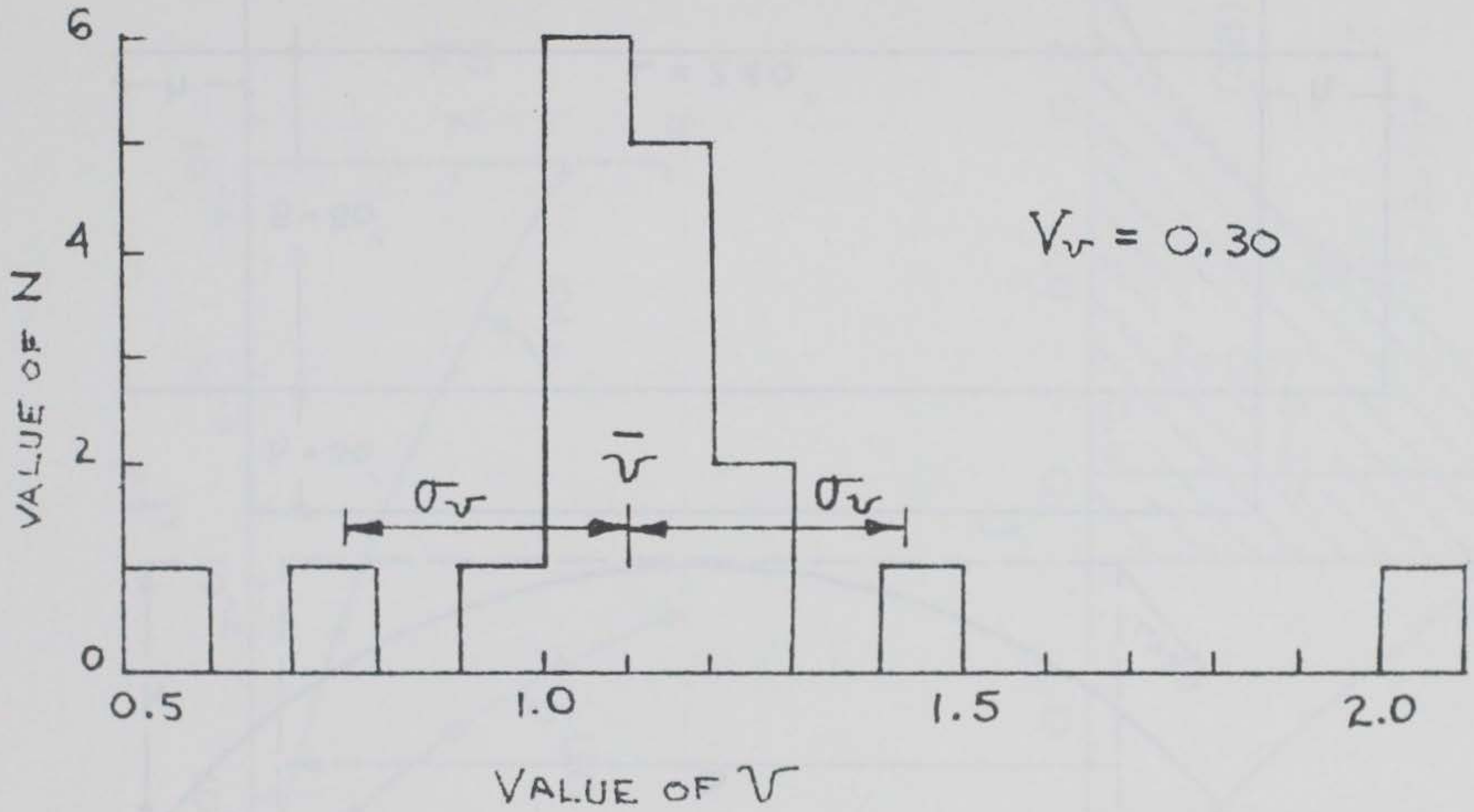
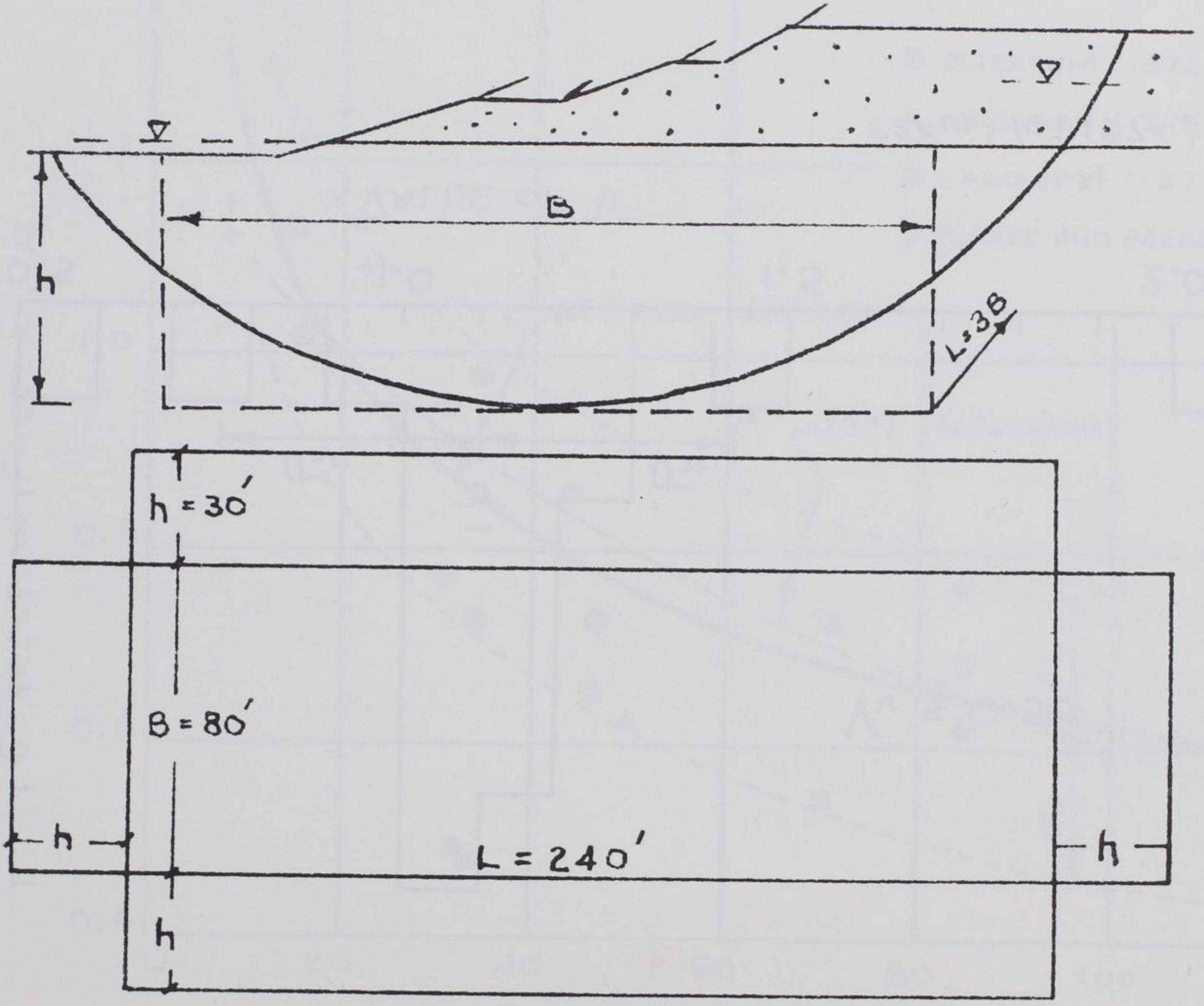


FIGURE 3-5

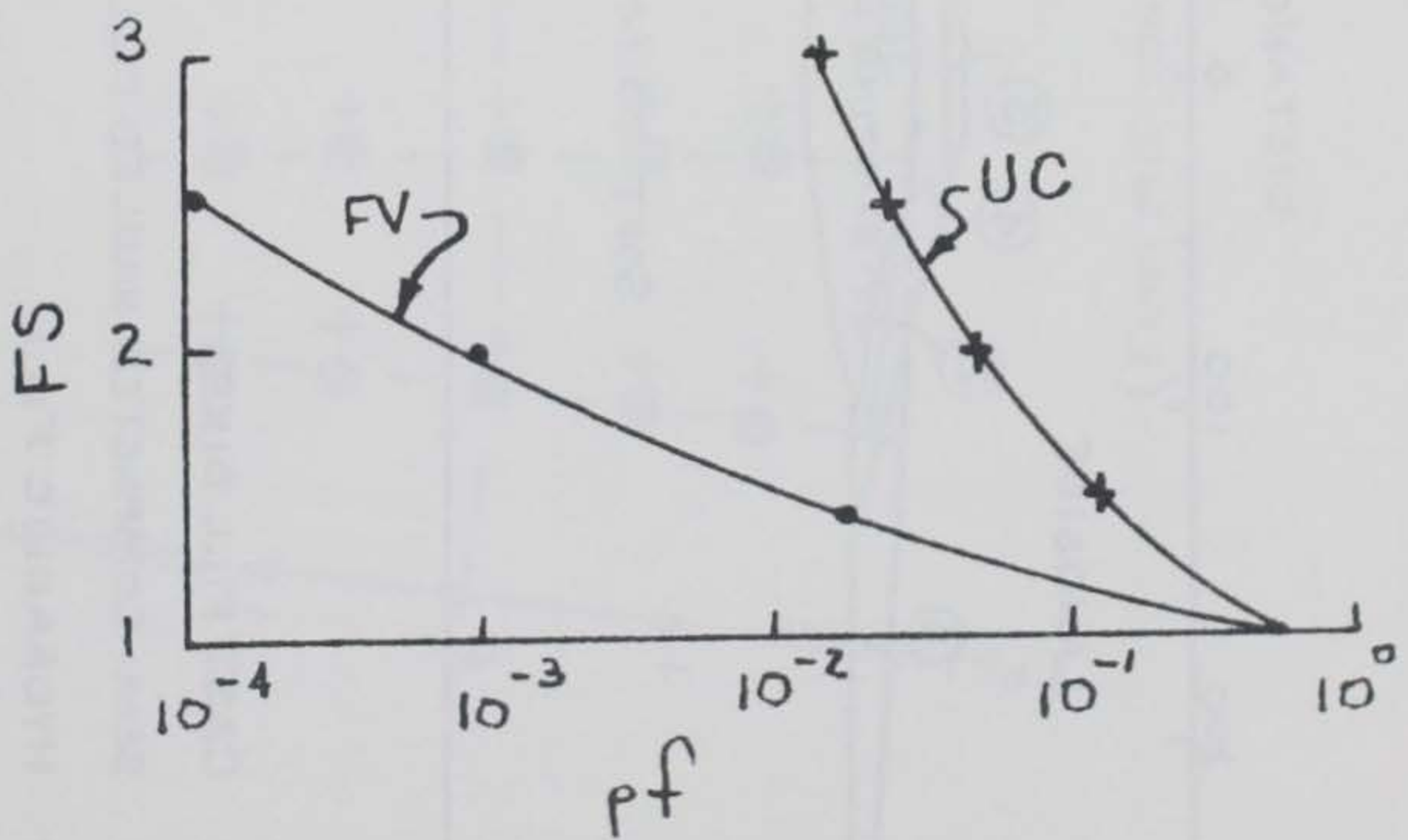
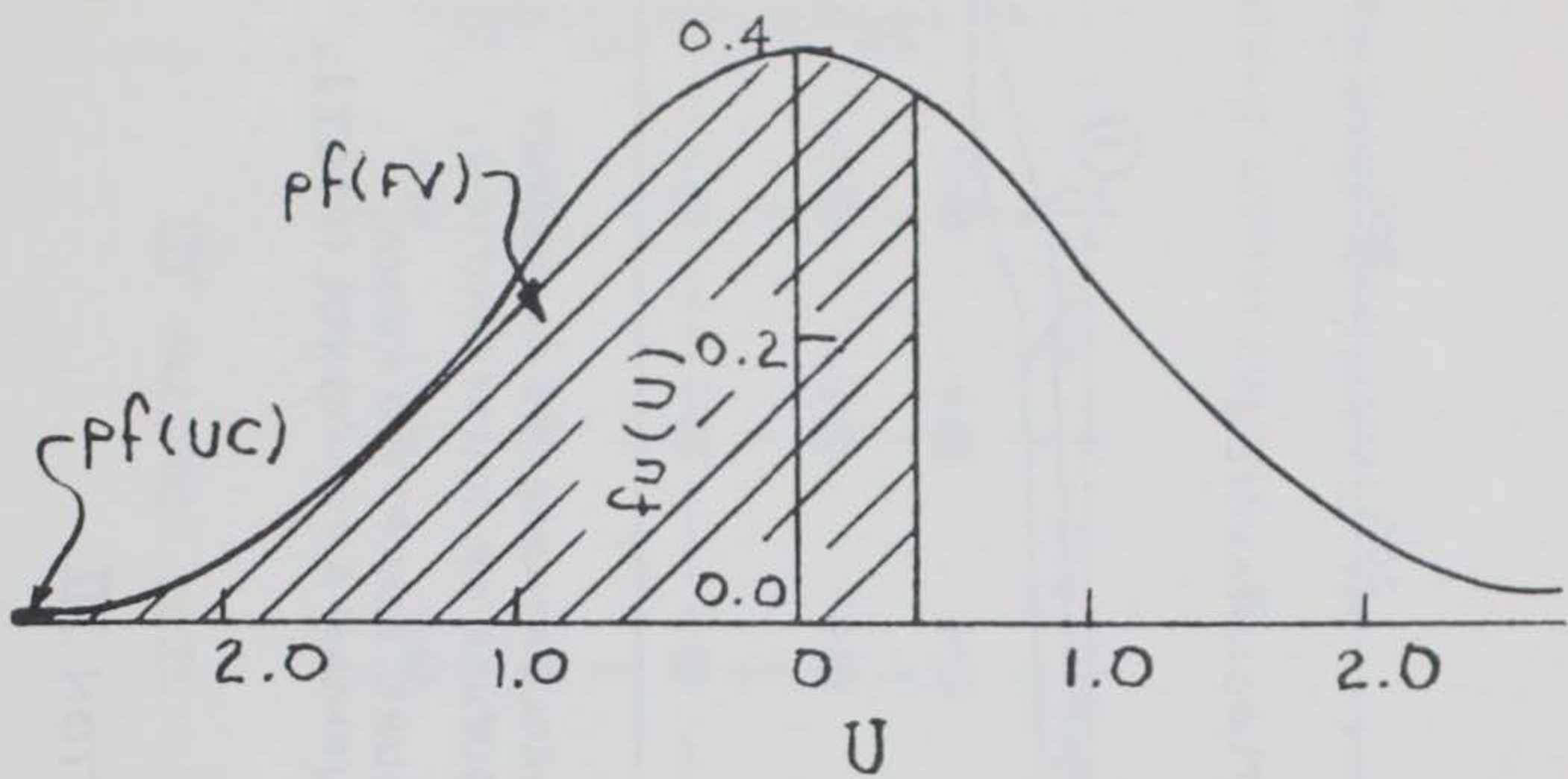
WU CORRECTION



FROM WU (1974)



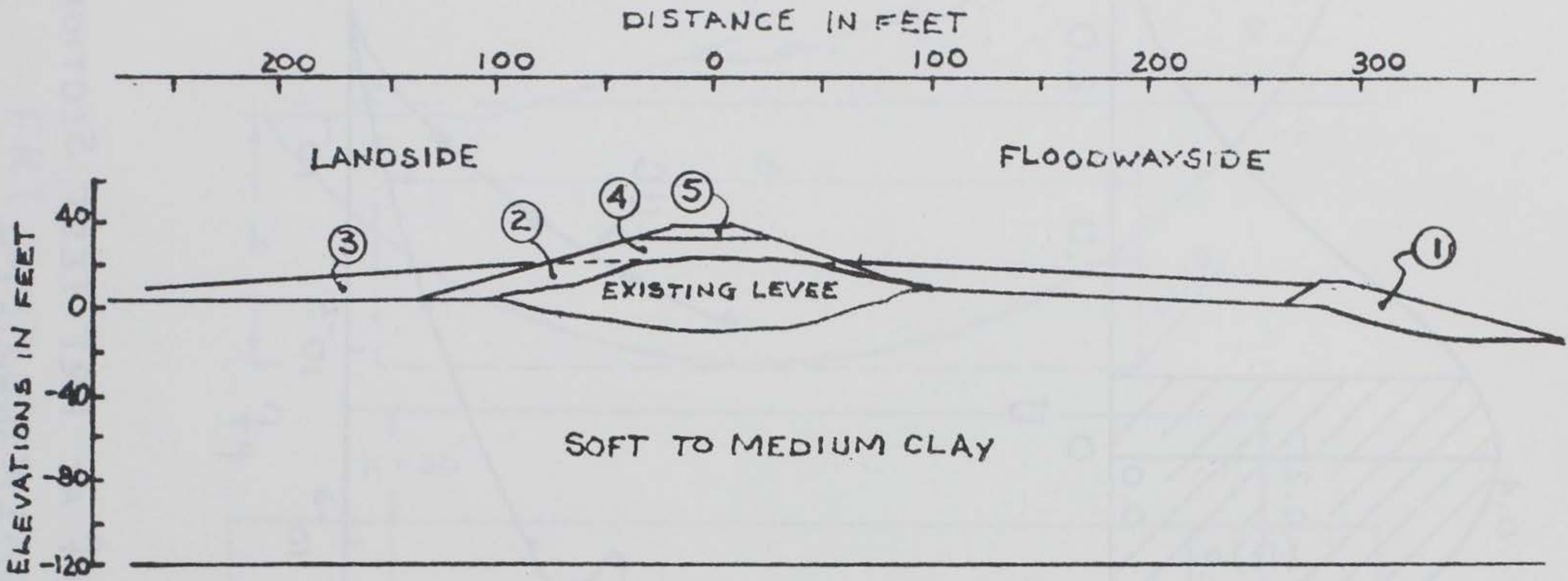
FRT SIMPLIFIED FAILURE SURFACE



CALCULATED pf AT FRT TEST SECTION
AND pf VERSUS FS

PLAN FOR RAISING LEVEL
GRADE

-108-



- ① CAST FILL DIKE
- ④ ⑤ ② SEMI COMPACTED HAULED FILL
- ③ HYDRAULIC FILL

ENCIRCLED NUMBERS REPRESENT SEQUENCE OF CONSTRUCTION.
FIGURE ADAPTED FROM KAUFMAN AND WEAVER (1967).

ATCHAFALAYA BASIN TEST SECTION III

FIGURE 3-9

PLAN OF TEST SECTION III

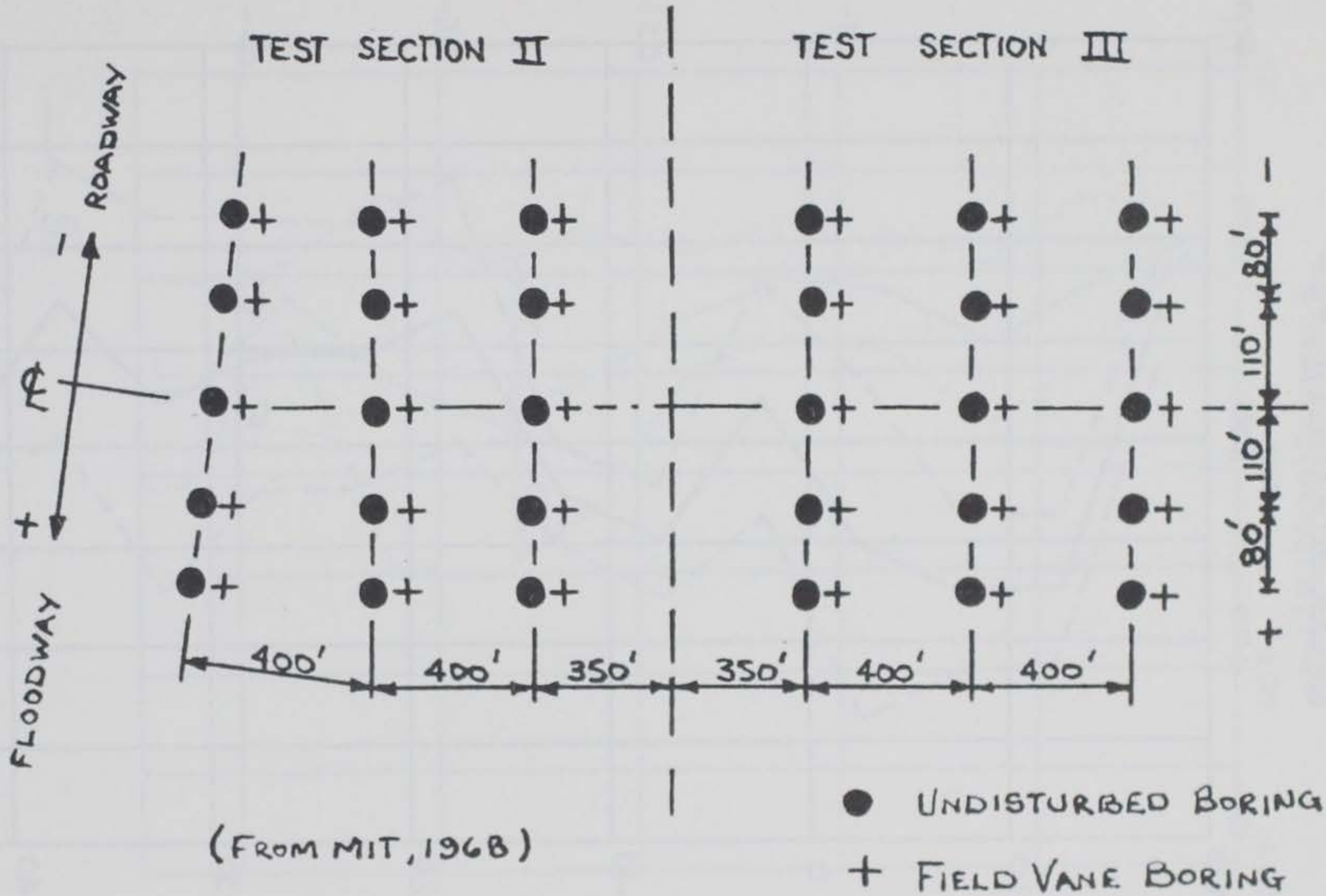
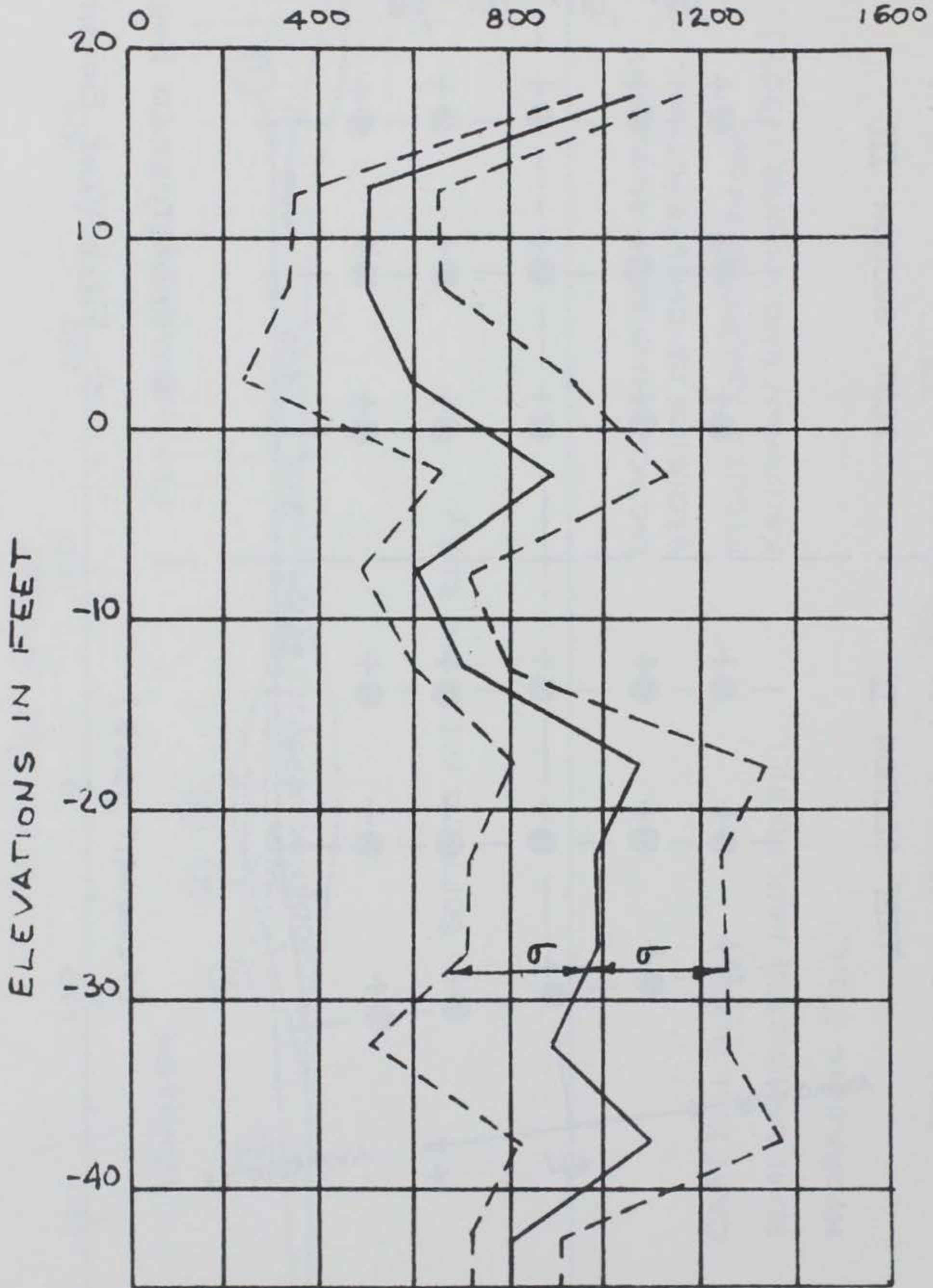


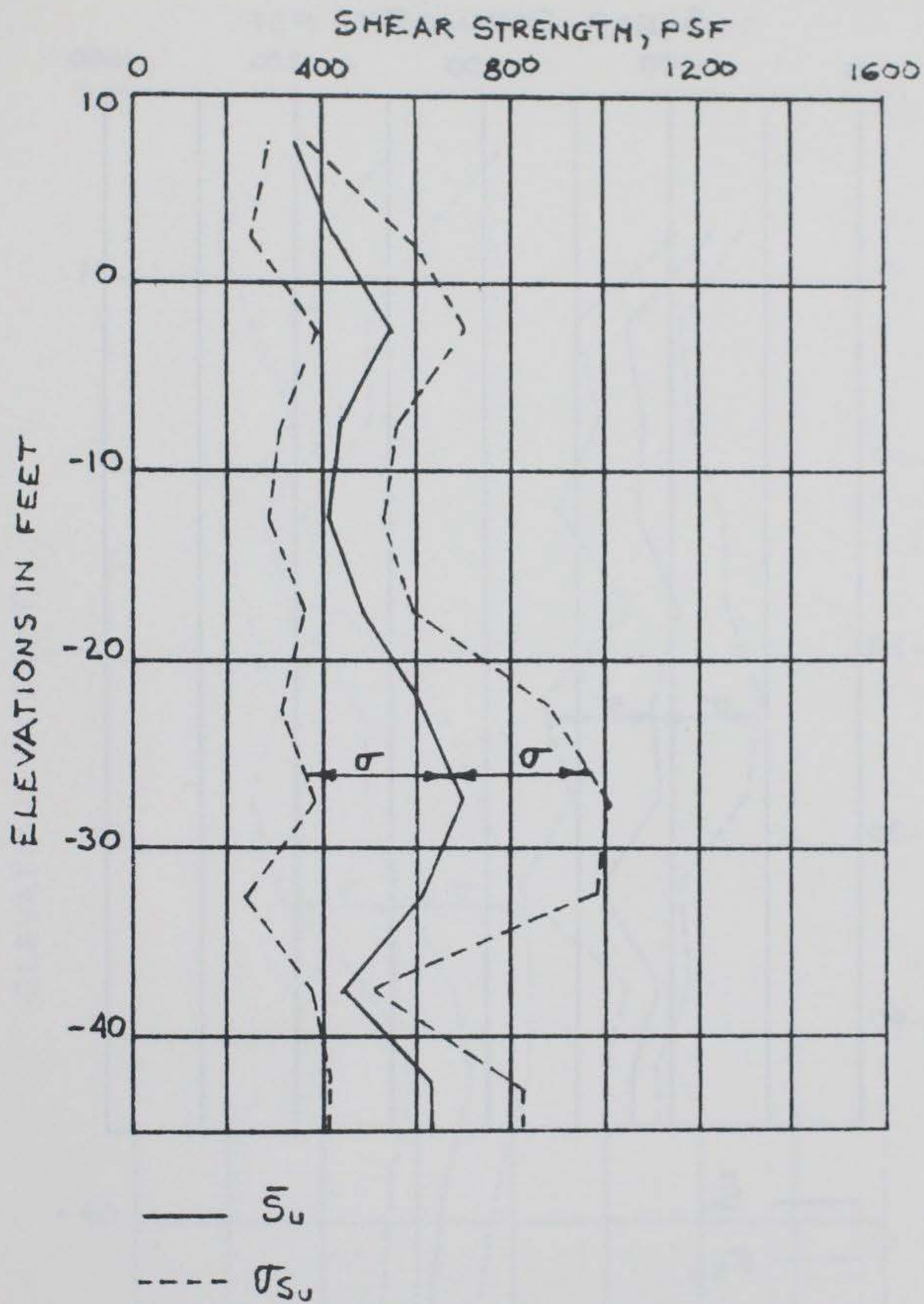
FIGURE 3-10

SHEAR STRENGTH, PSF

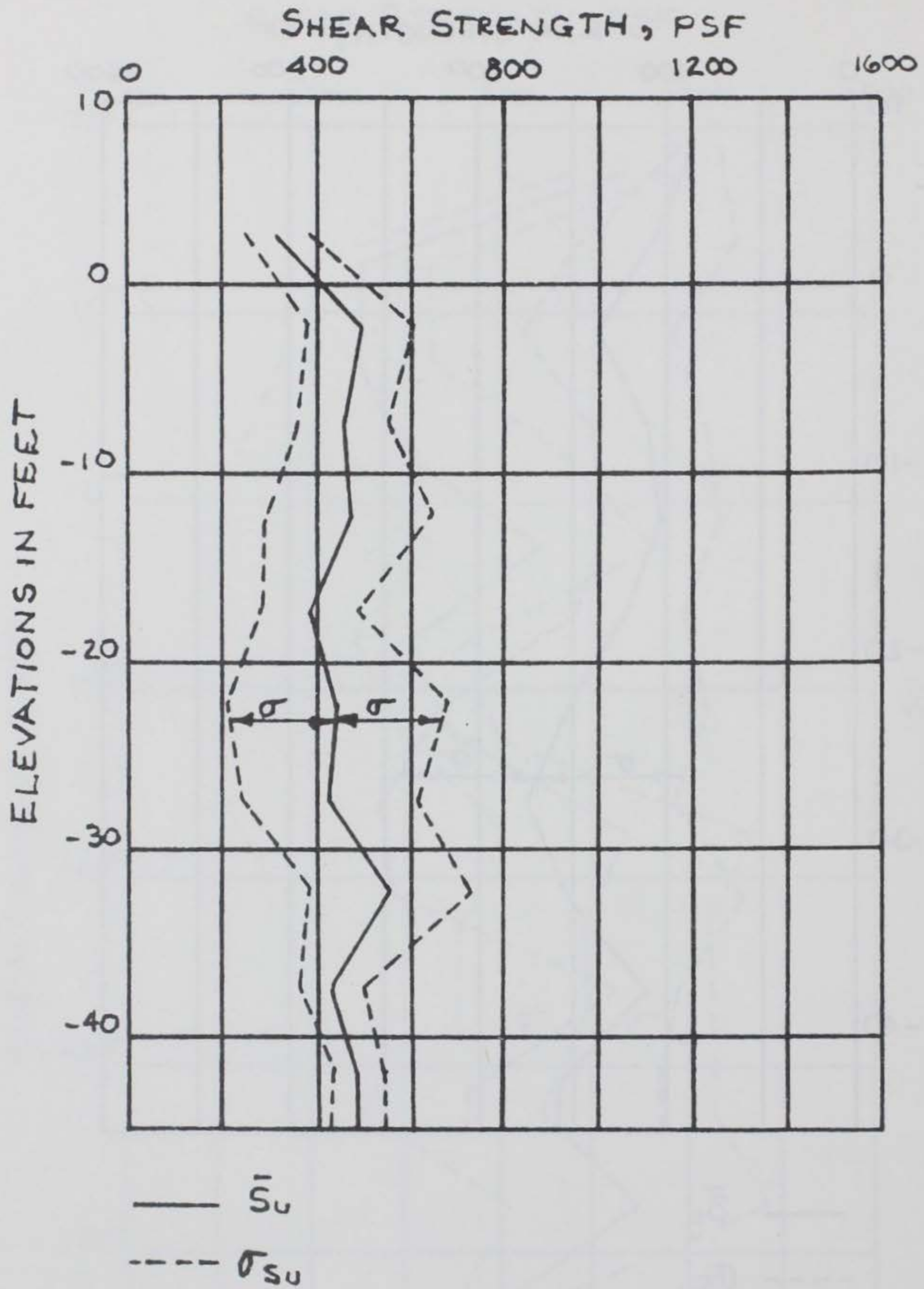


— \bar{S}_u
- - - σ_{Su}

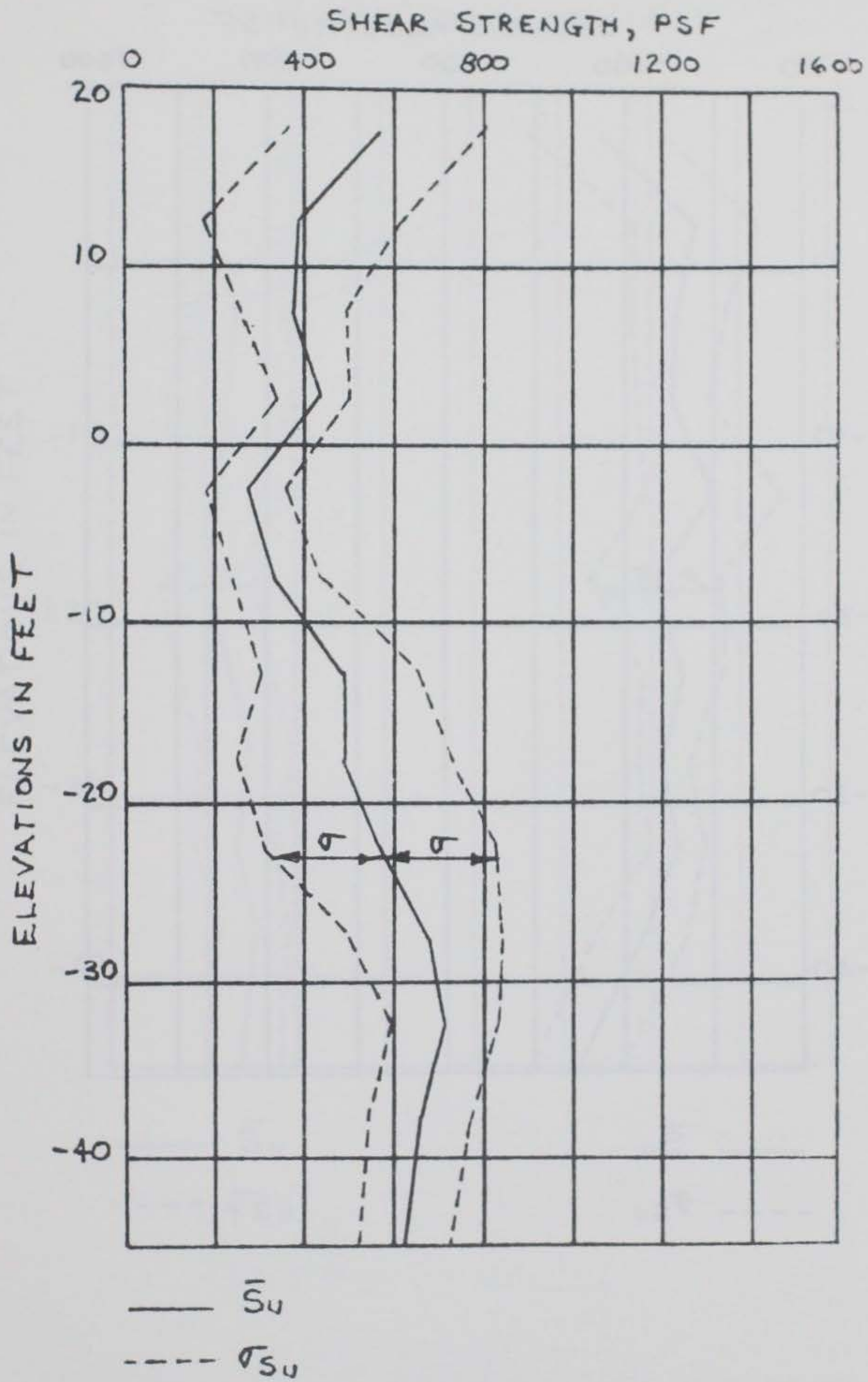
CENTERLINE FV STRENGTH (TS III)



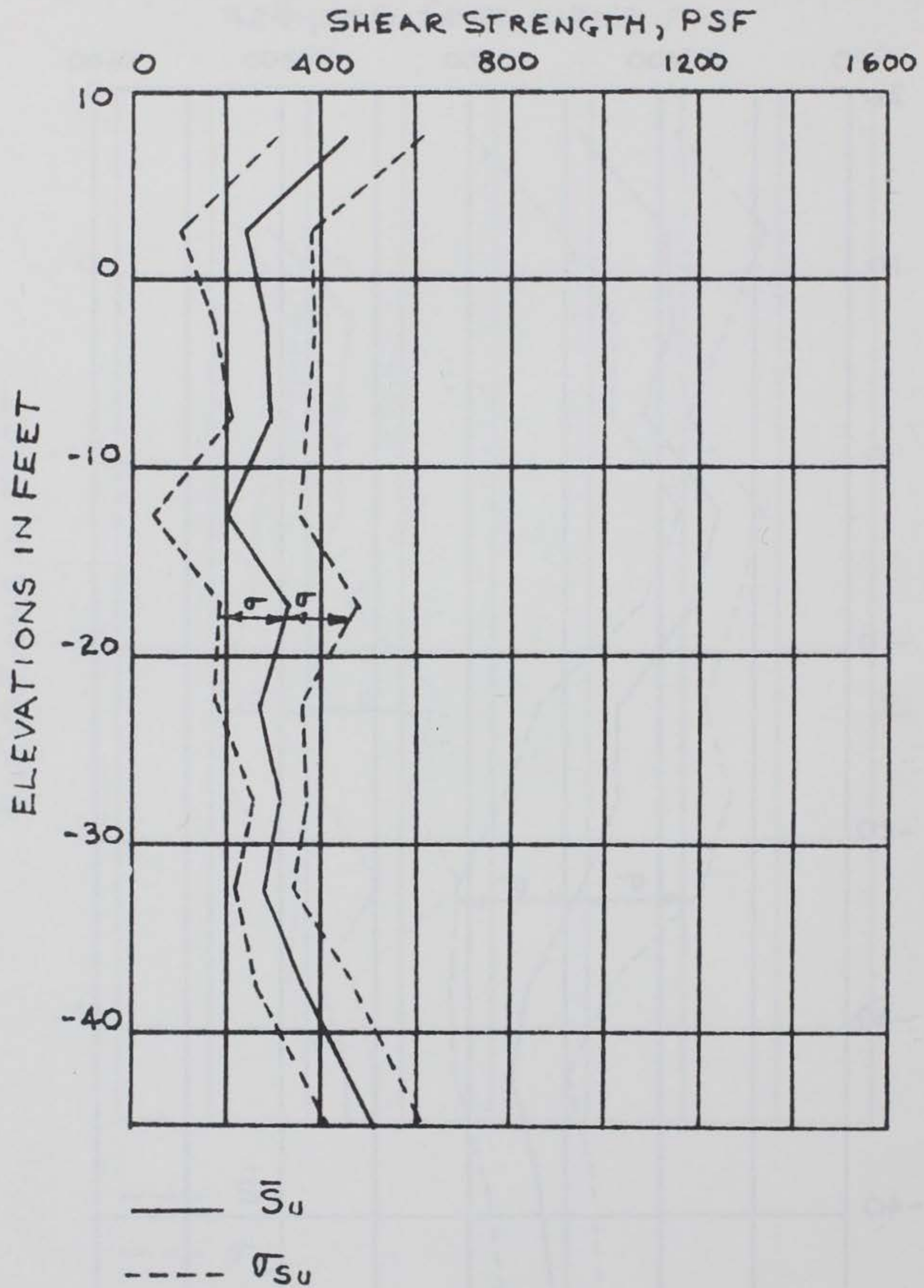
105 FEET FLOODWAYSIDE FV STRENGTH (TSIII)



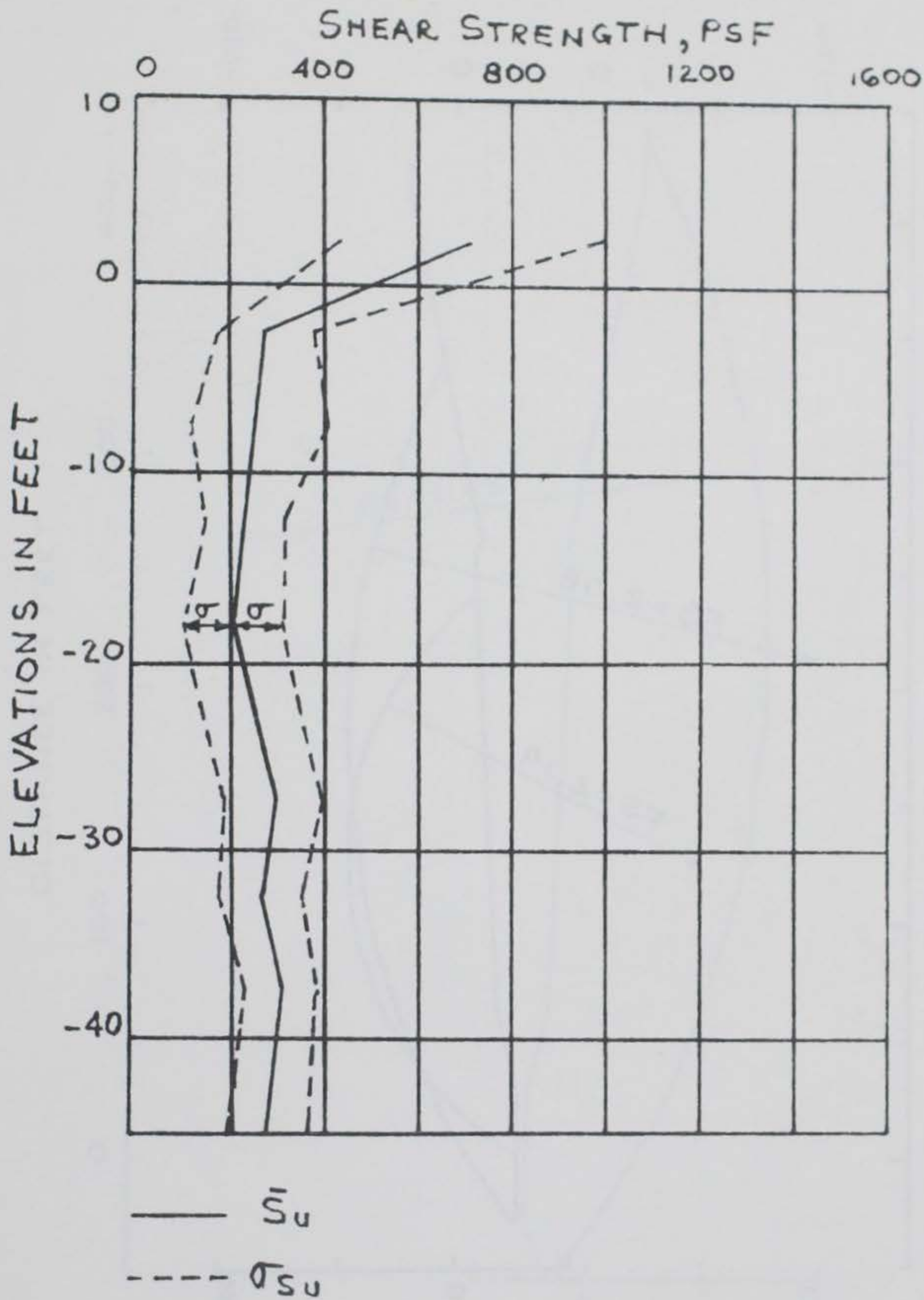
180 FEET FLOODWAYSIDE FV STRENGTH(TS III)



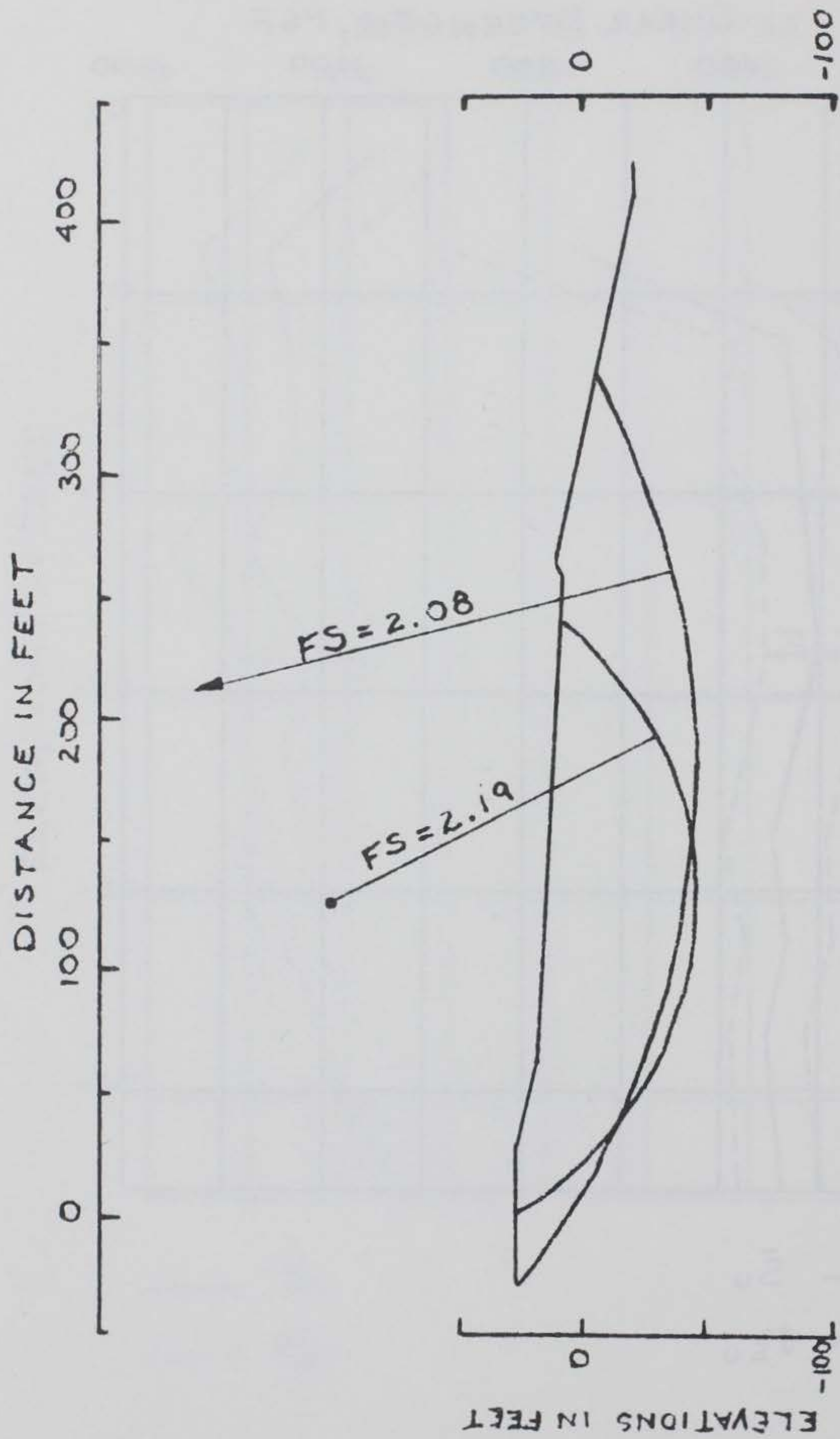
CENTERLINE UC STRENGTH (TS III)



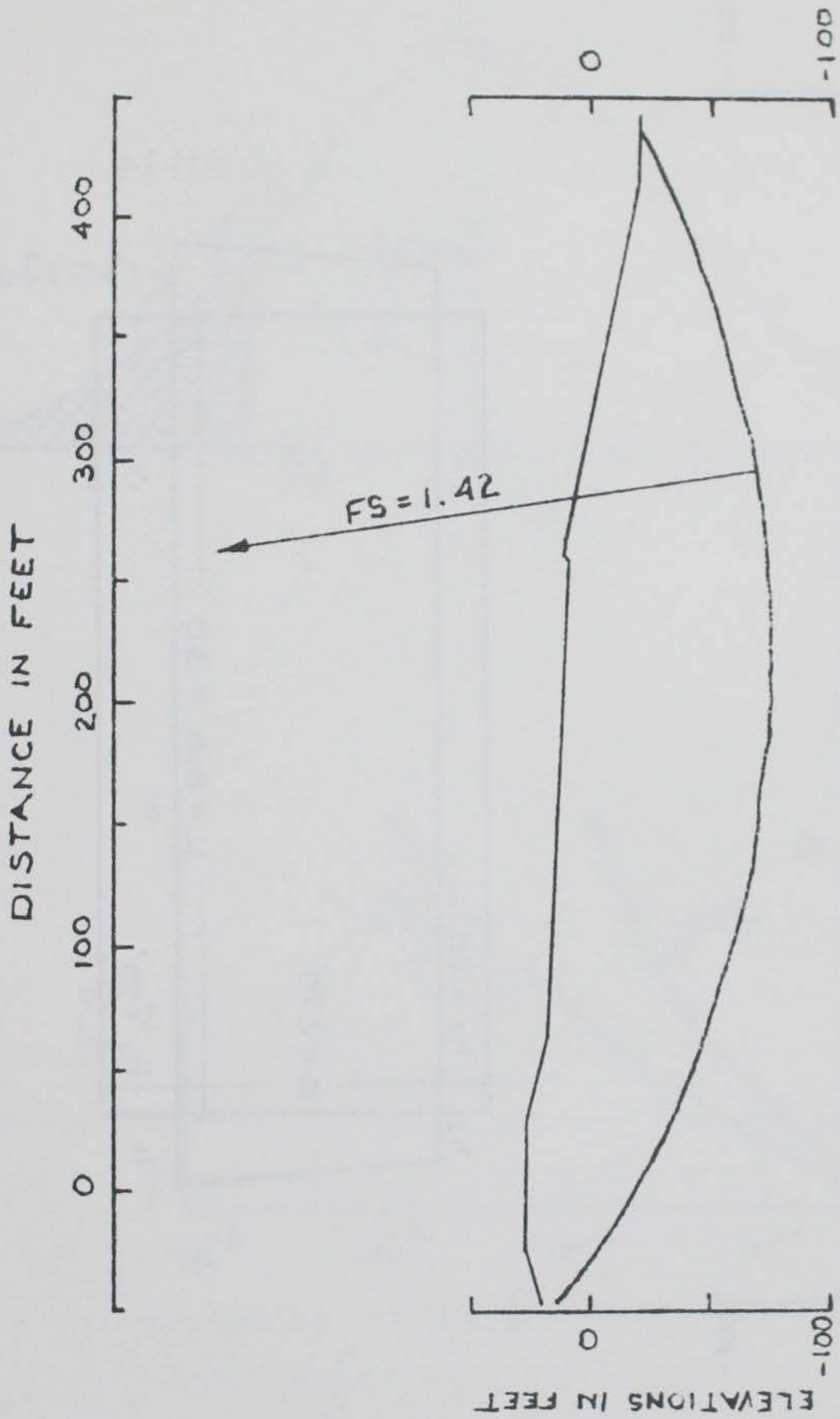
105 FEET FLOODWAYSIDE UC STRENGTH (TS III)



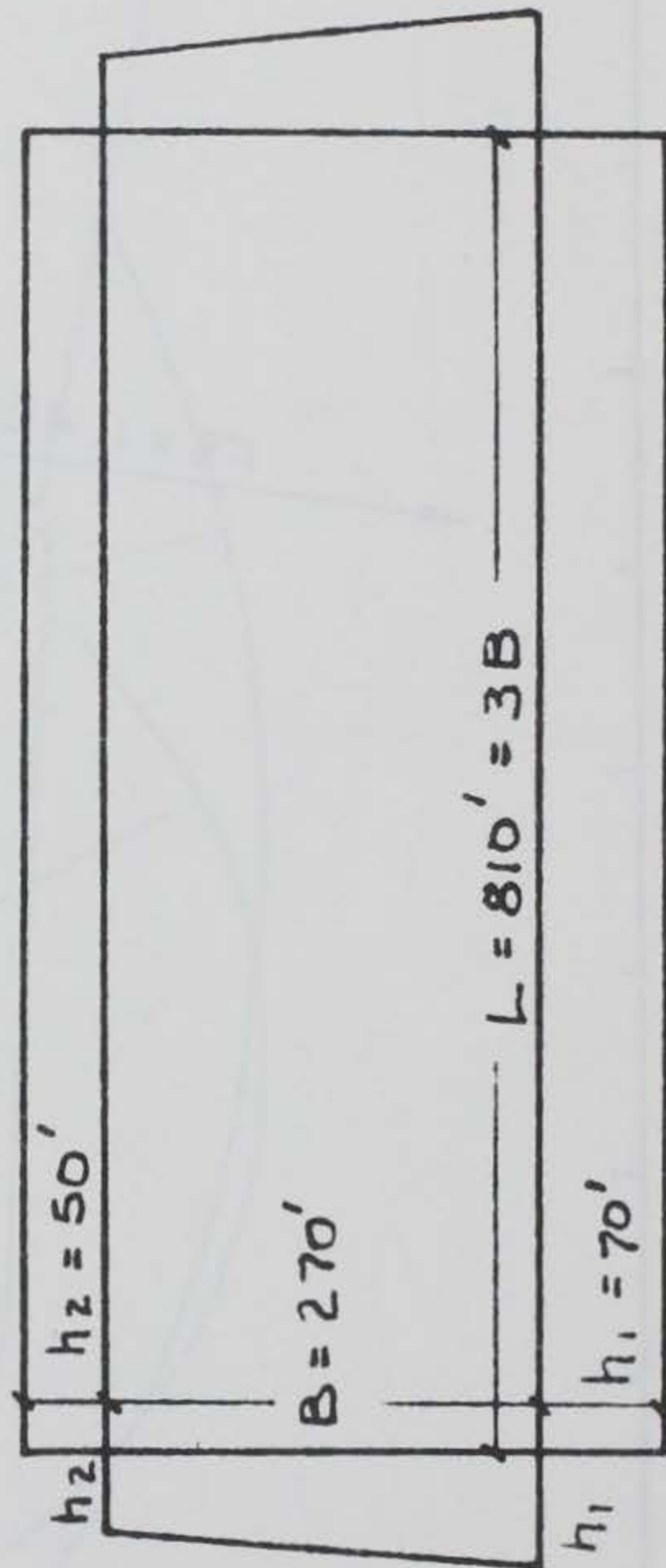
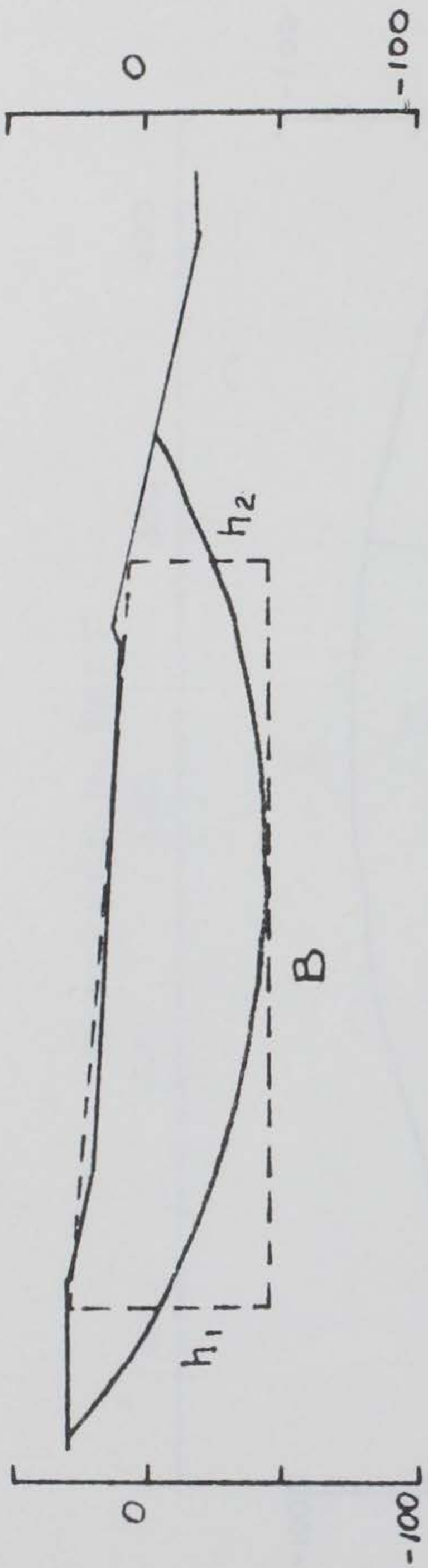
180 FEET FLOODWAYSIDE UC STRENGTH(TS III)



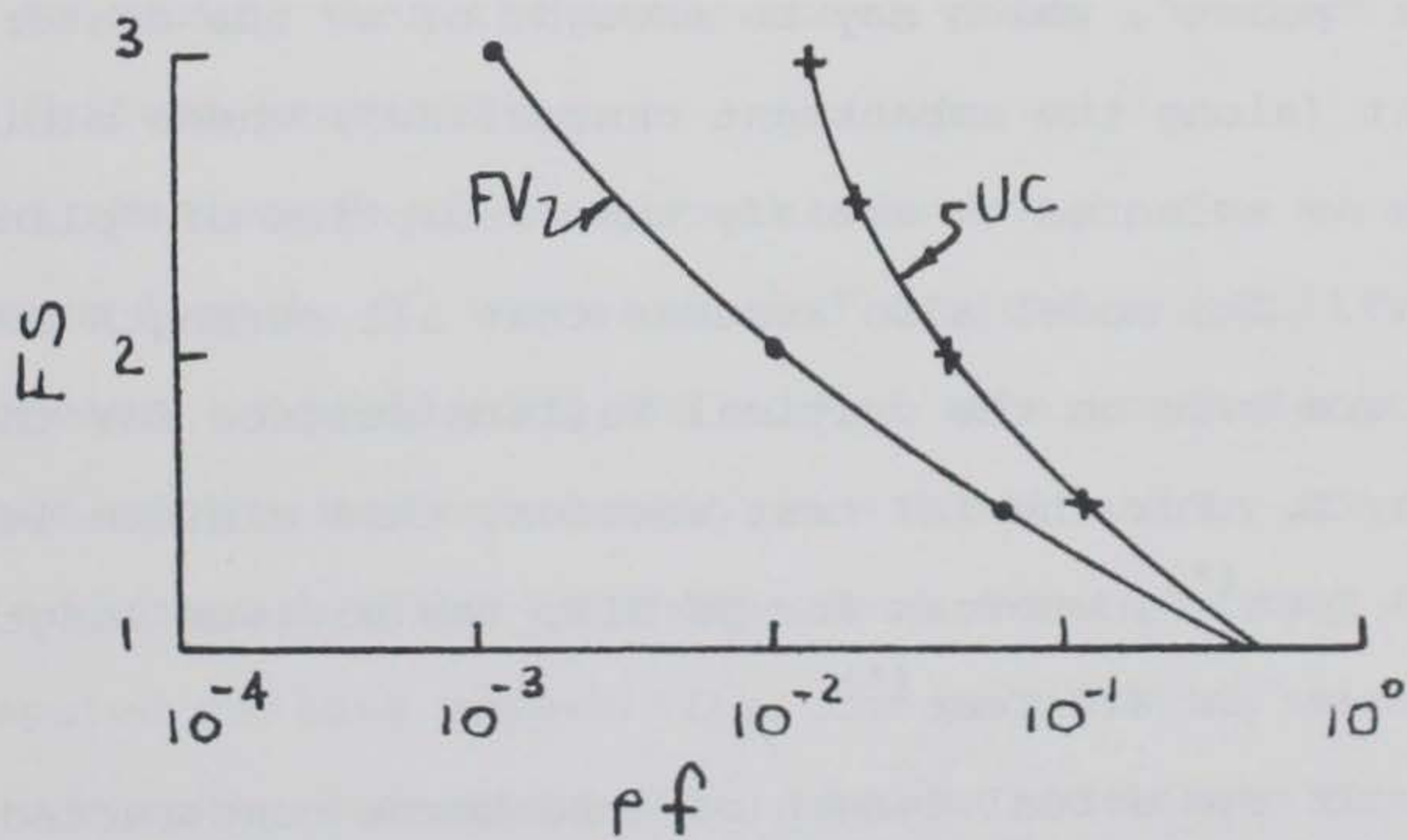
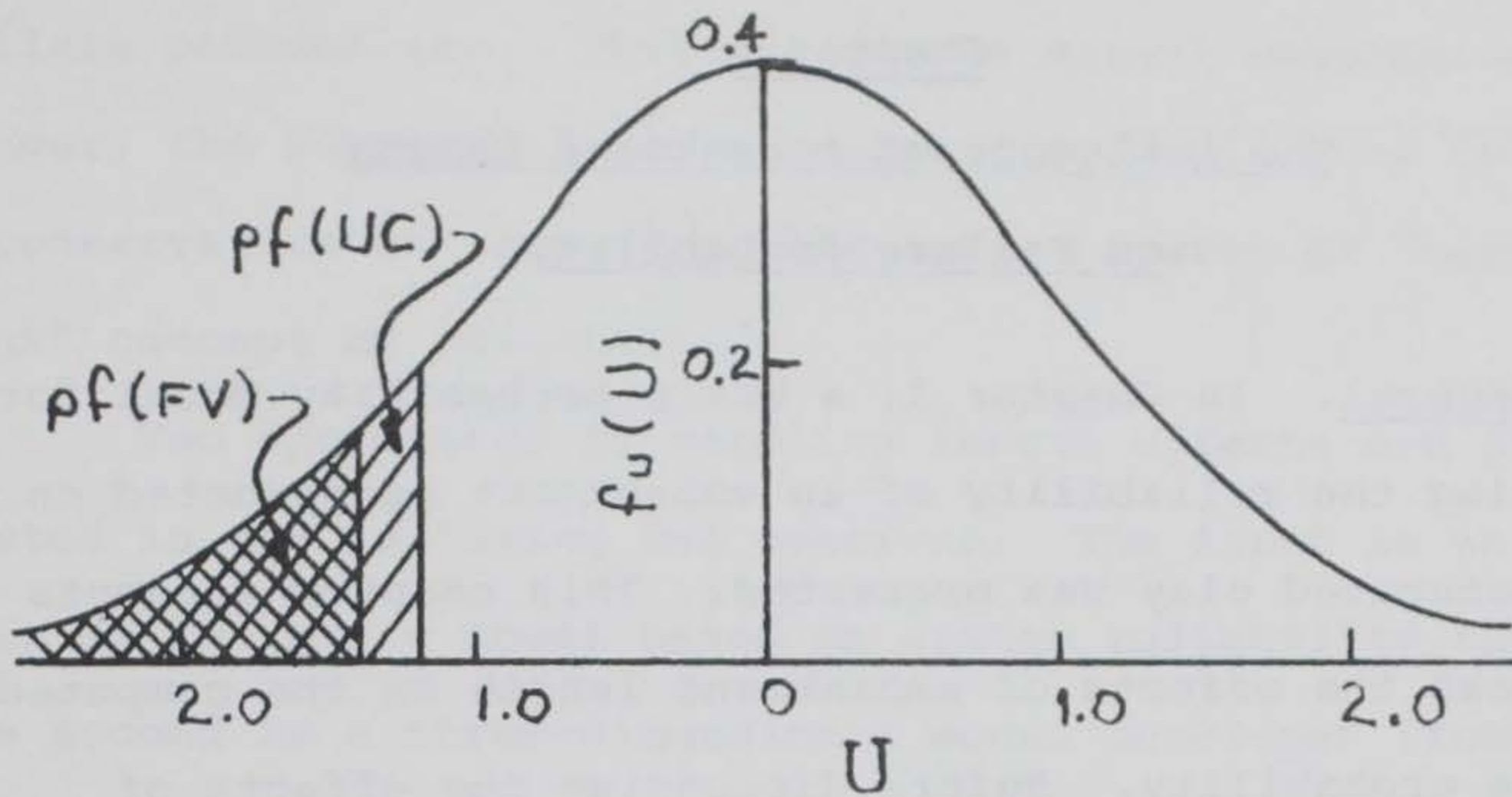
CIRCULAR ARC ANALYSES (TS III)
 FIELD VANE STRENGTHS



CIRCULAR ARC ANALYSIS (TS III)
UNCONFINED COMPRESSION STRENGTHS



TS III SIMPLIFIED FAILURE SURFACE



CALCULATED pf AT TEST SECTION III
AND pf VERSUS FS

Chapter 4

The Influence of Embankment Length on Failure Probability

4.1 General. In Chapter 2, a basic probability model for analyzing the reliability of an embankment constructed on soft saturated clay was presented. This chapter attempts to assess the effects of embankment length on the computed failure probability. Before discussing the effects of length, one must reflect on what the failure probability computed from the basic model represents.

The basic model computes the failure probability, p_f , at one "point", which may be thought of as the center of a segment (along the embankment centerline), whose minimum length is selected to satisfy the assumption of "plane strain". The model also assumes that all strength measurements are made on the critical failure surface for the length, L . For the FRT test section, this minimum length is 240 feet^(*), whereas for TS III, the minimum length of embankment is 810 feet^(*).

If the actual length of embankment constructed, L_a , were equal to these selected lengths, then the computed failure probability would correctly estimate the embankment

* These minimum lengths were computed in Chapter 3. By modeling the critical failure arc with a rectangular surface, the minimum length was assumed to be three times the base width of the simplified failure surface. These minimum lengths are presented in Figures 3-7 and 3-19.

failure probability. However, if the actual embankment were longer, the computed failure probability would tend to be unconservative on account of the series system or "weakest link" concept of reliability.

Two approaches to handling length effects are presented in the following two sections. The first is an extension of the basic model based on system reliability theory. The second is a three-dimensional model developed from a "first passage" failure criterion.

4.2 Series System Failure Criterion. As pointed out above, if an embankment is constructed just long enough for one failure to occur, then the basic model gives a correct estimate of failure probability.

As the length of the actual embankment, L_a , exceeds the minimum length, L , the estimated failure probability will increase. Considering the actual embankment length as a multiple of the minimum length ($n = L_a/L$) and by considering the adjacent lengths as independent events having the same computed failure probability, the probability of a failure occurring somewhere along the entire length can be expressed approximately as (Benjamin and Cornell, 1970):

$$P_f = 1 - (1 - p_f)^n \quad (4.2-1a)$$

or $P_f \approx n p_f \quad (\text{if } n p_f \ll 1) \quad (4.2-1b)$

where

P_f = the probability of a failure occurring at some location along the entire embankment length, L_a .

p_f = the probability of a failure occurring at one "point", centered at the minimum embankment length, L .

n = the number of minimum lengths contained within the actual embankment length^(*).

The implication of equation (4.2-1) can be shown by reviewing the failure probabilities of the two case studies presented in Chapter 3. Considering the calculations based on field vane testing, the Fore River Test Section had a computed failure probability of 0.4 percent for a minimum length equal to 240 feet. Since the FRT test section was itself approximately 240 feet square, n equals 4 for the entire length susceptible to failure. The probability of a failure occurring on one of the four sides of the test embankment is calculated as 1.6 percent^(**) from equation (4.2-1).

* This model is based on the assumption that the average strengths in adjacent segments are statistically independent. Since horizontal correlation distances (assumed equal to 100 feet for case studies in Chapter 3) are usually much smaller than the minimum lengths, this assumption appears justified.

** The clay layer under two of the sides (South&West) of the test section is not as deep and consequently not as likely to fail as the North and East slope. This effect of geometry is not considered in this analysis. It is assumed that the layer thickness is constant and equal to 30 feet.

For the Atchafalaya Basin Test Section III, the constructed length was 1500 feet, while the estimated minimum length for a "plane strain" failure was 810 feet. The probability of a failure occurring along the minimum length, based on field vane tests, was computed as 9 percent. This is compared to a failure probability for the entire length equal to 17 percent. The results of these two case studies are shown on Table 4-1.

Case Study	Minimum Length, L (ft)	Actual Length, La (ft)	pf for L* (%)	P _f for La* (%)
FRT	240	960	0.4	1.6
TS III	810	1500	9	17

*Based on Field Vane Tests

Failure Probabilities Including Length Effect

TABLE 4-1

4.3 "First Passage" Failure Criterion. An alternative to the above method of introducing the parameter, embankment length, into a probabilistic analysis of stability is developed from a "first passage" failure criterion.

For this analysis, the standardized safety margin, $U(x)$, is now thought of as a stationary Gaussian random process:

$$U_{(x)} = \frac{M_{(x)} - \bar{M}}{\sigma_M} \quad (4.3-1)$$

where

$$M_{(x)} = M_r(x) - M_o(x)$$

and

$M_r(x)$ = a "moving average" of strength as a function of position along the embankment length.

$M_o(x)$ = a "moving average" of the load, assumed constant.

The definition of $U_{(x)}$ is illustrated in Figure 4-1. The process $U_{(x)}$ begins and ends at a distance, $L/2$, from both ends of the embankment. Therefore, at $x = 0$, the actual embankment length, L_a , is equal to the minimum length required for a "plane strain" failure to occur.

The probability of a failure occurring at some location along a constructed embankment can be defined as the probability that the standardized safety margin lies below the reliability index at any point, or that the length to first passage of the reliability index is less than the length of the process, $U_{(x)}$, expressed as:

$$P_f = p [U_{(x)} \leq -\beta] = p [X_\beta < X] \quad (4.3-2)$$

where

X_β = the length to first passage of the barrier, $-\beta$ (failure).

A widely used approximation (Vanmarcke, 1972), based on the assumption that crossings of a sufficiently high barrier, $-\beta$, occur independently according to a Poisson process with rate, v_β , is:

$$P_s = (1 - pf) \exp \{-v_\beta X\} \quad (4.3-3a)$$

$$P_s = (1 - pf) \exp \{-v_0 X \exp(-\beta^2/2)\} \quad (4.3-3b)$$

where

P_s = the probability of complete survival of the embankment.

pf = the probability of a failure centered at a randomly-chosen point.

v_β = the mean rate of upcrossings (i.e., crossings with a positive slope) of a level, $-\beta$, by a stationary Gaussian process, $U(x)$.

v_0 = the mean rate of upcrossings of the level "zero".

X = the length or duration of the process, $U(x)$, equal to $L_a - L$.

These upcrossing rates and the length, X , are shown in Figure 4-1.

The probability of a failure occurring somewhere along the embankment length is equal to:

$$P_f = 1 - P_s \quad (4.3-4a)$$

$$P_f = 1 - (1 - pf) \exp \{-v_0 X \exp(-\beta^2/2)\} \quad (4.3-4b)$$

or $P_f \approx pf + v_0 X \exp(-\beta^2/2), \text{ if } \text{sum} \ll 1 \quad (4.3-4c)$

By inspecting equation (4.3-4b), it can be seen that as X equals zero (the actual embankment length, L_a , equals the minimum length, L), then

$$P_f = pf \quad (4.3-5)$$

This result from the three-dimensional model is consistent with the interpretation of the result of the basic probability model.

The major difficulty with this approach to length effects lies in the evaluation of v_0 . By definition, v_0 is a measure of how rapidly the standardized safety margin fluctuates with position along the embankment length. Considering the embankment load as deterministic and constant, soil strength and foundation geometry are the major sources that cause the standardized safety margin to fluctuate.

Considering only the soil strength as variable, what is important is the spatial average shear strength over the critical failure surface (three-dimensional). This spatial average shear strength should be highly correlated.

Referring back to Figure 4-1, the first possible failure surface with length, L , has some spatial average shear strength acting on it. This average shear strength can be thought of as centered at point c_0 . Now consider

another possible failure surface centered at some small distance from c_0 and having the same minimum length, L .

The latter failure surface has nearly the same spatial average shear strength as the former. This is true since a large portion of the two failure surfaces are common to each. It is this overlapping of individual failure surfaces when computing a "moving average", together with the large horizontal correlation distances estimated for strength, that cause the spatial average shear strength to be highly correlated.

The mean rate of zero upcrossings of the average process, $U(x)$, is linked to the correlation distance of the spatial average shear strength ($\delta\langle s \rangle$) as averaged over three-dimensional failure surfaces. If the coefficient of correlation of this spatial average shear strength can be considered to have the form:

$$\rho = e^{-x^2/\delta s^2} \quad (4.3-6)$$

then the rate of zero upcrossings becomes:

$$v_0' = \frac{2\sqrt{2}}{\delta\langle s \rangle} \quad (4.3-7)$$

Evaluating the correlation distance of the spatial average strength is a difficult task and is not undertaken in this thesis. However, to illustrate the application equation (4.3-4b), different values of v_0 are tried. The Atchafalaya Basin Test Section III analysis is used as an

example. The probability of failure of a minimum length of this embankment (810 ft) had a computed failure probability of failure equal to 9 percent based on field vane testing.

Figure 4-2 presents plots of failure probability versus embankment length. Curve 1 is based on the three-dimensional extension presented in Section 4.2 (equation 4.2-1). Curve 2 is computed from equation (4.3-4b) with v_0 set to yield the same results as curve 1. Curve 3 is also computed from equation (4.3-4b) with v_0 equal to $1/L$ for this case.

The results indicate that both methods of predicting the effect of embankment length on failure probability can be adjusted to yield the same results. From curves 1 and 2 on Figure 4-2, doubling the embankment length roughly doubles the failure probability.

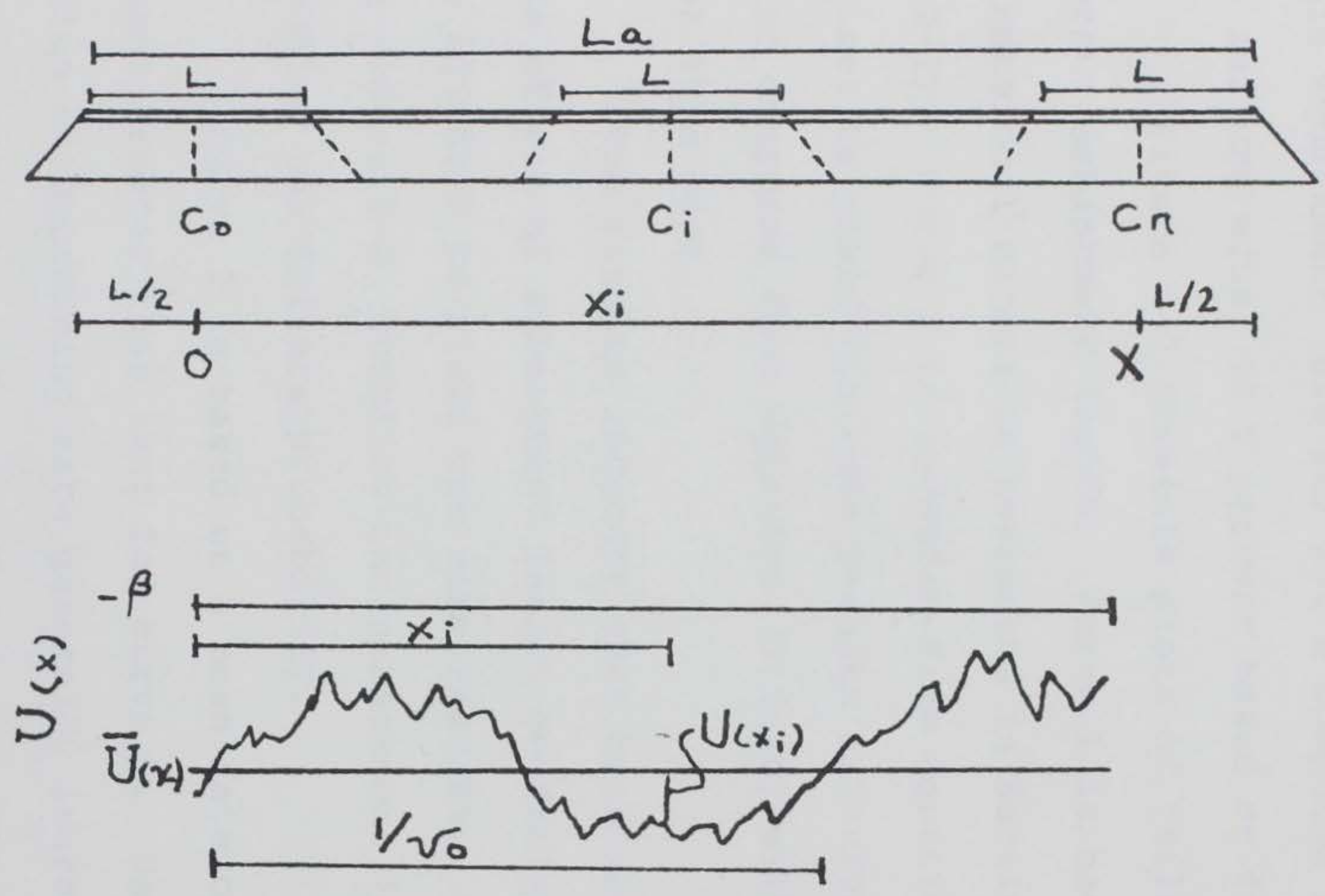
Curve 3 is based on a mean rate of upcrossings four times greater than that for curve 2. Using this greater value of upcrossing rate generally increases the failure probability by a factor of two over those from curves 2 and 3.

At present, it cannot be said as to which approach to length effect is better. More research is needed, especially in the area of spatial strength variability. Also, the effect of foundation geometry (e.g., natural variability

of depth of clay), neglected in this chapter, may be a major factor influencing failure probability versus length.

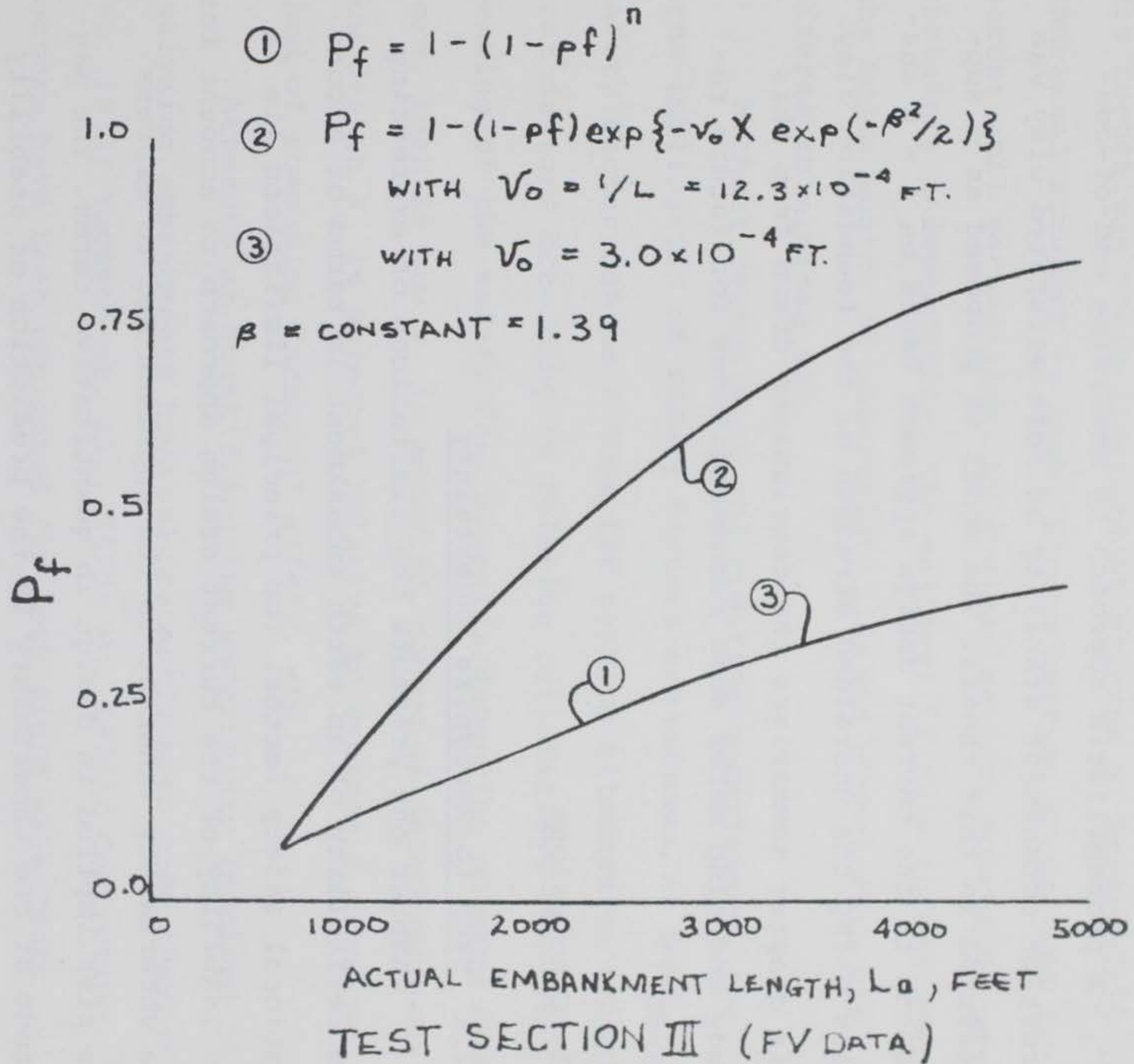


STANDARDIZED SAFETY MARGIN VERSUS
 POSITION ALONG EMBANKMENT LENGTH



- C_0 CENTER OF FIRST POSSIBLE FAILURE LENGTH
- C_i CENTER OF i^{TH} POSSIBLE FAILURE LENGTH
- C_n CENTER OF LAST POSSIBLE FAILURE LENGTH
- v_0 MEAN RATE OF UPCROSSINGS OF THE ZERO LEVEL

P_f VERSUS ACTUAL EMBANKMENT LENGTH



Chapter 5 Conclusions and Recommendations

5.1 General

A probabilistic approach to analyzing end-of-construction embankment stability on soft saturated clay was presented in this thesis. The model is proposed as a supplement to the current design approach based on $\phi = 0$ analyses using the undrained strength of the foundation clay. This chapter summarizes the conclusions drawn from this study and also makes some recommendations for future research.

5.2 Conclusions

5.2.1 Need to Recognize Uncertainty

Chapter one presents the limitations of expressing the reliability of an earth embankment in terms of a conventional safety factor. The principal limitations lie in the inability of the current design approach to account for the uncertainty inherent in the approach and to express the risk implied in design in quantitative terms. The magnitude of the uncertainty in the prediction of stability is a critical issue in geotechnical engineering.

It is the role of the geotechnical engineer to reduce unknowns and to evaluate and assess the degree of uncertainty. The probability model presents a systematic method of qualitatively evaluating uncertainty. It provides the en-

gineer with a mechanism that can indicate where additional investigation is needed to minimize risk.

The general probability model developed in this thesis recognizes three independent sources of uncertainty in undrained strength -- bias, random testing error, and inherent soil variability. By evaluating each source or uncertainty independently, the engineer is able to see where the major source of uncertainty lies and concentrate his efforts to minimize it.

Without recognizing and treating uncertainty, the true implication of safety factors are unknown. At best, the safety factor can be a tool for ranking alternative embankment designs according to relative reliability. The true meaning of the safety factor varies depending on many factors, such as how s_u is measured, number of determinations, how design s_u is selected relative to average s_u , and method of computing factor of safety, etc.

Attempts at quantifying the uncertainty involved in analyzing embankments have only recently been made (Barbatteu, 1972; Yucemen et. al., 1973; Wu, 1974). Correction factors have been published for both field vane tests (Bjerrum, 1972) and unconfined compression tests (Wu, 1974). These mean correction factors and the data from which they were developed allow one to evaluate the uncertainty associated with applying them.

A study is currently underway at M.I.T. to evaluate the spatial correlation properties of undrained shear strength. Through such a study, a better understanding of the uncertainty due to inherent soil variability will be available.

Although more refinement is, indeed, necessary, the probability model is a step in the right direction. The probability model does not eliminate any of the steps present in the current design approach. But it does attempt to standardize the approach and it introduces another set of parameters that truly enable assessments of reliability of analyses -- those that measure uncertainty.

5.2.2 Safety Factors as a Measure of Reliability

Historically, safety factors have been used as measures of reliability. In order to decide how good safety factors are at measuring reliability, it is necessary to reflect on the decisions that influence the determination of a safety factor of an embankment constructed on soft saturated clay.

A design engineer makes decisions that directly influence the calculated safety factor of an embankment. These decisions include selecting an appropriate method of analysis, planning the site exploration, laboratory and field testing programs, and selecting the "design" strength for the analysis.

These decisions generally do not follow a standardized pattern. For a given embankment of soft clay, an engineer may use a wedge or a circular arc analysis; 2½-inch or 5-inch diameter undisturbed samples; field vane or unconfined compression testing; and the use of mean strengths or lower than mean strengths for design. Different combinations of the above selections can result in a very wide range of safety factors for the same embankment. Consequently, the fact that one embankment has a computed safety factor equal to 1.5, while that of another equals 1.2, may have little real significance regarding the true "safety" or reliability.

However, safety factors can be used to reflect relative reliability, at least for the same soil deposit, if engineers or government organizations develop standardized procedures for investigating the stability of embankments. By building upon the experience of the engineer and by adjusting the design procedure, an engineer can develop a design procedure that can limit the number of actual failures to an acceptable percentage. This usually entails a trial and error approach. As one procedure leads to too many failures or too conservative of a design, one or a number of the steps are changed. This can ultimately lead to a combination of one method of analysis, a standardized field investigation program, one type of test for strength

determination, and one means of selecting a design value of strength. Such a combination plus a design safety factor can be successfully used as a semi-empirical procedure for investigating stability problems.

By standardizing the design procedure and by applying it to a particular geographic area, the uncertainty in the procedure is approximately constant. If the uncertainty (measured in terms of coefficients of variation and safety margin) is constant, the reliability index, and hence the failure probability, is proportional to the safety factor. For this case, the safety factor can be used as an indicator of the reliability of an embankment.

However, there are limitations to such semi-empirical procedures. Although a design safety factor is used, the true safety factor of an embankment remains unknown. Biases in strength measurements and the method of analysis are hidden in the steps of the procedure. The working procedure often involves an cancellation of errors.

If another method of determining strength were used to better define the true in situ strength, the balance of the procedure can be destroyed and the probability of failure will change - even though the design safety factor is constant. Also, a working procedure developed for a particular geologic deposit, if extrapolated to different geologic areas, may prove to be ineffective.

Although a working factor of safety procedure does allow a ranking according to relative reliability, safety factors cannot be combined with the cost associated with an embankment to optimize design. The effect on the failure probability by raising or lowering the safety factor cannot be evaluated without explicitly accounting for the uncertainty entering into the analysis. Although increasing the safety factor decreases the probability of failure, one is unable to answer the question "By how much?"

While the current design approach has often proved to be an effective tool, a systematic consideration of uncertainty can give better measure of true risk. With such an assessment of true risk, the engineer is better equipped to optimize the design and judge its acceptability.

5.2.3 The Uncertainty of Bias

The two case studies presented in this thesis indicate that the bias inherent in field vane and unconfined compression testing can be the major source of uncertainty in design. Depending on soil type and depth and type of test, measured strength can be equal to, less than, or greater than the true in situ undrained strength. Bias is a persistent source of uncertainty regardless of the number of independent strength tests performed.

Comparing the uncertainty of the two correction

factors used for the examples presented in this thesis, the correction factor for unconfined compression tests showed the larger scatter about its mean. This would tend to indicate that the field vane test is a better measure of strength trends in space than the unconfined compression test.

The reason for field vanes being better measures of strength is that the field vane test introduces less (and generally a constant amount of) sample disturbance. Varying degrees of sample disturbance are exhibited by unconfined compression tests by different size and type of sampling tubes, different field and lab handling techniques, different type soils tested. It also tends to vary with depth. The field vane tests minimize sample disturbance by performing the test in situ. It also generally involves a more standardized test procedure.

There appears to be two different ways to reduce the uncertainty due to test bias. The first involves restricting the source of data for the correction factor. The second way is to use a more rational method of measuring strength.

By limiting the source of data to a particular geologic deposit, the effect of soil type on the correction factor will be approximately constant. By standardizing both the equipment and the method of testing (i.e., strain

rate, depth of penetration of the vane, size of the vane), the bias due to these sources of error will also be approximately constant.

The effect of restricting the method of testing and source of data for the correction factor was illustrated in Chapter 1. By limiting the source of case studies to embankment failures in Boston Blue Clay and by performing the field vane test in a standardized manner, scatter in a correction factor developed from this information should be smaller than that for the revised Bjerrum factor (developed from a wide variety of case studies).

Of course, one problem with developing local correction factors is that it takes time to accumulate a sufficient amount of data. Performing strength tests at sites of embankment failures after the failures have occurred would hasten the acquisition of local data.

The second way to reduce the uncertainty due to bias is to improve on the conventional method of measuring soil strength. Such a method has been proposed by Ladd and Foott (1973) and has shown to be more effective in predicting unbiased strength for uniform soil deposits. The Stress History and Normalized Soil Engineering Properties (SHANSEP) method is based on the principle that stress-strain-strength properties of clay are uniquely related to the overconsolidation ratio (OCR). By reconsolidating a sample

in the laboratory to the same stress ratio as in the field, one can obtain a sample having normalized properties similar to those in situ. By shearing the reconsolidated sample under the same stress conditions expected in the field (plane strain active, direct shear, plane strain passive), normalized strength parameters (undrained strength divided by vertical effective stress) can be determined for a soil deposit.

The measurement of strength by the SHANSEP method does not involve a direct measurement of in situ strength at a point. Rather, normalized soil properties are obtained for an entire soil deposit. The evaluation of the uncertainty of strength determined by SHANSEP requires an evaluation of the uncertainty in the steps followed to measure normalized soil properties (total weight, pore pressures, coefficient of lateral earth pressure, maximum past pressure, laboratory strength testing). Preliminary studies in this area indicate that uncertainty in stress history (especially maximum past pressure) is the dominant source of uncertainty for strength measured by SHANSEP.

5.3 Recommendations

5.3.1 Other Failure Modes

The probability model developed in this thesis assumes only one mode of embankment failure, an undrained

shear failure. It neglects other possible modes of failure, such as excessive consolidation deformations, deformations due to undrained creep, piping, and overtopping or erosion.

If other modes of failure are to be considered, an assessment of the probability of failure for each individual mode has to be made. Once the individual failure probabilities are assessed, they can be combined using basic probability to give a failure probability resulting from the system of failure modes.

More study on a probabilistic basis is needed on other modes of failure of earth embankments. Without a full understanding of these other modes, the actual failure probability is indeterminate. This area of study would also involve introducing another variable, time, into the problem.

5.3.2 Spatial Variability

The uncertainty due to inherent soil variability was shown to be proportional to the point coefficient of variation of in situ strength and inversely proportional to the equivalent number of independent soil elements, N_e . In order to evaluate N_e , the correlation of in situ strength has to be measured. Determining the correlation of in situ strength would generally require a close, well tested grid of borings

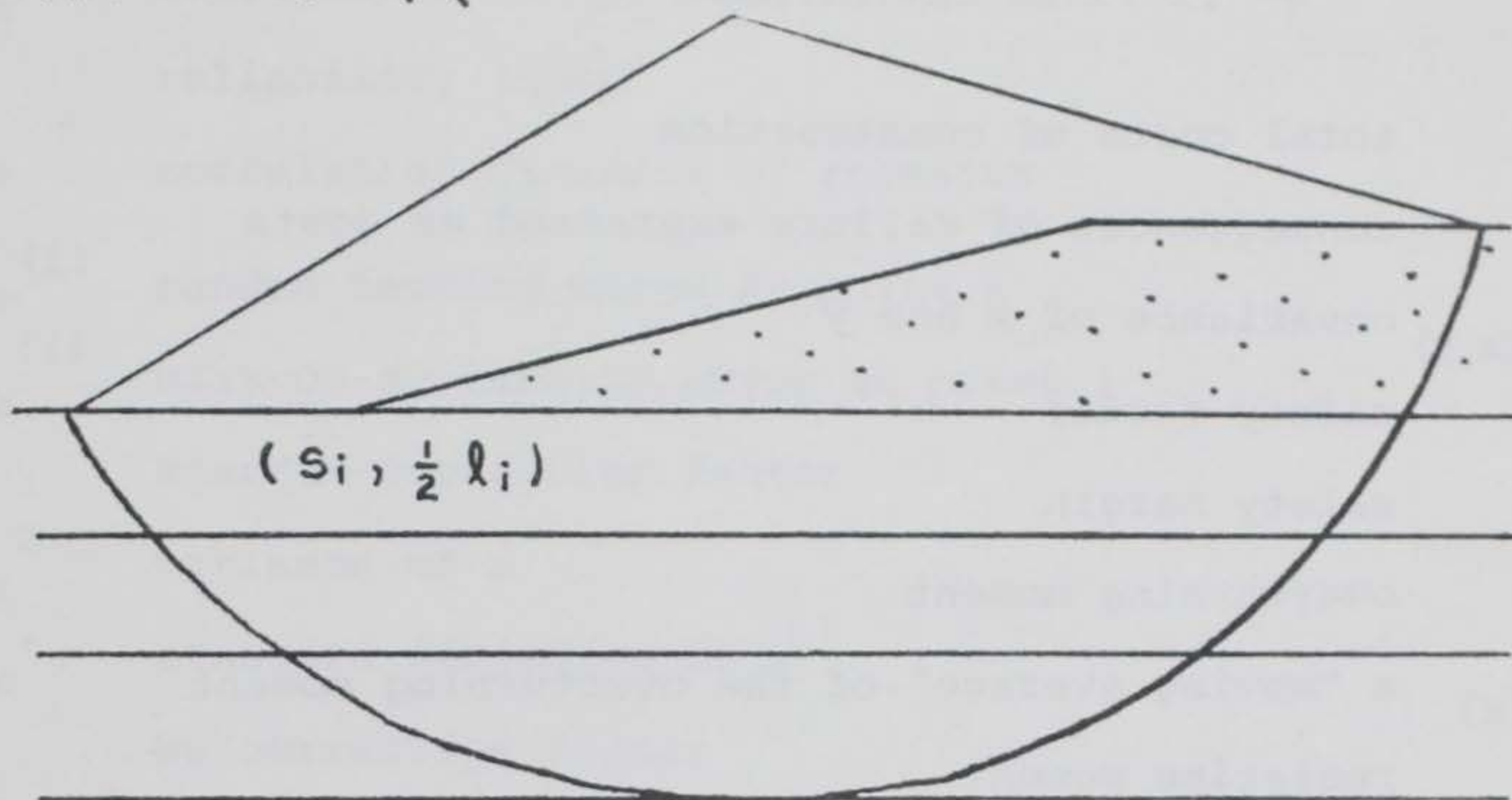
A study is currently underway at M.I.T. to evaluate

strength correlation distances for various soil deposits. More research is needed in this area of uncertainty in order to better understand the true importance of inherent soil variability.

5.3.3 Other Measures of Strength

As previously stated, the Stress History and Normalized Soil Engineering Properties approach has been effectively used to measure undrained strength. A study of the sources of uncertainty in the approach and a method for measuring the uncertainty should be made. This would allow for the results from SHANSEP to be applied in probabilistic studies of embankment reliability. Also, more studies of other embankment failures, as well as of satisfactorily performing embankments, should be made. This will provide a better feel for the results of probabilistic analyses.

APPENDIX A



$$\bar{M}_r = r \sum \bar{l}_i \bar{s}_i$$

$$\sigma_{M_r}^2 = \sum_i \sigma_{(l_i s_i)} + \sum_i \sum_j \rho(l_i s_i)(l_j s_j) \sigma_{l_i s_i} \sigma_{l_j s_j}$$

$$= \sum_i V_{(l_i s_i)}^2 \bar{l}_i^2 \bar{s}_i^2 + \sum_i \sum_j \rho [V_{l_i s_i} \bar{l}_i \bar{s}_i V_{l_j s_j} \bar{l}_j \bar{s}_j]$$

$$= \sum_i (V_{l_i}^2 + V_{s_i}^2) (\bar{l}_i^2 \bar{s}_i^2) + \sum_i \sum_j \rho [(V_{l_i}^2 + V_{s_i}^2)^{\frac{1}{2}} \bar{l}_i \bar{s}_i \times$$

$$(V_{l_j}^2 + V_{s_j}^2)^{\frac{1}{2}} \bar{l}_j \bar{s}_j]$$

$$\rho(l_i s_i)(l_j s_j) = 1 \text{ FOR } i = j \left. \begin{array}{l} \text{BOTH } s \text{ AND } l \\ \text{ARE INDEPENDENTLY} \\ \text{PERFECTLY} \\ \text{CORRELATED.} \end{array} \right\}$$

$$= 0 \text{ FOR } i \neq j$$

$$\sigma_{M_r}^2 = \sum_i (V_{l_i}^2 + V_{s_i}^2) (\bar{l}_i^2 \bar{s}_i^2) + 2 \sum_i (V_{l_i}^2 + V_{s_i}^2)^{\frac{1}{2}} \bar{l}_i \bar{s}_i$$

NOTATION

cc	total costs of construction
CF	consequences of failure expressed as costs
$COV_{(x,y)}$	covariance of x and y
FS	safety factor
M	safety margin
M_o	overturning moment
$M_o(x)$	a "moving average" of the overturning moment
M_R	resisting moment
$M_R(x)$	a "moving average" of the resisting moment
pf	probability of failure at one "point"
P_f	probability of a failure occurring at some location along the actual embankment length
$S_{(meas)}^{(i)}$	measured strength at point i
$S_{(true)}^{(i)}$	true strength at point i
S_u	undrained shear strength
TEC	total expected costs
U	standardized safety margin at a "point"
$U_{(x)}$	standardized safety margin as a stationary Gaussian random process.
$VAR_{(x)}$	Variance of x
V_x	coefficient of variation of x
X	length or duration of the process, $V_{(x)}$
\bar{X}	mean of x

x_{β}	length to first passage of the barrier, $-\beta$
β	reliability index
δs	correlation distance of strength
$\epsilon_r^{(i)}$	random testing error at point i
$\epsilon_b^{(i)}$	bias or systematic error at point i
μ	Bjerrum correction factor
σ_x^2	variance of x
σ_x	standard deviation of x
ν	Wu correction factor
ν_{β}	mean rate of upcrossings of a level, $-\beta$
ν_0	mean rate of upcrossings of the level, zero

REFERENCES

1. Ang, A.H.-S (1972), "Probability Bases of Safety, Performance, and Design", Proceedings, Specialty Conference on Safety and Reliability of Metal Structures, ASCE, Pittsburgh, Pennsylvania.
2. Barboteu, G. (1972), "Reliability of Earth Slopes", M.S. Thesis, M.I.T.
3. Benjamin, J.R. and Cornell, C.A. (1970), Probability Statistics and Decision for Civil Engineers, McGraw-Hill, New York.
4. Bishop, A.W. and Bjerrum, L. (1960), "The Relevance of the Triaxial Test to the Solution of the Stability Problems", Proceedings, Research Conference on Shear Strength of Cohesive Soils, ASCE, June, Boulder Colorado.
5. Bjerrum, L., Clausen, C.J.F., and Duncan, J.M., (1972), "Earth Pressures on Flexible Structures - A State-of-the-Art Report".
6. Duckstein, L., Bogardi, I., Szidarovszky, F., and Kisiel, C., (1973), "Reliability of a Levee Reach", Submitted for Publication, JGED, ASCE, November.
7. Flaate, K., (1966), "Factors Influencing the Results of Vane Tests", Canadian Geotechnical Journal, Vol. 3, No. 2.
8. Flaate, K., and Preber, T., (1974), "Stability of Road Embankments in Soft Clay", Canadian Geotechnical Journal, Vol. 11, No. 1, February.
9. Foott, R. and Ladd, C.C. (1973) "The Behavior of Atchafalaya Test Embankments During Construction", M.I.T. Department of Civil Engineering, Research Report R73-27, May.
10. Gordon, M.. (1973), "A Comparison of Effective and Total Stress Stability Analyses of Embankments on Soft Ground", M.S. Thesis, M.I.T.
11. Haley and Aldrich, Inc. (1967), "Interim Report on Embankment Failure at Fore River Test Section, Portland, Maine", Report Written for Maine State

Highway Commission by Haley and Aldrich, Inc.,
Cambridge, Massachusetts.

12. Höeg, K. and Murarka, R.P. (1974), "Probabilistic Analysis and Design of a Retaining Wall", JGED ASCE, Vol. 100, GT3, March.
13. Hooper, J.A. and Butler, F.G. (1966), "Some Numerical Results Concerning the Shear Strength of London Clay", Geotechnique, Vol. 16, No. 4.
14. Kaufman, R.I. and Weaver, R.J. (1967), "Stability of Atchafalaya Levees", JSMFD, ASCE, Vol. 93, No. SM 4, July.
15. Ladd, C.C. (1964), "Strength Parameters and Stress Strain Behavior of Saturated Clays", M.I.T. Department of Civil Engineering, Research Report R71-23.
16. Lambe, T.W. and Whitman, R.V. (1969), Soil Mechanics John Wiley and Sons, Inc., New York.
17. LaRoche, P. Track, B., Travenas, F., and Ray, M., "Failure of a Test Embankment on a Sensitive Champlain Clay Deposit", Canadian Geotechnical Journal, No.1, February.
18. Lefebure, K. and Preber, T. (1974), "Stability of Road Embankments in Soft Clay", Canadian Geotechnical Journal, Vol. 11, No. 1, February.
19. Lumb, P. (1966), "The Variability of Natural Soils", Canadian Geotechnical Journal", Vol. 3., No. 2.
20. Lumb, P. (1970), "Safety Factors and Probability Distributions of Soil Strengths", Canadian Geotechnical Journal, Vol. 7, No. 3.
21. Meyerhof, G.G. (1970), "Safety Factors in Soil Mechanics", Canadian Geotechnical Journal, Vol. 7, No. 4, November.
22. M.I.T. (1968) "The Selection of Foundation Soil Properties for Levee Design", M.I.T. Department of Civil Engineering, Research Report R69-17, Soil Publication No. 232, December.
23. Morla-Catalan, J. and Cornell, C.A. (1974), "Slope Stability Reliability as a Spatial First-Passage Problem", Paper Presented at ASCE-EMD Specialty Conference, Stanford University, June.

24. Padilla, J.D. and Vanmarcke, E.H. (1974), "Settlement of Structures on Shallow Foundations: A Probabilistic Analysis", M.I.T. Department of Civil Engineering, Soil Publication No. 334.
25. Sowers, G.F. (1969), Introductory Soil Mechanics and Foundations, The MacMillan Co., New York.
26. USCE (1968), "Interim Report on: Field Tests of Levee Construction Test Sections I, II, and III", New Orleans District, Corps of Engineers, New Orleans, Louisiana.
27. Vanmarcke, E.H. (1969) "First Passage and Other Failure Criteria in Narrow-Band Random Vibration: A Discrete State Approach", M.I.T. Department of Civil Engineering, Research Report R69-68
28. Vanmarcke, E.H. (1970), "Some Basic Results for I-D Random Processes", Course Notes, 1.34, M.I.T.
29. Vanmarcke, E.H. (1972), "Properties of Spectral Moments with Applications to Random Vibrations", JEMD, ASCE, Vol 98., No. EM 2, April.
30. Vanmarcke, E.H. (1974), "A Model of Soil as a Random Medium", Paper Presented at ASCE-EMD Specialty Conference, Stanford University, June.
31. Vanmarcke, E.H. (1973), "Matrix Formulation of Reliability Analysis and Reliability-Based Design", Computers and Structures, Vol. 3, No. 4.
32. Wright, S.G. and Duncan, J.M. (1972), "Analysis of Waco Dam Slide", Ph.D. Thesis, Berkeley.
33. Wu, T.H. (1974), "Uncertainty, Safety, and Decision in Soil Engineering", JGED, ASCE, Vol. 100, No. GT 3, November.
34. Wu, T.H. and Kraft, L.M. Jr. (1970), "Seismic Safety of Earth Dams", JSMFD, ASCE, Vol. 96, No. SM 6, November.
35. Wu, T.H. and Kraft, L.M. Jr. (1970), "Safety Analysis of Slopes", JSMFD, ASCE, Vol. 96, No. SM 2, March.
36. Yucemen, M.S., Tang, W.H. and Ang, A. H-S. (1973), "A Probabilistic Study of Safety and Design of Earth Slopes", University of Illinois, Department of Civil Engineering, Structural Research Series, No. 402.

In accordance with ER 70-2-3, paragraph 6c(1)(b), dated 15 February 1973, a facsimile catalog card in Library of Congress format is reproduced below.

Gilbert, Lawrence William

A probabilistic analysis of embankment stability problems, by Lawrence W. Gilbert. Vicksburg, U. S. Army Engineer Waterways Experiment Station, 1977.

148 p. illus. 27 cm. (U. S. Waterways Experiment Station. Miscellaneous paper S-77-10)

Prepared for Office, Chief of Engineers, U. S. Army, Washington, D. C., under CWIS 31173, Task 21.

References: p. 146-148.

1. Embankment stability. 2. Embankments. 3. Models.
4. Probability theory. I. U. S. Army. Corps of Engineers. (Series: U. S. Waterways Experiment Station, Vicksburg, Miss. Miscellaneous paper S-77-10)
TA7.W34m no.S-77-10